

**Translational control in autism spectrum disorder and memory:
a novel role for 4EHP**

by Shane Wiebe

Department of Biochemistry
Rosalind and Morris Goodman Cancer Institute
McGill University
Montréal, Québec, Canada

April 2022

A thesis submitted to McGill University in partial fulfillment of the requirements for the degree
of Doctor of Philosophy.

©Shane Wiebe, 2022

TABLE OF CONTENTS

TABLE OF CONTENTS.....	ii
LIST OF TABLES AND FIGURES.....	vi
English abstract.....	vii
French abstract.....	viii
Preface.....	x
Contribution of authors to each chapter.....	xi
Contributions to knowledge and elements of original scholarship.....	xiii
Acknowledgements.....	xiv
List of abbreviations.....	xvi
Chapter 1: General Introduction.....	1
1.1. 4EHP, a multifaceted cap-binding protein.....	2
1.1.1. 4EHP inhibits translation initiation.....	5
1.1.1.1. Non-canonical initiation.....	5
1.1.2. miRNA-mediated silencing.....	6
1.1.2.1. 4EHP and 4E-T.....	7
1.1.3. 4EHP and GIGYF2.....	7
1.1.3.1. Role in development.....	8
1.1.3.2. Regulation of ERK signalling and implications.....	9
1.1.3.3. Protection of host during viral infection.....	10
1.1.3.4. Ribosome collisions and quality control.....	11
1.1.3.5. Link to autism spectrum disorder.....	12
1.1.4. Concluding remarks.....	13
1.2. Neurological Disorders and mRNA Translation.....	14
1.2.1. The mTOR pathway: mTORC1 and mTORC2.....	14
1.2.2. Cap-dependent mRNA translation: eIF4E and 4E-BP2.....	19
1.2.3. Cap-dependent mRNA translation: FMRP and CYFIP1.....	20
1.2.4. Integrated stress response: eIF2.....	24
1.2.5. Concluding remarks.....	26

1.3.	Translational control in learning and memory	29
1.3.1.	Mechanisms of short-term memory.....	32
1.3.1.1.	Working memory	32
1.3.2.	Mechanisms of long-term memory	33
1.3.2.1.	Phosphorylation of eIF2 α is a molecular memory switch	34
1.3.3.	The role of miRNAs in synaptic plasticity and memory	35
1.3.4.	Concluding remarks	36
Chapter 2:	The eIF4E homolog 4EHP (eIF4E2) regulates hippocampal long-term depression and impacts social behavior	37
2.1.	Abstract	38
2.2.	Background	40
2.3.	Methods	43
2.3.1.	Mice.....	43
2.3.2.	Generating <i>Eif4e2</i> conditional knockout (KO) mice.....	43
2.3.3.	Synaptic protein extraction.....	44
2.3.4.	Western blot	44
2.3.5.	Primary hippocampal neuron cultures	46
2.3.6.	Immunofluorescence on primary neuron cultures.....	46
2.3.7.	Immunofluorescence on brain slices	47
2.3.8.	Electrophysiological recordings	48
2.3.9.	Measurement of global protein synthesis	49
2.3.10.	Three-chamber social interaction	49
2.3.11.	Marble burying.....	50
2.3.12.	Direct social interaction	50
2.3.13.	Self-grooming.....	51
2.3.14.	Isolation-induced ultrasonic vocalizations.....	51
2.3.15.	Open field.....	51
2.3.16.	Rotarod	52
2.3.17.	Olfactory preference	52

2.3.18. Elevated plus maze	52
2.3.19. Contextual fear conditioning	53
2.3.20. Statistical analysis	53
2.4. Results	54
2.4.1. 4EHP is primarily expressed in neurons and synaptosomes and its amount increases during development.....	54
2.4.2. 4EHP in excitatory neurons regulates hippocampal mGluR-LTD and is necessary for normal social behaviors.....	57
2.4.3. ASD-like behavioral impairments in 4EHP-eKO mice are specific to social interaction and are not confounded by deficits in locomotion, motor function, olfaction, or anxiety	61
2.4.4. <i>GIGYF2</i> mutations are linked to ASD, but heterozygous deletion of <i>Gigyf2</i> , <i>Eif4e2</i> , or both in mice does not elicit ASD-like behaviors	64
2.5. Discussion.....	68
2.5.1. Limitations.....	74
2.5.2. Conclusions	74
2.6. Connecting text.....	75
Chapter 3: Cell-type-specific translational control of spatial working memory by the cap-binding protein 4EHP.....	76
3.1. Abstract	77
3.2. Background	78
3.3. Methods.....	80
3.3.1. Mice.....	80
3.3.2. Generating conditional knockout (KO) mice.....	80
3.3.3. Genotyping.....	81
3.3.4. Western blot	81
3.3.5. Immunofluorescence on brain slices	82
3.3.6. Administration of anisomycin	83
3.3.7. Morris Water Maze	83

3.3.8. T-maze.....	84
3.3.9. Contextual fear conditioning	84
3.3.10. Statistical analysis	85
3.4. Results	86
3.4.1. Conditional deletion of 4EHP in CaMKII α -positive excitatory neurons.....	86
3.4.2. 4EHP in excitatory neurons is not required for long-term memory.....	89
3.4.3. Spatial working memory requires 4EHP in both excitatory and inhibitory neurons.	92
3.4.4. Sustained, but not acute inhibition of translation impairs working memory	97
3.5. Discussion.....	100
Chapter 4: General Discussion.....	103
4.1. Summary and integration of findings	104
4.1.1. How might <i>GIGYF2</i> mutations engender ASD?.....	104
4.1.2. What is the link between working memory and ASD?	106
4.1.3. What are the implications of altered translation in working memory?	107
4.1.4. What are the potential mechanisms of 4EHP in the brain?	108
4.1.4.1. Post translational modifications	108
4.1.4.2. Phase separation and biomolecular condensates	109
4.1.5. Concluding remarks	110
References	111
Appendix A: Supplementary tables and figures	140

LIST OF TABLES AND FIGURES

Figure 1.1.	Mechanism of interaction between 4EHP and the m7GTP cap structure.	4
Figure 1.2.	Neurological disorders linked to regulation of cap-dependent translation initiation.	18
Figure 1.3.	Integrated stress-response related neurological disorders.	28
Figure 1.4.	Memory classification in humans.	31
Table 2.1:	Mutations in <i>GIGYF2</i> are linked to autism spectrum disorder.	42
Figure 2.1.	4EHP expression in the brain.	56
Figure 2.2.	Loss of 4EHP in excitatory neurons exaggerates hippocampal mGluR-LTD and impairs social behavior.	60
Figure 2.3.	4EHP-eKO mice do not present wide-spread behavioral alterations.	63
Figure 2.4.	Heterozygous deletion of <i>Gigyf2</i> , <i>Eif4e2</i> , or both in mice does not result in ASD-like behavioral deficits.	67
Figure 2.5.	Proposed model.	73
Figure 3.1.	Conditional deletion of 4EHP in CaMKII α -positive excitatory neurons.	88
Figure 3.2.	Long-term memory is normal in 4EHP-CaMKII α KO mice.	91
Figure 3.3.	Working memory is impaired in 4EHP-CaMKII α KO mice.	94
Figure 3.4.	Working memory is impaired in 4EHP-GAD65 KO mice.	96
Figure 3.5.	Working memory is impaired after sustained, but not acute inhibition of protein synthesis.	99
Table S2.1:	Details of statistical analyses for Chapter 2	140
Table S3.1:	Details of statistical analyses for Chapter 3	152
Figure S2.1.	Codeletion of 4EHP and GIGYF2 occurs as early as P0 in the brain of 4EHP-eKO mice.	161
Figure S2.2.	Analysis of global protein synthesis.	162
Figure S2.3.	Analysis of long-term contextual fear memory and p-ERK.	163
Figure S3.1.	4EHP expression pattern in the prefrontal cortex.	164
Figure S3.2.	Inhibitory interneuron-specific deletion of 4EHP does not affect ASD-like behaviors.	165

English abstract

Control of protein synthesis (mRNA translation) is essential for proper brain development and function. Perturbations to the mechanisms governing mRNA translation have repeatedly been shown to constitute a risk factor for neuropathological conditions, such as autism spectrum disorder (ASD). Developing effective therapeutics for brain dysfunction will require a better understanding of the molecular mechanisms underlying the control of protein synthesis in brain function. The eukaryotic initiation factor 4E homologous protein (4EHP) is a mRNA 5' cap-binding protein that represses translation in complex formation with GRB10 interacting GYF protein 2 (GIGYF2), which is required for the stability of both proteins. Mutations in human *GIGYF2* are linked to ASD, but causality is lacking. We hypothesized that *GIGYF2* mutations cause ASD by disrupting 4EHP function. In genetic mouse models lacking expression of 4EHP and GIGYF2 in excitatory neurons we observed robust ASD-like social behavior impairments and exaggerated mGluR-LTD, a synaptic plasticity dysfunction frequently observed in mouse models of ASD. These phenotypes were not attributed to changes in hippocampal global protein synthesis, which suggests that 4EHP and GIGYF2 regulate the translation of specific mRNAs to mediate these effects. Next, given the prominent role of protein synthesis in memory formation, we assessed long-term memory in mice lacking cell-type-specific 4EHP expression. Surprisingly, long-term memory was not affected in mice lacking 4EHP expression in either excitatory (CaMKII α -positive) or inhibitory (GAD65-positive) neurons whereas short-term working memory was impaired in both models. This finding suggests that cooperation of these circuits is necessary for higher-order cognition. Together these findings provide the first insights into the cellular and molecular function of 4EHP in brain function, namely in ASD and memory.

French abstract

Le contrôle de la synthèse des protéines (traduction de l'ARNm) est essentiel au bon développement et au bon fonctionnement du cerveau. Il a été démontré à maintes reprises que les perturbations des mécanismes régissant la traduction de l'ARNm constituent un facteur de risque pour les conditions neuropathologiques, telles que les troubles du spectre autistique (TSA). Le développement de thérapies efficaces pour le dysfonctionnement cérébral nécessitera une meilleure compréhension des mécanismes moléculaires sous-jacents au contrôle de la synthèse des protéines dans la fonction cérébrale. La protéine homologue du facteur d'initiation eucaryote 4E (4EHP) est une protéine de liaison à la coiffe 5' de l'ARNm qui réprime la traduction dans la formation de complexes avec la protéine GYF 2 interagissant avec GRB10 (GIGYF2), qui est nécessaire à la stabilité des deux protéines. Les mutations du GIGYF2 humain sont liées au TSA, mais la causalité fait défaut. Nous avons émis l'hypothèse que les mutations GIGYF2 provoquent un TSA en perturbant la fonction 4EHP. Dans des modèles génétiques de souris dépourvus d'expression de 4EHP et de GIGYF2 dans les neurones excitateurs, nous avons observé de robustes troubles du comportement social de type TSA et un mGluR-LTD exagéré, un dysfonctionnement de la plasticité synaptique fréquemment observé dans les modèles murins de TSA. Ces phénotypes n'ont pas été attribués à des changements dans la synthèse protéique globale de l'hippocampe, ce qui suggère que 4EHP et GIGYF2 régulent la traduction d'ARNm spécifiques pour médier ces effets. Ensuite, étant donné le rôle prépondérant de la synthèse des protéines dans la formation de la mémoire, nous avons évalué la mémoire à long terme chez des souris dépourvues d'expression de 4EHP spécifique au type de cellule. Étonnamment, la mémoire à long terme n'a pas été affectée chez les souris dépourvues d'expression de 4EHP dans les

neurones excitateurs (CaMKII α -positifs) ou inhibiteurs (GAD65-positifs) alors que la mémoire de travail à court terme était altérée dans les deux modèles. Cette découverte suggère que la coopération de ces circuits est nécessaire pour la cognition d'ordre supérieur. Ensemble, ces découvertes fournissent les premières informations sur la fonction cellulaire et moléculaire de 4EHP dans la fonction cérébrale, notamment dans les TSA et la mémoire.

Preface

The present thesis consists primarily of manuscripts published or in preparation for submission to peer-reviewed journals, of which I am the first or co-first author. Below are their citations, with permission where required, and are included in the text as follows:

Chapter 1 (section 1.2):

Wiebe S*, Nagpal A*, Sonenberg N. Dysregulated translational control in brain disorders: from genes to behavior. *Curr Opin Genet Dev.* 2020 Jun 11;65:34-41. (*equal contribution)

Chapter 2:

Wiebe S, Meng XQ, Kim SH, Zhang X, Lacaille JC, Aguilar-Valles A, Sonenberg N. The eIF4E homolog 4EHP (eIF4E2) regulates hippocampal long-term depression and impacts social behavior. *Mol Autism.* 2020 Nov 23;11(1):92.

Chapter 3:

Wiebe S, Huang Z, Skalecka A, Amiri M, Cagnetta R, Lacaille JC, Aguilar-Valles A, Sonenberg N. Cell-type-specific translational control of spatial working memory by the cap-binding protein 4EHP. *To be submitted for publication.*

Contribution of authors to each chapter

The following text provides details on the contribution of the authors to the manuscripts presented in each chapter. All experiments were performed by Shane Wiebe, except where specifically mentioned and credited to the author below. Author contributions are listed in order of their appearance as presented in the manuscripts.

Chapter 1:

This section of the thesis is a literature review which contains the content of the review paper titled: “Dysregulated translational control in brain disorders: from genes to behavior” published in *Curr Opin Genet Dev* in June of 2020. Authorship contributions are as follows. Shane Wiebe: conceptualization, writing – original draft, writing – review and editing, visualization; Anmol Nagpal: conceptualization, writing – original draft, writing – review and editing, visualization; Nahum Sonenberg: writing – review and editing, supervision, and funding acquisition.

Chapter 2:

The second chapter consists entirely of the manuscript titled “The eIF4E homolog 4EHP (eIF4E2) regulates hippocampal long-term depression and impacts social behavior” published in *Mol Autism* in November of 2020. For this publication, Shane Wiebe designed the study, carried out the majority of experiments, analyzed and interpreted data, and wrote the manuscript. Xiang Qi Meng assisted with experiments and provided conceptual support. Sung-Hoon Kim carried out primary neuron culture experiments, analyzed and interpreted data. Xu Zhang and Jean-Claude Lacaille contributed to data analysis and/or provided technical and conceptual support. Argel

Aguilar-Valles and Nahum Sonenberg provided supervision and oversaw the study. Nahum Sonenberg provided funding for the present study. All authors revised the manuscript and approved the final version.

Chapter 3:

The third chapter consists entirely of the manuscript titled “Cell-type-specific translational control of spatial working memory by the cap-binding protein 4EHP” which is in preparation for submission to a peer reviewed journal. Shane Wiebe designed the study, carried out the majority of experiments, analyzed and interpreted data, and wrote the manuscript. Ziyang Huang performed the following experiments in the 4EHP-GAD65 knockout mice: immunofluorescence validation of the model, immunofluorescence analysis of p-S6, T-maze working memory, contextual fear conditioning, and ASD behavior experiments. Agnieszka Skalecka performed immunofluorescence on Raptor-CaMKII α knockout mice. Roberta Cagnetta assisted with immunofluorescence validation of the 4EHP-CaMKII α knockout mice. Mehdi Amiri and Jean-Claude Lacaille contributed to data analysis and/or provided technical and conceptual support. Argel Aguilar-Valles and Nahum Sonenberg provided supervision and oversaw the study. Nahum Sonenberg provided funding for the present study.

Contributions to knowledge and elements of original scholarship

Listed below are the novel discoveries and significant contributions to the scientific field of translational control in neurological function presented in this thesis. These elements were considered original scholarship at the time the research was conducted.

1. 4EHP protein is expressed in multiple brain regions including the cortex, hippocampus, and cerebellum where its levels increase developmentally.
2. 4EHP is expressed in both excitatory and inhibitory neurons, but not in endothelial cells.
3. Neuronal 4EHP localizes to subcellular synaptic compartments.
4. Loss of 4EHP in excitatory neurons in mice results in ASD-like phenotypes including impaired social behavior and exaggerated mGluR-LTD.
5. Behavioral deficits in 4EHP-excitatory neuron knockout mice are specific to sociability and not confounded by deficits in olfaction, anxiety, locomotion, or motor ability.
6. Heterozygous deletion of *Eif4e2*, *Gigyf2*, or one copy of both genes does not impact ASD-associated behaviors.
7. Codeletion of 4EHP and GIGYF2 occurs as early as P0 in the brain of 4EHP-eKO mice.
8. Global regulation of protein synthesis is not mediated by 4EHP and GIGYF2 in adult brain excitatory neurons.
9. Long-term memory is not dependent on 4EHP.
10. 4EHP mediates working memory ability in both excitatory and inhibitory neurons.
11. mTORC1 activity is reduced in excitatory neurons lacking 4EHP.
12. Sustained mTORC1 activity in excitatory neurons is necessary for working memory.

Acknowledgements

Listed below are the acknowledgements for contributions to each chapter of this thesis, including funding where appropriate. First, however, I would like to sincerely thank Dr. Sonenberg for his most excellent supervision and guidance during the tenure of my doctoral studies. This work would not have been possible without his continued guidance and support. My time in Dr. Sonenberg's lab has been an extraordinary learning experience which was beyond the scope of typical graduate studies; for this I am very thankful. Second, I would like to thank Anmol Nagpal for his excellent contributions to our review paper. We also co-authored a study published in PNAS (Wiebe et al. 2019) which is not included in this thesis. It was most fun and exciting to work together. Third, I wish to extend my gratitude for everyone who keeps our lab functioning so smoothly on a regular basis, including Isabelle Harvey, Meena Vipparthi, Annie Sylvestre, Annik Lafrance, Eva Migon, and Annamaria Kiss. Thanks to my research advisory committee Jerry Pelletier and Keith Murai, as well as Argel Aguilar-Valles for the insightful discussions and helping to keep my projects on track. And to all members of the Sonenberg lab, thank you very much for being amazing colleagues and making me a friend. I wish you all the best. Lastly, I would like to thank my family for their never-ending support, my friends Camille, Cynthia, Jeff, Brittany, and Colten for all the good times, and my wife Jovyn for walking with me through every step of the journey.

Chapter 1:

We thank Dr. Ilse Gantois for insightful comments and suggestions on the numerous versions of the manuscript. Funding was provided by a Brain Canada/FNC grant (Nahum Sonenberg), a

Canadian Institutes of Health Research foundation grant (Nahum Sonenberg), A Senior International Research Scholar award from the Howard Hughes Medical Institute (Nahum Sonenberg), a Brain & Behaviour Research Foundation grant (Nahum Sonenberg), the Richard Tomlinson Doctoral Fellowship (Shane Wiebe), and the Healthy Brains for Healthy Lives Fellowship (Canada First Research Excellence Fund to McGill University) (Anmol Nagpal).

Chapters 2 and 3:

We thank Karim Nader (McGill University) for providing access to his behavioral testing rooms. For their help with animal husbandry we thank Annie Sylvestre and Annik Lafrance. We thank Mehdi Hooshmandi from Arkady Khoutorsky's lab (McGill University) for sharing P5 to P120 brain samples. Funding was provided by a Brain Canada/FNC grant, a Canadian Institutes of Health Research (CIHR) foundation grant (FDN-148423), Howard Hughes Medical Institute Distinguished Researcher (#55007654), and Brain & Behavior Research Foundation grant to N.S. and the Richard Tomlinson Doctoral Fellowship, Fonds de Recherche du Québec – Santé (FRQS) Doctoral Scholarship, and Québec Autism Research Training (QART) program scholarship to S.W. J.C.L. was supported by a CIHR project grant (PJT-153311), a FRQS Research Center grant (Centre Interdisciplinaire de Recherche sur le Cerveau et l'Apprentissage [CIRCA]), and is the recipient of the Canada Research Chair in Cellular and Molecular Neurophysiology (CRC-950-231066).

List of abbreviations

4EHP-eKO: 4EHP knockout in EMX1 neurons; **4EHP-cKO**: 4EHP knockout in CaMKII α neurons; **4EHP-gKO**: 4EHP knockout in GAD65 interneurons; **EMX1**: empty spiracles homeobox 1; **PV**: parvalbumin; **SST**: somatostatin; **LAMA1**: laminin; **eIF4E2**: eukaryotic initiation factor 4E homologous protein; **GIGYF2**: GRB10 interacting GYF protein 2; **PABP**: poly A binding protein; **HIF-2 α** : hypoxia-inducible factor; **RBM4**: RNA Binding Motif Protein 4; **miRISC**: miRNA-induced silencing complex; **AGO**: Argonaute; **CCR4-NOT**: carbon catabolite repression 4-negative on TATA-less; **4E-T**: eIF4E transporter; **Bcd**: Bicoid; **cad**: caudal; **DUSP6**: Dual Specificity Phosphatase 6; **p-ERK**: phospho-extracellular-signal-regulated kinase; **TTP**: tristetraprolin; **IFN**: interferon; **EDF1**: endothelial differentiation related factor 1; **mTOR**: mechanistic target of rapamycin; **Raptor**: regulatory associated protein of mTOR; **TSC**: tuberous sclerosis complex; **Rheb**: Ras homolog enriched in brain; **PTEN**: phosphatase and tensin homolog; **S6Ks**: ribosomal protein S6 kinases; **MNKs**: MAPK-interacting serine/threonine-protein kinases; **TNF α** : tumor necrosis factor α ; **FMRP**: fragile X mental retardation protein; **CYFIP1**: cytoplasmic FMR1 interacting protein 1; **4E-BP2**: eIF4E-binding protein 2; **NMDA**: N-methyl-D-aspartate; **AMPA**: α -amino-3-hydroxy-5-methyl-4-isoxazolepropionic acid receptor; **NDRG1**: N-Myc Downstream Regulated 1; **CNTNAP2**: contactin associated protein 2; **ISR**: integrated stress response; **GCN2**: general control nonderepressible 2; **PKR**: protein kinase RNA-activated; **PERK**: protein kinase RNA-like endoplasmic reticulum kinase; **HRI**: heme-regulated inhibitor; **TC**: ternary complex; **uORFs**: upstream open reading frames; **RQC**: ribosome-associated quality control; **NMD**: nonsense mRNA decay; **NSD**: nonstop mRNA decay; **NGD**: no-go decay; **ISG15**: interferon-stimulated gene 15; **P-bodies**: processing bodies; **ARE**: AU-rich element; **E/I**: excitatory to inhibitory balance; **MDD**:

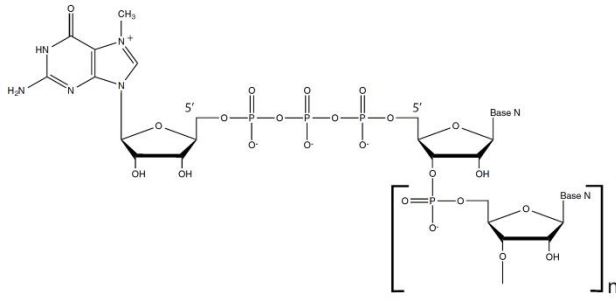
major depressive disorder; **AD**: Alzheimer's disease; **DS**: Down syndrome; **FXS**: Fragile X Syndrome; **SCZ**: schizophrenia; **ASD**: autism spectrum disorder; **VSWM**: visuospatial working memory; **ADHD**: attention deficit/hyperactivity disorder; **IQ**: intelligence quotient; **ID**: intellectual disability; **SFARI**: Simons Foundation Autism Research Initiative; **DSM-5**: Diagnostic and Statistical Manual of Mental Disorders; **GWLA**: genome-wide linkage analysis; **GWAS**: genome-wide association studies; **WGS**: whole genome sequencing; **P**: postnatal day; **e**: embryonic day; **KO**: knockout; **RIPA**: radioimmunoprecipitation assay; **BSA**: bovine serum albumin; **TBST**: Tris-Buffered Saline with Tween 20; **RT**: room temperature; **HRP**: horseradish peroxidase; **HBSS**: Hank's Balanced Salt Solution; **FBS**: fetal bovine serum; **DMEM**: Dulbecco's Modified Eagle Medium; **DIV**: days in vitro; **PBS**: phosphate-buffered saline; **PFA**: paraformaldehyde; **ACSF**: artificial cerebrospinal fluid solution; **fEPSPs**: field excitatory postsynaptic potentials; **mGluR-LTD**: metabotropic glutamate receptor-mediated long-term depression; **DHPG**: (S)-3,5-Dihydroxyphenylglycine; **SUnSET**: surface sensing of translation; **DREADDs**: designer receptors exclusively activated by designer drugs; **TRAP**: translating ribosome affinity purification; **BONCAT**: biorthogonal non-canonical amino-acid tagging; **S1**: stranger 1; **E**: empty cage; **S2**: stranger 2; **LTD**: long-term depression; **LTP**: long-term potentiation; **USVs**: ultrasonic vocalizations; **MEFs**: mouse embryonic fibroblasts; **HEK**: human embryonic kidney; **iPSCs**: induced pluripotent stem cells; **AAV**: adeno-associated virus; **TE**: translational efficiency; **STM**: short-term memory; **LTM**: long-term memory; **WM**: working memory; **DNMTP**: delayed nonmatching-to-place; **MWM**: Morris Water Maze.

Chapter 1: General Introduction

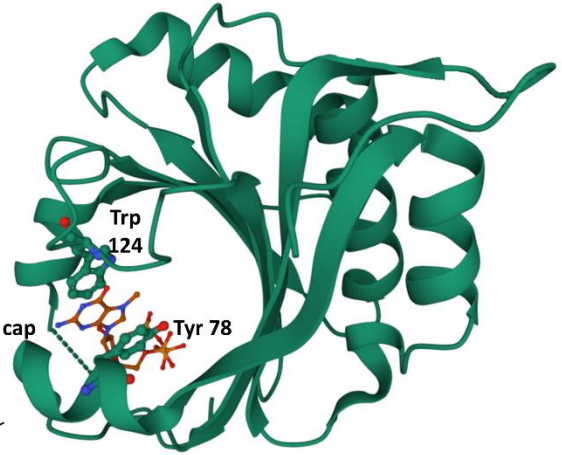
1.1. 4EHP, a multifaceted cap-binding protein

The co-transcriptional addition of a 7-methylguanosine to the terminal nucleotide of nuclear-encoded mRNAs via a unique 5'-5' triphosphate linkage results in a structure known as the 5' cap (m⁷GpppN cap, where N is any nucleotide and m is a methyl group): one of the essential features required for eukaryotic translation [1]. This structure is important for nuclear export of mRNA, splicing, polyadenylation, stability, and translation initiation [2]. The 5' cap is recognized by various cap-binding proteins to mediate translation initiation [1,3]. Among the mammalian cap-binding proteins is the eukaryotic initiation factor (eIF) 4E (eIF4E or eIF4E1), the eIF4E homologous protein (4EHP or eIF4E2), and eIF4E3 [4]. These proteins contain aromatic residues, such as tryptophan or tyrosine, in their cap binding pocket which interacts with the m⁷GTP structure through pi stacking [5,6] (Exemplified by 4EHP in Fig. 1.1). In the case of eIF4E, translation initiation is achieved through recruitment of a DEAD box RNA helicase eIF4A and a molecular scaffold eIF4G, which also interacts with the 3' tail poly A binding protein (PABP) to circularize the mRNA [7–9]. The eIF4E, eIF4G, and eIF4A factors together constitute the eIF4F complex and are necessary to recruit the 43S preinitiation complex to capped mRNA [10]. Unlike eIF4E, 4EHP binds the 5' cap to repress translation initiation under most conditions [4,11–14]. The following sections are dedicated to detailing the multifarious methods of translation regulation by 4EHP and the various contexts under which its unique function is achieved.

A



Human 4EHP



B

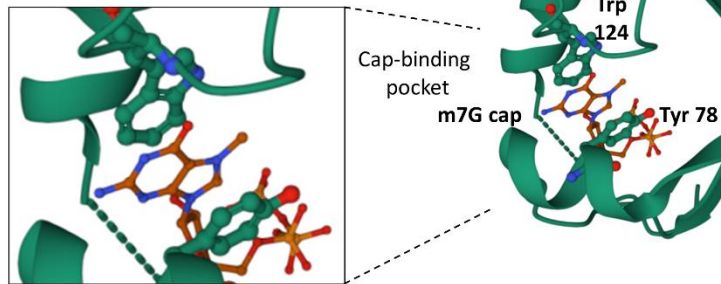


Figure 1.1. Mechanism of interaction between 4EHP and the m7GTP cap structure.

A Structure of the mRNA 5' cap linked to the first nucleoside of the mRNA via an inverted 5'-to-5' triphosphate bridge. At position N7 the 5' guanosine is methylated. The base N can be any nucleotide. Image is modified from [15]. **B** Crystal structure of 4EHP interaction with m7GTP between Trp124 and Tyr 78. 4EHP crystal structure is from PDB [16].

1.1.1. 4EHP inhibits translation initiation

The first cloning and characterization of 4EHP identified it as a specific 5' cap binding protein with an amino acid sequence 30% identical and 60% similar to eIF4E [12]. However, 4EHP was found to be 5-10 times less abundant than eIF4E [12] and bind the cap up to 200-fold more weakly than eIF4E [16,17]. Despite binding to the 5' cap, 4EHP does not form a complex with eIF4G and therefore fails to initiate translation under most conditions [4,18,19]. These findings have raised a paradox as to how 4EHP can out-compete eIF4E for cap-binding and successfully repress translation of its target mRNAs. The most plausible explanation is that 4EHP function requires multiple factors and complex formation depending on the cellular context. Through these interactions, the affinity of 4EHP for the cap may be enhanced. The function of 4EHP and the proteins that regulate its function are also highly context specific which will be discussed in detail in the following sections.

1.1.1.1. Non-canonical initiation

Most cellular stresses reduce global translation to both conserve energy and prevent the production of unwanted proteins [20], yet selective translation of a subset of mRNAs is required for cell survival under stress [21,22]. This poses a fundamental issue in biology as to how cells maintain proteostasis during conditions of stress. One possible means is through the integration of a non-canonical translation initiation machinery. This was observed to be the case during hypoxic stress where 4EHP directly interacts with hypoxia-inducible factor (HIF)-2 α , RNA Binding Motif Protein 4 (RBM4), eIF4A, and eIF4G3 to form a non-canonical initiation complex and allow active translation thereby overcoming hypoxia-induced repression of protein synthesis [23,24].

The enhanced association of 4EHP with actively translating polysomes occurred concurrently while eIF4E-polysome association was reduced. This mechanism was shown to be important for tumor cell growth during hypoxia as deletion of 4EHP in cancer cells rendered them indistinguishable from control cells under normal oxygen conditions, yet they failed to survive and proliferate in hypoxic conditions [25]. The authors argued that this mechanism represents a global remodeling of translation efficiencies, rather than changes in transcript abundance, to regulate protein output during oxygen deprivation [24]. However, later studies discovered that HIF-1 α up-regulates expression of eIF4E, but not 4EHP, by utilizing hypoxia response elements in the eIF4E proximal promoter region to promote cap-dependent translation of hypoxia-responsive mRNAs [26]. More research is required to fully understand how non-canonical cap-dependent translation initiation mechanisms operate during hypoxia.

1.1.2. miRNA-mediated silencing

The most recent lines of evidence suggests that 4EHP represses mRNA translation via a microRNA (miRNA)-mediated silencing mechanism [18,27–29]. miRNAs constitute a class of short (~22 nucleotide) non-coding RNAs which target mRNAs to regulate their stability and translation [30]. The miRNA-induced silencing complex (miRISC), which consists of Argonaute (AGO) and GW182/TNRC6 proteins, is critical for miRNA target recognition and gene silencing. Upon target recognition, a series of events are initiated including translational repression, deadenylation, and mRNA decay [31]. Deadenylation is orchestrated by the cap-dependent deadenylation complex (CCR4-NOT) on TATA-less (CCR4-NOT) deadenylase multi-subunit complex, maintained by the CNOT1 scaffolding protein [32]. Importantly, CCR4-NOT interacts with the 5' cap indirectly via a chain of

interactions including the RNA helicase DDX6 [33], which then binds 4E-T (eIF4E transporter) [34,35], which then binds 4EHP [36,37]. Together this network of interactions is fundamental for miRISC repression of translation initiation [13].

1.1.2.1. 4EHP and 4E-T

4E-T is a conserved eIF4E-binding protein, which was first shown to shuttle eIF4E into the nuclear compartment [36]. 4E-T directly binds to the dorsal surface of eIF4E through its canonical eIF4E-binding motif, impairs the eIF4E/eIF4G interaction, and inhibits translation initiation. 4EHP interacts with 4E-T [36,37] to facilitate miRNA-mediated silencing via the CCR4-NOT and miRISC complexes [18]. The affinity of 4EHP for the 5' cap structure is fourfold greater in the presence of the N terminus of 4E-T [18]. This finding provides evidence that other important 4EHP-binding factors can increase its affinity for the cap which is necessary to out-compete eIF4E. Further work is required to fully understand the specific context and conditions where this would occur.

1.1.3. 4EHP and GIGYF2

GIGYF2 [GRB10 (growth factor receptor bound-10)-interacting GYF (Glycine-Tyrosine-Phenylalanine) protein 2] was first identified to bind the insulin receptor and insulin-like growth-factor receptor adaptor protein GRB10 in a yeast two-hybrid screen [38]. The *GIGYF2* gene maps to human chromosome 2q37 within a region linked to familial Parkinson's disease (PARK11 locus) and was thought to be genetically linked to Parkinson's disease as mutations in this gene were observed in patients [39,40,49,41–48]. Moreover, aged mice (12-15 months) lacking one copy of *Gigyf2* show motor impairments, histopathological evidence of neurodegeneration, and rare

intracytoplasmic Lewy body-like inclusions in spinal anterior horn motor neurons [50]. However, recent studies in different populations have been unable to replicate the association in Parkinson's disease patients [51,52,61–67,53–60]. Mounting evidence, detailed in the following sections, suggests the main role of GIGYF2 is in translational regulation. It was first identified to bind 4EHP through far-Western analysis, co-immunoprecipitation assay, and mass spectrometry (MS) analysis [14]. This interaction was observed to be critical for the stable expression of both proteins, as deletion of one resulted in loss of the other. GIGYF2 binds 4EHP through a conserved N-terminal binding motif (YXYXXXXLΦ, where Φ is a hydrophobic amino acid), but more recent work demonstrated that GIGYF2 also uses auxiliary sequences to bind the dorsal and lateral surfaces of 4EHP [68]. Specific deletion of either 4EHP or GIGYF2 in HeLa cells results in a roughly 30% increase in [³⁵S]-methionine incorporation which suggests that these proteins regulate either a relatively large number of mRNAs or a small proportion of mRNAs that represent a significant part of the total translation profile [14]. Since these findings, the physiological role of 4EHP and GIGYF2 in various contexts has been further characterized and this regulatory axis has been implicated in disease states.

1.1.3.1. Role in development

The first line of evidence implicating an important role for 4EHP in development was in *Drosophila* embryos, where 4EHP was shown to bind with Bicoid (Bcd) in the anterior segments to suppress translation of the uniformly distributed caudal (*cad*) mRNA [11]. This is necessary to create a differential distribution of Cad protein expression to allow asymmetric development. Abrogation of the 4EHP-Bcd interaction resulted in reduced numbers of hatching embryos. In *C.*

elegans, 4EHP interacts with the GIGYF1/2 ortholog, GYF-1, which utilizes specific miRNAs to mediate translational repression necessary for development [27]. Similarly, in full-body 4EHP knockout mice, only 1/3rd of the expected number of mice are born relative to wildtype and die shortly after birth [14]. This finding is consistent with observations that GIGYF2 null mice, which undergo seemingly normal embryonic development, die within the first 2 postnatal days from failure to feed [50]. One possible explanation for the perinatal lethality of 4EHP and GIGYF2 is that among the mRNAs they translationally regulate, some belong to factors in cell signalling pathways necessary for growth and development.

1.1.3.2. *Regulation of ERK signalling and implications*

Previous work from the Sonenberg lab assessed mRNAs which are translationally regulated by 4EHP. Ribosome profiling is a technique that utilizes RNase digestion of polysomes that are carrying out translation and deep sequencing of these ribosome-protected mRNA fragments to derive information about mRNA translation efficiency and identify the regions of the transcriptome that are actually translated [69]. Using this approach, a subset of mRNAs that are translationally controlled by 4EHP were identified [28]. Among the targets, Dual Specificity Phosphatase 6 (*Dusp6*) mRNA, which encodes an ERK1/2 phosphatase, was translationally repressed by 4EHP via miR-145. Deletion of 4EHP in mouse embryonic fibroblasts (MEFs) resulted in increased protein expression of DUSP6 and a concomitant reduction in ERK1/2 phosphorylation. As a result, cell growth was impaired, and markers of apoptosis accumulated, consistent with the known role of the ERK signalling pathway [70,71]. In addition, HEK293T cells

transfected with siRNA against GIGYF2 showed a 75% reduction in levels of p-ERK1/2 [72] further implicating 4EHP/GIGYF2 translational control in ERK signalling.

1.1.3.3. *Protection of host during viral infection*

A role for 4EHP and GIGYF2 in immune regulation was first implicated in the identification of the zinc finger protein tristetraprolin (TTP) as a co-factor in the 4EHP-GIGYF2 complex [73,74]. TTP is a ribosome binding protein (RBP) that regulates cytokine expression during immune responses via translational repression of 3' UTR AU-rich element (ARE)-containing cytokine mRNAs [75–77]. This function is carried out in part through interaction with the CCR4-NOT deadenylase complex [78–81] and DDX6 [82]. Most recently, 4EHP was shown to regulate the innate immune response via miRNA-dependent translation silencing [83]. Mechanistically, 4EHP suppresses type-I interferon (IFN- β) production during viral infection via miR-34a-induced translational repression of *Ifnb1* mRNA [83]. This mechanism is likely physiologically adaptive to prevent exacerbated immune responses and inflammation which have potentially harmful auto-immune effects [84]. However, this function positions 4EHP as an ideal target for viruses to evade innate immunity. This is exemplified in the case of the novel SARS-CoV-2 coronavirus responsible for the 2019 global pandemic [85]. In a study that identified human proteins that physically associate with each of the SARS-CoV-2 proteins using affinity-purification mass spectrometry, 4EHP and GIGYF2 were found to associate with the vesicle trafficking protein NSP2 (non structural protein 2) of the SARS-CoV-2 virus [86,87]. The viral non-structural proteins are necessary for various functions including double-membrane vesicle formation, RNA replication, and replication proofreading [88]. Mutations of NSP2 residues (G262V/G265V) which are implicated in modulating ribosome-

associated quality control, disrupts interaction with 4EHP-GIGYF2 [89]. These finding not only support a role of 4EHP-GIGYF2 in immune regulation, but also suggest an involvement in the ribosome-associated quality control pathway.

1.1.3.4. Ribosome collisions and quality control

Ribosome stalling can occur on defective or damaged mRNAs such as those lacking stop codons, containing premature stop codons, or non-optimal codons [90–92]. If not properly resolved, ribosome stalling can be problematic for cells as protein synthesis output is reduced [93] and truncated peptides may form toxic aggregates [94]. Cells have therefore evolved a method to prevent continued translation of defective mRNAs called the ribosome-associated quality control (RQC) pathway [95]. This pathway is further linked to downstream mRNA decay mechanisms such as nonsense mRNA decay (NMD), which degrades mRNA with premature stop codons, nonstop mRNA decay (NSD), which targets mRNAs that lack stop codons, and no-go decay (NGD), which targets mRNA that present obstacles to elongation [96]. In a genome-wide CRISPR-Cas9-based screen to characterize the RQC pathway in mammals, Hickey and colleagues discovered that 4EHP, GIGYF2, and ZNF598 (an E3 ubiquitin ligase) were among the top proteins important for preventing translation of mRNAs with stalled ribosomes [97]. Here, ZNF598 detects collided ribosomes [98], recruits 4EHP and GIGYF2 to inhibit translation of the defective mRNA which prevents further ribosome recruitment. As a ubiquitin ligase, ZNF598 mono-ubiquitinates truncated polypeptides for their degradation [99] and ribosomal subunits on premature polyadenylated mRNAs to trigger RQC [100,101]. The authors also observed that 4EHP and GIGYF2 can repress translation independently of ZNF598, suggesting additional adapters are

redundant with ZNF598 or activated as a compensatory mechanism to ZNF598. Indeed, endothelial differentiation related factor 1 (EDF1) was identified using quantitative proteomics as a ZNF598-independent sensor of ribosome collisions capable of stabilizing GIGYF2 at collisions to inhibit translation initiation via 4EHP [102,103]. 4EHP and GIGYF2 were further shown to mediate translational repression of NMD-target mRNAs with premature termination codons [104] or those with prominent ribosome pausing [105]. In the brain, NMD is critical for proper neuron development and synaptic plasticity [106–108]. Human mutations in NMD factor genes are associated with neurodevelopmental disorders, including schizophrenia [109], intellectual disability [110], and autism spectrum disorder (ASD) [108,111]. These observations suggest 4EHP and GIGYF2 may contribute to the pathophysiology of neurological disorders such as ASD, which is discussed in detail in the following section.

1.1.3.5. *Link to autism spectrum disorder*

Translational dysregulation constitutes a strong risk factor for neuropathological conditions, such as ASD [112]. Of particular relevance to this thesis are the numerous mutations that have been reported in *GIGYF2* in patients with ASD [113–119]. Among these mutations are large truncations (nonsense), splice donor, missense, large exon deletion, and loss of stop codon mutations. Given the nature and frequency of these mutations, Simons Foundation Autism Research Initiative (SFARI) Gene predicts them to be deleterious, placing *GIGYF2* as a category 1 (high confidence) risk-factor for ASD. SFARI Gene defines a category 1 ASD-linked gene using the following criteria: “Genes in this category are all found on the SPARK [Simons Foundation Powering Autism Research] gene list, or on the list of genes reported by Satterstrom et al. 2020 [120]. Each of these

genes has been clearly implicated in ASD—typically by the presence of at least three de novo likely-gene-disrupting mutations being reported in the literature—and such mutations identified in the sequencing of the SPARK cohort are typically returned to the participants. Some of these gene meet the most rigorous threshold of genome-wide significance; all at least meet a threshold false discovery rate of < 0.1 ". Given this strong genetic link between *GIGYF2* and ASD in conjunction with the well-known role of GIGYF2 as a critical binding partner of 4EHP, the Sonenberg lab investigated the hypothesis that *GIGYF2* mutations cause ASD by disrupting 4EHP function. Consistent with this link, deletion of 4EHP in excitatory neurons destabilized GIGYF2 expression and resulted in ASD-like social behavior deficits and synaptic plasticity impairments [121]. The results of this study constitute Chapter 2 of this thesis.

1.1.4. Concluding remarks

Proper regulation of translation is critical for organismal development and physiology; the dysregulation of which has been implicated in various disease contexts. Since its initial discovery, 4EHP has proven to have an important role in modulating the translation of specific mRNAs and is a critical player in cellular mechanisms preventing the accumulation of aberrantly expressed polypeptides in cells. Future studies in the field should address how 4EHP effectively competes with eIF4E for cap-binding, given its relatively weak affinity for the cap, to perform its function and under what circumstances the various complexes associated with 4EHP are utilized. Addressing these questions will be invaluable for further elucidating the complexity of mRNA translation control and may provide a foundation for novel drug discovery in the treatment of diseases of dysregulated translation.

1.2. Neurological Disorders and mRNA Translation

Gathering genetic information from patients using techniques such as genome-wide linkage analysis (GWLA), genome-wide association studies (GWAS), and whole genome sequencing (WGS) is becoming cheaper and more accessible. As a result, hundreds of genes and genetic loci have been linked to various neurological disorders thereby helping to uncover their etiology. These studies, in addition to the known monogenic causes of some neurological disorders, have revealed interesting patterns in the types of genes often mutated. Among these, the genes encoding for proteins involved in regulating mRNA translation are afflicted by disruptive mutations [122]. These include the regulators of the mTOR pathway (e.g. PTEN and TSC1/2) and cap-dependent mRNA translation (e.g. eIF4E, FMRP, and CYFIP1). Overactivation of the integrated stress response pathway (i.e. eIF2) has also been observed in numerous neurological disorders. Using transgenic animal models, exciting progress has been made towards understanding how these proteins function to govern brain function and how their dysregulation underlies brain disorders.

1.2.1. The mTOR pathway: mTORC1 and mTORC2

The mechanistic target of rapamycin (mTOR) is a protein serine/threonine kinase present in two distinct functional complexes. mTOR complex 1 (mTORC1), contains as the indicative subunit the regulatory associated protein of mTOR (Raptor) and is sensitive to inhibition by rapamycin [123]. mTOR complex 2 (mTORC2) instead contains as a subunit the rapamycin-insensitive companion of mTOR (Rictor). In the brain, mTORC1 integrates synaptic signals through a variety of postsynaptic receptors such as the NMDA receptors (glutamate) and TrkB receptors (BDNF and

NGFs). Downstream of these receptors, phosphatidylinositol 3-kinase (PI3K) and the tuberous sclerosis complex (TSC) proteins TSC1 and TSC2 activate the Ras homolog enriched in brain (Rheb), which in turn stimulates mTORC1 [123]. The negative regulator phosphatase and tensin homolog (PTEN) directly counteracts PI3K activity, thereby attenuating mTORC1 function (Fig. 1.2). There are many direct downstream targets of mTORC1, of which the best studied are ribosomal protein S6 kinases (S6Ks) and the eukaryotic initiation factor 4E (eIF4E)-binding proteins (4E-BPs). Activation of mTORC1 results in phosphorylation of the S6Ks and 4E-BPs (see below, and legend to Fig. 1.2 for details) to promote mRNA translation.

Conditions associated with abnormal mTORC1 function, aptly named ‘mTORopathies’, define a large class of neurodevelopmental disorders. The function of mTORC1 in neurodevelopmental disorders like autism spectrum disorder (ASD) has been extensively reviewed [124–126]. Individuals with ASD harbor mutations in the upstream mTORC1 regulating proteins *TSC1*, *TSC2* and *PTEN*. Mice lacking the genes *Tsc1*, *Tsc2*, or *Pten* either full-body or in specific cell types exhibit abnormally high mTORC1 activity and recapitulate ASD-related behavioral deficits observed in patients. Treatment of these mice with rapamycin rescued the observed impairments [127–129]. However, chronic treatment of rapamycin also inhibits mTORC2 along with mTORC1 [130]. Building on this, Chen and colleagues discovered that mice lacking *Pten* exclusively in excitatory neurons displayed autism-like behaviors that were not rescued by co-deletion with mTORC1 but only with co-deletion of mTORC2 [131]. Further, chronic rapamycin treatment of mice that lack both *Pten* and mTORC1 in excitatory neurons rescued the observed impairments, indicating an mTORC1-independent role for rapamycin-mediated treatment of

PTEN-related mTORopathies. However, it is not clear what role mTORC2 plays in ASD that is not *PTEN* mutation associated, given that deletion of *Pten* in mice is itself known to increase mTORC2 activity [123]. The inhibitory neuron-specific role of mTORC1 and mTORC2 also remains to be evaluated to fully understand the individual contributions of the two mTOR complexes in ASD-related behaviors.

Over the last decade, a new role for mTORC1 has emerged in neuropsychiatric disorders, adding major depressive disorder (MDD) to a growing list of mTORopathies. Exposure of mice to chronic stress results in the reduction of mTORC1 signaling [132], which is consistent with findings that the antidepressant effect of ketamine, an anesthetic, in mouse models of MDD is mediated through mTORC1 activation [132–134]. Most recently, Kato and colleagues used the new drug NV-5138, which is the first brain-selective mTORC1 activator [135], in a mouse model of MDD [136]. Treatment with NV-5138 using a single dose was sufficient to reverse depressive-like behaviors in the mouse model, similar to ketamine. Importantly, infusion of rapamycin prior to NV-5138 treatment rendered the depressive-like behavior in the mice non-reversible, indicating that mTORC1 activation is required for the antidepressant effects of NV-5138 [136].

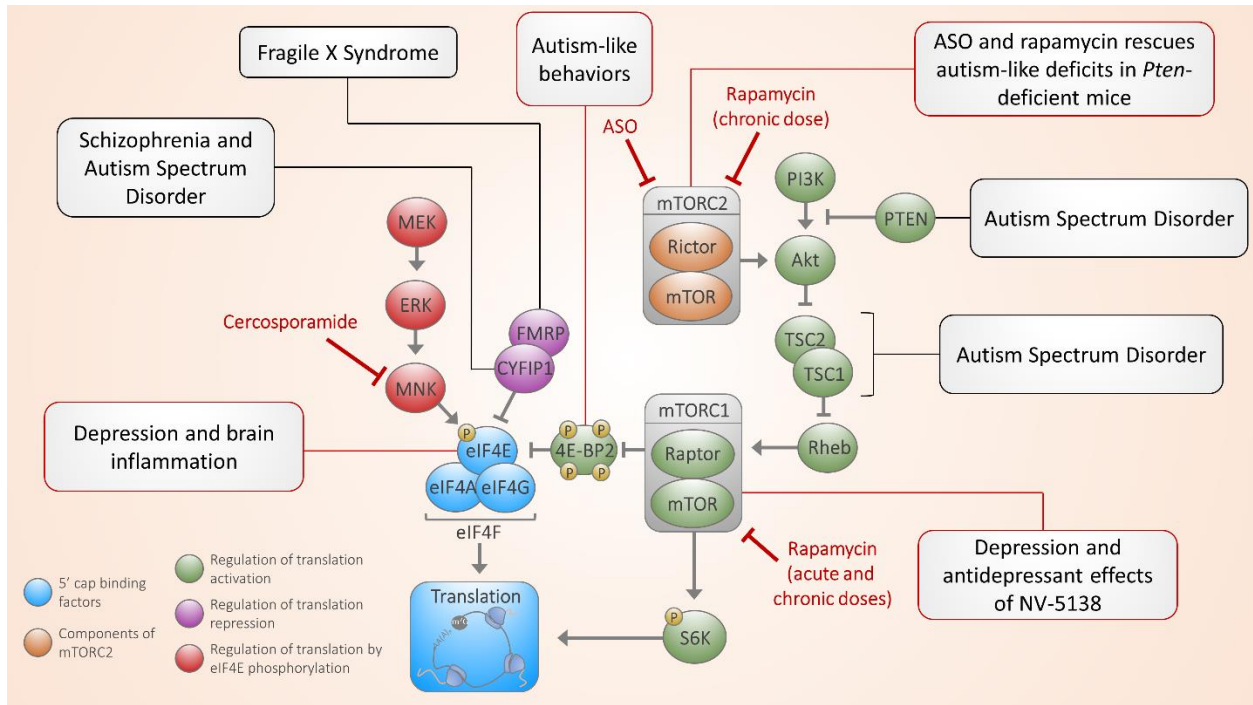


Figure 1.2. Neurological disorders linked to regulation of cap-dependent translation initiation.

Initiation of translation requires binding of the eukaryotic initiation factor (eIF) 4F (eIF4F) complex to the 5' end of the mRNA. eIF4F is composed of eIF4E, the 5' cap-binding protein, eIF4G, a scaffolding protein, and eIF4A, an RNA helicase. eIF4E is a downstream effector of MAPK-interacting serine/threonine-protein kinases (MNKs), mechanistic target of rapamycin complex 1 (mTORC1), and the fragile X mental retardation protein (FMRP)-cytoplasmic FMR1 interacting protein 1 (CYFIP1) complex. MNKs can phosphorylate eIF4E at Ser 209 to regulate the translation of a subset of mRNAs. Phosphorylation and therefore activity of the eIF4E-binding protein 2 (4E-BP2) is regulated by mTORC1 (inhibited by rapamycin) in response to various complex upstream signaling pathways. FMRP/CYFIP1 regulate translation by forming the FMRP-eIF4E-CYFIP1 complex at the 5' end of the mRNA, repressing translation. Abbreviations: Mitogen-activated protein kinase kinase (MEK); extracellular signal-regulated kinases (ERK), regulatory-associated protein of mTOR (Raptor), mechanistic target of rapamycin (mTOR), ribosomal protein S6 kinase (S6K), phosphoinositide 3-kinase (P13K), phosphatase and tensin homolog (PTEN), mechanistic target of rapamycin complex 2 (mTORC2), protein kinase B (Akt), tuberous sclerosis 1 (TSC1), tuberous sclerosis 2 (TSC2), ras homolog enriched in brain (Rheb). Neurological disorders associated with factors that control of cap-dependent translation initiation from recent patient and animal model studies (in black bordered boxes) or from animal studies only (in red bordered boxes) are presented.

1.2.2. Cap-dependent mRNA translation: eIF4E and 4E-BP2

Most eukaryotic mRNAs require binding of eIF4E to the 5' cap to initiate translation. Together with an RNA helicase, eIF4A, and a scaffolding protein, eIF4G, these proteins form the eIF4F complex, which facilitates the attachment of the 43S preinitiation complex to the mRNA [137]. Being the least abundant initiation factor, eIF4E activity is rate-limiting for translation initiation and constitutes a key translational regulatory mechanism (Fig. 1.2). For example, eIF4E activity is regulated via phosphorylation on serine (Ser) 209 by upstream MAPK-interacting serine/threonine-protein kinases (MNKs) [138,139]. This mechanism is important for controlling the translation of a subset of mRNAs and impacts oncogenesis [140]. Little was known about how eIF4E phosphorylation regulates brain function until two studies demonstrated that mice containing an eIF4E with a Ser 209 mutation to alanine (Ala), thereby preventing eIF4E phosphorylation, exhibit depressive-like behavior and exaggerated brain inflammatory responses via increased production of tumor necrosis factor α (TNF α) [141,142]. Treating eIF4E mutant mice with a dominant negative TNF α rescued depression-like behaviors and restored serotonin responsiveness in the dorsal raphe nucleus [141]. Importantly, these phenotypes were consistent with deletion of the MNKs or by pharmacologically inhibiting the phosphorylation [141]. Taken together, these data suggest that deregulation of p-eIF4E is a potential underlying pathology mediating brain inflammation and depression.

Another mechanism regulating eIF4E activity is through competitive binding of the 4E-BPs for a conserved sequence shared by the 4E-BPs and eIF4G, thereby inhibiting translation initiation [143] (Fig. 1.2). Several studies have implicated eIF4E overactivity through enhanced expression of

eIF4E [144] or by deletion of 4E-BP2 [145,146], the predominant 4E-BP isoform in the brain, in the development of autistic-like features, including behavioral deficits reminiscent of ASD. Interestingly, deletion of 4E-BP2 only in GABAergic interneurons was sufficient to elicit many of the core behavioral deficits observed in full-body knockout (KO) mice [147]. This finding suggests that translational control via 4E-BP2 in selective cell types might be more critical than others in regulating complex behaviors. Consistent with this notion, other studies have documented an important role for mTOR signaling in somatostatin neurons, which constitute a subset of GABAergic neurons, in synaptic plasticity and memory [148]. In the case of fragile X mental retardation protein (FMRP) translational regulator 1 (*Fmr1*) KO mice, chemogenetic stimulation of parvalbumin-specific GABAergic interneurons using designer receptors exclusively activated by designer drugs (DREADDs) reversed behavioral impairments [149]. These findings prompt the utilization of cell-type-specific protein analysis techniques to further elucidate the role of translational control in brain function and behavior.

1.2.3. Cap-dependent mRNA translation: FMRP and CYFIP1

FXS is the leading monogenic cause of ASD, which is engendered by >200 CGG trinucleotide repeats in the promoter region of the *FMR1* gene, leading to hypermethylation and gene silencing [150]. *FMR1* encodes the RNA binding protein FMRP, which functions in part to inhibit eIF4E and translation initiation [151] (Fig. 1.2). Using the FXS mouse model (*Fmr1* KO mice), progress has been made in identifying differentially translated genes with techniques such as ribosome footprinting [152], translating ribosome affinity purification (TRAP) [153], and biorthogonal non-canonical amino-acid tagging (BONCAT) [154]. Using cell-type-specific TRAP

and RNA-Seq, Thomson and colleagues demonstrated that deletion of FMRP in CA1 pyramidal neurons of the hippocampus resulted in differential translation of 121 mRNAs with the muscarinic acetylcholine receptor 4 (M₄) being significantly overexpressed [153]. Interestingly, positive allosteric modulation of M₄, rather than inhibition, normalized excessive protein synthesis and the exaggerated metabotropic glutamate receptor-mediated long-term depression (mGluR-LTD), and reduced the incidence of audiogenic seizures in *Fmr1* KO mice. This finding revealed that aberrant translation of some genes may be a protective adaptation, rather than a cause of the pathophysiology. Taking a different approach, the Darnell lab used conditional tagging of FMRP and UV cross-linking immunoprecipitation (FMRP cTag CLIP) to examine FMRP-associated mRNA targets in CA1 pyramidal neurons [155]. This technique utilizes the Cre-lox system to knock-in epitope tags on the RNA binding protein of interest for CLIP purification of protein-RNA complexes. The authors observed enriched binding of FMRP to autism candidate mRNAs as classified in the SFARI Gene database [155]. Interestingly, the CA1 hippocampal targets were not observed in cerebellar granule neurons suggesting that FMRP differentially regulates translation in specific cell types which may contribute to particular phenotypes associated with FXS [155]. Together these studies highlight the importance of investigating the cell-type-specific contribution of translation control mechanisms towards brain function, the results of which may inform more precise therapeutic interventions.

While much work has elucidated the cellular and molecular function of FMRP, current studies focus on drug discovery and the identification of novel FMRP targets, such as M₄ [153] and β -arrestin 2 [156]. The repurposing of FDA-approved drugs such as lovastatin [157,158] and

metformin [159] have proven to be effective at reversing the behavioral, electrophysiological and biochemical impairments in the FXS mouse model. Both lovastatin and metformin correct these deficits by normalizing exaggerated protein synthesis and extracellular signal-regulated kinase (ERK) 1/2 activity. Similarly, pharmacological inhibition of the PI3K catalytic isoform p110 β ameliorated FXS-associated phenotypes in FMRP-deficient mice [160]. Taken together these findings suggest that drugs which rectify aberrations in the cell signaling pathways upstream of FMRP may be a potential therapeutic option for treating FXS patients. These drugs are currently being tested in clinical trials (Lovastatin: NCT02680379, NCT02998151, NCT02642653 and Metformin: NCT03722290, NCT04141163, NCT03862950, NCT03479476).

Unfortunately, some of the drugs that are effective in reversing phenotypes in the FXS mouse, such as mavoglurant and arbaclofen, failed to adequately improve FXS patients in clinical trials [161]. One possible explanation is that the age-point at which a drug is administered is critical in determining the effectiveness of the treatment. This was the case for the GABA_B receptor agonist, arbaclofen, which manifested therapeutic effects in children, but not in young adults [162]. Similarly, Asiminas and colleagues found that treating *Fmr1* KO rats with lovastatin during an early stage of development (between 5 and 9 weeks of age), restored associative memory deficits observed in spatial memory tasks [163]. Importantly, this rescue was sustained for several months after treatment further highlighting the necessity of therapeutic intervention during key developmental windows.

Translation repression by FMRP is achieved in part through physical interaction with cytoplasmic FMRP interacting protein 1 (CYFIP1) which directly binds to and sequesters eIF4E thereby inhibiting translation initiation [151]. CYFIP1 also interacts with the Rac1-Wave complex to regulate actin dynamics [164]. By shuttling between the FMRP-eIF4E and Rac1-Wave complexes, CYFIP1 activity links translation regulation with actin dynamics and dendritic spine morphology in a homeostatic balance [165], which is dysregulated in *Fmr1* KO mice. Since loss of FMRP also causes increased binding between eIF4E and eIF4G [166], Santini and colleagues hypothesized that blocking eIF4E-eIF4G interaction using the specific small molecule inhibitor, 4EGI-1, would increase the pool of available eIF4E to bind CYFIP1 [167]. Consistent with this hypothesis, the authors observed that loss of FMRP destabilizes the interaction between CYFIP1 and the 5' cap complex in the hippocampus. In addition, treatment of *Fmr1* KO mice with 4EGI-1 restored CYFIP1 interaction with the 5' cap, reversed hippocampal-dependent memory deficits, corrected aberrant spine morphology and restored exaggerated mGluR-LTD to control levels [167]. These results suggest that targeting eIF4F under conditions of dysregulated translation may be a potential therapeutic option for patients with neurological disorders.

In the human genome, *CYFIP1* resides in the 15q11.2 region for which copy number variants are associated with neurological/psychiatric disorders such as schizophrenia (SCZ) and ASD [168]. Polymorphisms and rare mutations in *CYFIP1* are also linked to SCZ [169] and ASD [170], further implicating disrupted CYFIP1 activity in neurological/psychiatric disorders. Since both microduplications and microdeletions in 15q11.2 are associated with these disorders, Davenport and colleagues sought to determine how CYFIP1 gene dosage affects neuronal function in rodents.

They observed that either up or downregulation of CYFIP1 in hippocampal neurons resulted in alterations in the ratio of excitatory to inhibitory (E/I) currents [171]. However, a comprehensive behavioral study of CYFIP1 overexpression in mice did not reveal any ASD-associated behavioral impairments [172]. Instead, the mice presented mild learning deficits and an exaggerated fear response, suggesting that the E/I deficits observed with increasing CYFIP1 gene dose may not contribute to ASD-associated behaviors, but towards cognitive ability. Similarly, heterozygous deletion of CYFIP1 in both mice [173] and rats [174] resulted in white matter thinning of the corpus callosal axons and the rats exhibited cognitive inflexibility. The mice, however, presented abnormalities in motor coordination, sensorimotor gating, and sensory perception which are consistent with the neuropsychiatric deficits observed in ASD and SCZ patients [173]. In summary, these findings suggest that CYFIP1 abundance is important for functional brain connectivity which may underlie the behavioral features in 15q11.2 patients, particularly for cognition.

1.2.4. Integrated stress response: eIF2

The integrated stress response (ISR) is a mechanism that evolved to halt the production of proteins in order to conserve energy during cellular stress. The ISR targets ternary complex (TC) availability in the cell. The TC is comprised of the initiator methionine-tRNA, GTP and the translation initiation factor eIF2, which contains 3 subunits (α , β , and γ) [175] (Fig. 1.3). The cellular availability of the TC is controlled by the phosphorylation status of eIF2 at Ser 51 in its alpha (α) subunit [175]. Under conditions of cell stress, eIF2 α is phosphorylated (p-eIF2 α) by one of four kinases (general control nonderepressible 2, GCN2; protein kinase RNA-activated, PKR; protein kinase RNA-like endoplasmic reticulum kinase, PERK; or heme-regulated inhibitor, HRI),

thereby inhibiting TC formation and arresting general translation, while paradoxically increasing translation of a subset of mRNAs containing 5' upstream open reading frames (uORFs) [176]. Dephosphorylation of eIF2 α is carried out by 2 protein complexes (PP1/CR ϵ P or PP1/GADD34), thus normalizing mRNA translation [176] (Fig. 1.3).

It is well established that genetic or pharmacological reduction of p-eIF2 α enhances memory formation and long-term potentiation (LTP), and impairs mGluR-LTD [177–182]. In contrast, elevation of p-eIF2 α impairs memory formation and LTP, but facilitates mGluR-LTD [178,181,183]. Importantly, eIF2 α hyperphosphorylation is observed in neurodegenerative diseases that manifest deficits of learning and memory, such as Alzheimer's disease (AD), Parkinson's disease, Huntington's disease, and frontotemporal dementia [184,185]. In a mouse model of AD, pharmacological inhibition of p-eIF2 α alleviated hippocampal-dependent memory deficits [186], highlighting the potential of targeting the ISR to treat neurodegenerative disorders.

More recently, Zhu and colleagues implicated the phosphorylation of eIF2 α in Down syndrome (DS) [187], a neurological condition caused by the presence of an extra copy of human chromosome 21 (ch 21) that results in hippocampal-dependent learning and memory deficits [188]. Here, the authors observed exaggerated levels of p-eIF2 α in brain tissue and induced pluripotent stem cells (iPSCs) from individuals with DS as well as reduced general translation in the iPSCs. The authors show that a mouse model of DS, that contains 3 copies of the mouse gene orthologue of ch 21 (Ts65Dn mice), recapitulates exaggerated hippocampal p-eIF2 α levels and decreased general translation. Consistent with DS, Ts65Dn mice displayed impaired

hippocampal-dependent memory and LTP. Genetic deletion of the eIF2 α kinase PKR in Ts65Dn mice normalized p-eIF2 α and general translation, reversing the memory and synaptic plasticity impairments [187]. Furthermore, Zhu et al reversed memory and synaptic impairments in Ts65Dn mice by (1) genetically replacing the eIF2 α Ser 51 residue with an Ala to reduce p-eIF2 α levels and (2) pharmacologically inhibiting the ISR [187]. Thus, these findings implicate the ISR as a potential target for the treatment of DS.

1.2.5. Concluding remarks

The control of protein synthesis is essential for proper brain functioning and its dysregulation is a frequent cause of neurological disorders. We highlighted recent progress made in understanding how translational control modifies brain function, from the genetic to the behavioral level. Considering the challenges of translating basic neuroscience into clinical practice, these studies are imperative to provide the foundation for the discovery of novel treatments for neurological disorders.

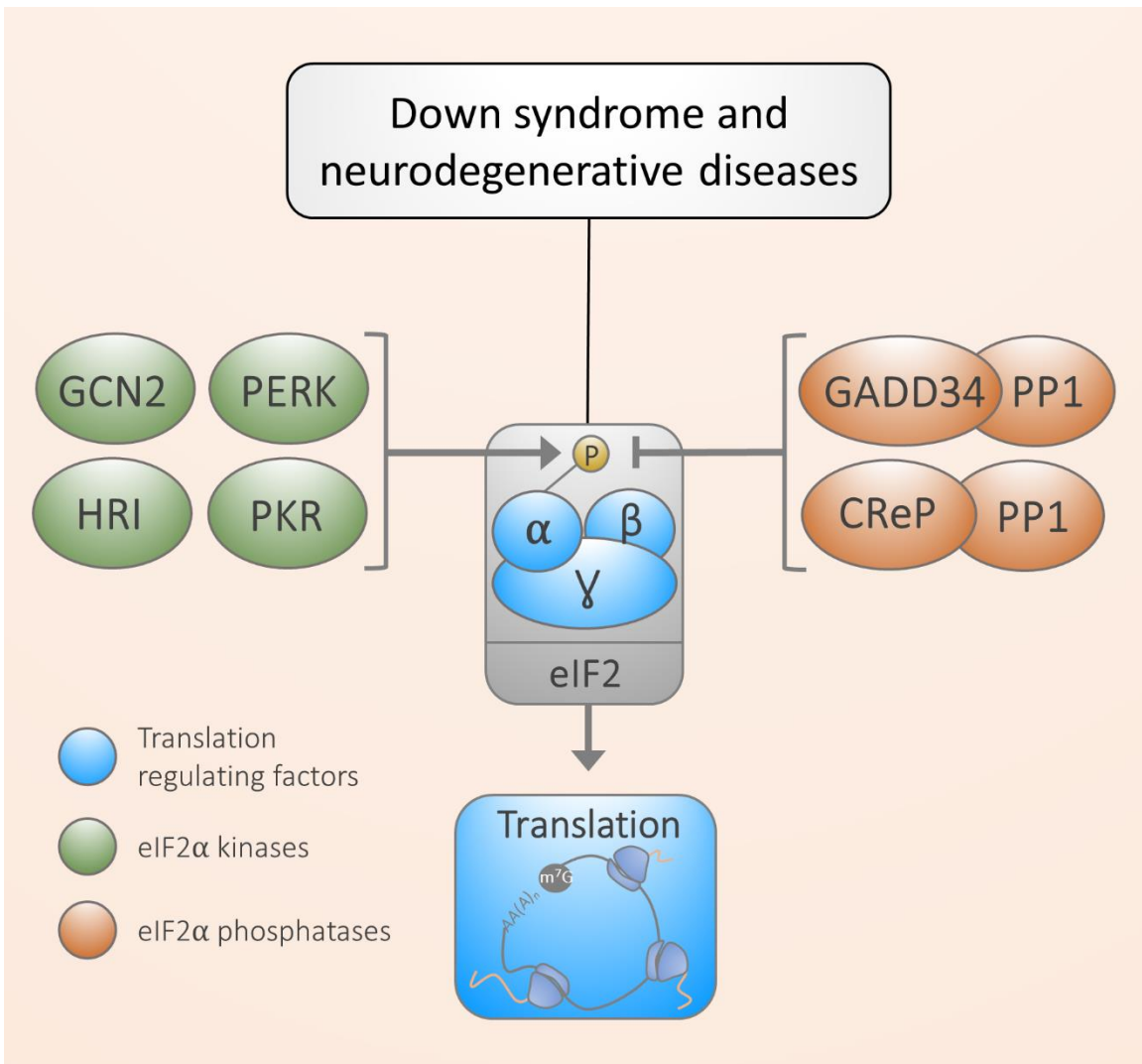


Figure 1.3. Integrated stress-response related neurological disorders.

Cellular stress results in activation of the integrated stress response (ISR) and phosphorylation of the eukaryotic initiation factor 2 (eIF2). eIF2 is composed of three subunits: α (eIF2 α), β (eIF2 β) and γ (eIF2 γ). Phosphorylation of eIF2 occurs on the Ser 51 residue of eIF2 α by one of four kinases: general control nonderepressible 2 (GCN2), PKR-like endoplasmic reticulum kinase (PERK), protein kinase RNA-activated (PKR) and heme-regulated inhibitor (HRI), each of which respond to different cell stressors (not shown). To attenuate levels of phosphorylated eIF2 α , protein phosphatase 1 (PP1) bound to regulatory subunits growth arrest and DNA damage-induced protein (GADD34) or constitutive revertor of eIF2 α phosphorylation (CReP) will remove the phosphate at Ser 51. Neurological disorders associated with eIF2 α function from recent patient and animal studies are highlighted in boxes with black borders.

1.3. Translational control in learning and memory

Learning and memory is the process of receiving stimuli and storing information for later recollection and use. Memory is broadly categorized as either short-term or long-term memory (STM or LTM) (Fig. 1.4), which lasts seconds to hours and days to decades, respectively. STM can be further categorized into working memory, which is the process of using a recently learned stimuli in executing a decision [189], or sensory memory which is used for briefly retaining sensory information from environmental stimuli through integration of the senses [190]. LTMs are further classified into explicit: memory about life events (episodic) or factual information (semantic), and implicit: priming or procedural (motor) memory [190]. At the molecular level, STMs depend on transient events (such as post-translational modifications) locally in the synapse and are insensitive to disruption by protein synthesis inhibitors. The formation of LTMs, however, requires translation for both immediate early gene expression and to maintain translation of newly transcribed memory-related mRNAs. Disruption of protein synthesis within the memory consolidation window results in retrograde amnesia [191]. Not surprisingly, regulators of cap-dependent translation are integral for LTM formation [192,193]. Much less is known about the role of de novo protein synthesis, if any, in STMs. The body of literature on memory is incredibly vast and multidisciplinary. Much of this work is beyond the scope of this literature review, except where necessary to provide the essential background information. The following sections will focus primarily on a few key examples of translational control mechanisms involved in learning and memory provided in the given context which are of relevance for the present thesis.

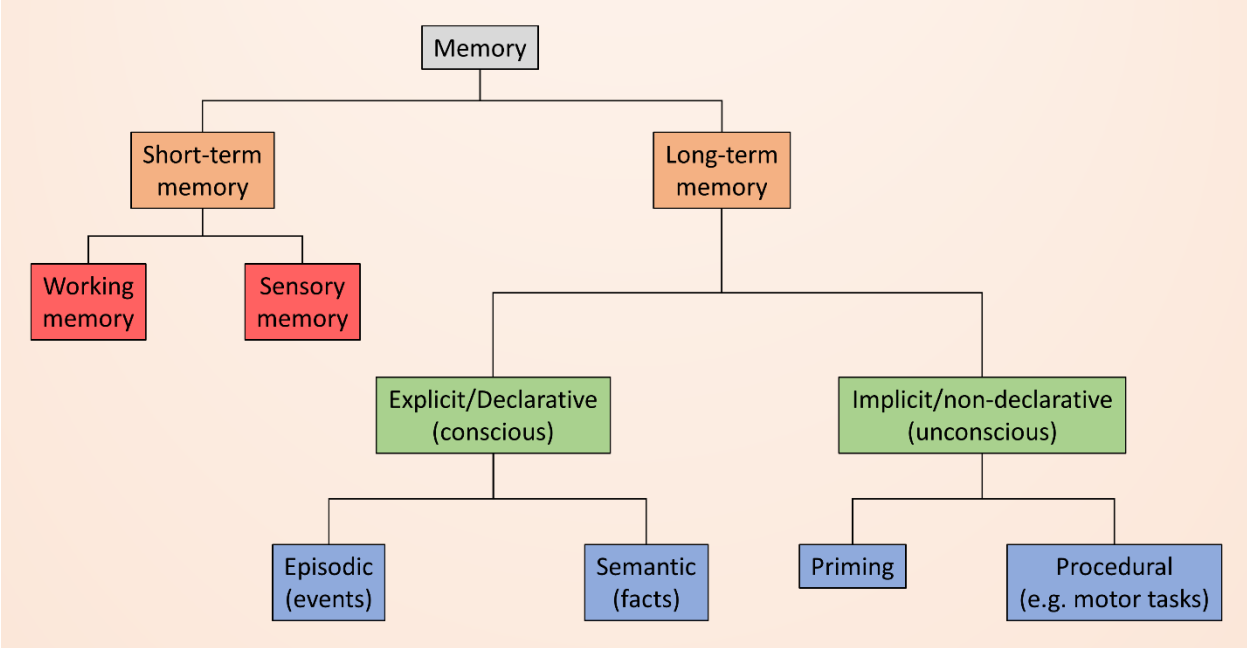


Figure 1.4. Memory classification in humans.

Memories are classified as either short- or long-term. Short-term memory duration is on the timescale of seconds to hours and can be further divided into either working or sensory memories. A working memory, by definition, utilizes information previously learned in decision-making [189]. A sensory memory requires the ability to retain an impression of a sensory stimuli [190]. Long-term memories are stored as either explicit (conscious) or implicit (unconscious) information. Explicit memories include information about events (episodic) or information as facts (semantic). Implicit memories are those gained from procedural learning, such as in motor skills, or from priming. Diagram is derived from information presented in Squire and Zola-Morgan 1991 [194].

1.3.1. Mechanisms of short-term memory

While the exact molecular mechanisms underlying STMs are not fully known, there is a plethora of evidence implicating an important role of a synaptic plasticity phenomenon known as long-term potentiation (LTP), specifically early (e) LTP, as the cellular mechanism underlying STMs. Decades of research has provided insight into the molecular events underlying eLTP [195]. To briefly highlight the basic mechanism, during postsynaptic depolarization upon induction of eLTP, extracellular Mg^{2+} ions are electrostatically dislodged from N-methyl-D-aspartate (NMDA) receptors allowing an influx of Ca^{2+} ions. As a secondary cell signalling molecule, Ca^{2+} initiates a cascade of events including, but not limited to, activation of α -calcium-calmodulin-dependent protein kinase II (CaMKII), which is found at high density in the postsynaptic compartment [196]. CaMKII supports both α -amino-3-hydroxy-5-methyl-4-isoxazolepropionic acid receptor (AMPA) and NMDAR basal synaptic transmission and LTP, but the mechanistic details by which this occurs are currently under debate [197]. These mechanisms are likely supporting diverse forms of STM such as working memory, although direct evidence is lacking.

1.3.1.1. Working memory

Working memory (WM) is defined as a short-term cognitive buffer of limited capacity that holds and manipulates information for the guidance of decision-making behavior [198]. WM is a core component of executive functions (i.e. cognitive control) which are important for many aspects of human life, including selective attention, self-control, creativity, reasoning, mental flexibility, and fluid intelligence [199]. In other animals such as rodents, WM is important for appropriate exploratory behavior and navigation of their environment [200]. Brain recording experiments in

primates during WM tasks have revealed an important role of prefrontal cortical neuron firing in WM [201]. More recent work using optogenetics has shown that medial prefrontal cortical units require ventral hippocampal inputs during encoding but not retrieval of a WM task [202]. Little is known about the cellular and molecular substrate of WM, particularly those involved in translation control. Given the short-term nature of WM (on the scale of seconds to hours, depending on the species [203]), it is not intuitive to suppose that de novo protein synthesis would be necessary for WM. Indeed injection of anisomycin in the medial prefrontal cortex of mice after the last training session of the delayed nonmatching-to-place (DNMTP) task did not affect working memory performance [204]. Long-term consolidation required for learning the DNMTP task over multiple days was, however, sensitive to protein synthesis inhibition by anisomycin [204]. Alternatively, there is evidence that repression of protein synthesis may in fact be a requirement for WM. This notion is supported by findings that WM is impaired in genetic mouse models lacking translation repressor proteins such as 4E-BP2 [205] and PERK [206]. However, these findings cannot implicate a direct mechanistic role for protein synthesis in working memory as the effects may be due to structural changes in the synaptic protein landscape or developmental abnormalities. The use of more advanced genetic models where protein expression can be transiently regulated will be required to reach a definitive conclusion. It is interesting, however, to speculate that one or multiple molecular mechanisms exist to discriminate which stimuli are encoded into long-term memory and which are retained for short-term purposes only.

1.3.2. Mechanisms of long-term memory

Memory consolidation is the process by which temporary and labile learned information is transformed to become more stable and long-lasting through time [207]. This transformation is thought to occur through two processes: synaptic consolidation, which occurs locally at the synapses and corresponds with a long-lasting form of plasticity called late (L)-LTP [208], and systems consolidation which involves large-scale transfer of information across brain regions [209]. The classic example for transfer of memory across brain regions is the case of patient H.M. who underwent hippocampal resection surgery to alleviate chronic seizures [210,211]. Although this surgery subdued the seizures, H.M. was left with anterograde amnesia, yet retrograde amnesia was limited to recent memories whereas old memories, such as those from childhood, were spared [210,211]. This discovery implicated a critical role for the hippocampus in memory consolidation and the ability to make new memories. The molecular mechanisms in the hippocampus mediating memory and L-LTP have been well-characterized and extensively reviewed [208,212–214]. Highlighted below are some important examples of the key players in L-LTP and LTM via translation control.

1.3.2.1. Phosphorylation of eIF2 α is a molecular memory switch

More than a decade ago, work from the Sonenberg lab defined the phosphorylation of eIF2 α as a critical event in determining whether a STM is switched to long-term [178]. Here, reduction of eIF2 α phosphorylation enhanced long-term memory formation in rodents which was later shown to also enhance auditory imprinting in birds [215]. In the opposite scenario, preventing eIF2 α dephosphorylation impaired long-term memory formation [178]. A few years prior to this discovery, there were already hints for a critical role of p-eIF2 α in memory regulation as mice

lacking the eIF2 α kinase GCN2 exhibit enhanced memory given a weak training stimulus and conversion of e-LTP to L-LTP [177]. Work from other investigators has greatly expanded these initial findings. Most notably, the Walter lab discovered a compound called ISRIB (integrated stress response inhibitor) which blocks the effects of p-eIF2 α and enhances memory formation in several models [182,216]. Most recently, the role of p-eIF2 α in memory was determined to be cell-type-specific as preventing its phosphorylation in either excitatory or somatostatin-expressing (but not parvalbumin-expressing) inhibitory neurons enhanced synaptic plasticity and long-term memory [217]. These findings have together uncovered a critical node for memory and have fueled investigation for targeting the ISR for the development of cognitive enhancers, particularly in the context of neurodegenerative diseases [218].

1.3.3. The role of miRNAs in synaptic plasticity and memory

miRNAs are expressed throughout the brain and play an important role in neurological processes such as presynaptic vesicle release, glutamatergic receptor activity, dendritic spine size, and LTP-related gene expression [219]. Being functional immediately after transcription and processing, miRNAs can rapidly regulate the translation of specific mRNAs, making them ideally suited to regulate synaptic plasticity and memory formation [220]. Evidence for miRNAs in the synapse comes from the observation that components of the miRNA processing machinery, such as the ribonuclease protein Drosha, microprocessor complex subunit protein DGCR8, and the endoribonuclease enzyme Dicer, are located in mouse hippocampal post-synaptic densities [221,222]. Furthermore, in a study analyzing miRNA representation in five different rat brain regions (cortex, hippocampus, cerebellum, brainstem, and olfactory bulb), purified synapto-

neurosomal miRNAs from all regions accounted for over 50% of all miRNAs tested compared to total fractions [223]. It is thought that translation of mRNAs in synapses are kept suppressed by miRNAs until they are needed [224]. For example, miR-26a and miR-384-5p generally suppress the expression of ribosomal S6 kinase 3, a translational regulator [225]. However, during L-LTP their expression is reduced, thereby increasing the levels of S6 kinase which in turn supports the maintenance of L-LTP [225]. These are a few examples which substantiate the important function of miRNAs as epigenetic regulators contributing to fundamental cellular and molecular mechanisms underlying learning and memory in the adult brain [220].

1.3.4. Concluding remarks

Despite the wealth of knowledge gained on the remarkable ability of the brain to learn and store information, there is still much that remains to be appreciated. The mechanisms governing translational control and de novo protein synthesis provide an unequivocal level of regulation for learning and memory, particularly in the process of long-term consolidation. New technologies are making it possible to dissect the spatial and temporal regulation of translation in memory more precisely. This can be achieved, for example, with techniques that allow cell-type-directed and doxycycline-controlled expression of shmiRs [226], and chemically inducible/reversible translation inhibitory proteins, such as PKR [227].

Chapter 2: The eIF4E homolog 4EHP (eIF4E2) regulates hippocampal long-term depression and impacts social behavior

2.1. Abstract

Background: The regulation of protein synthesis is a critical step in gene expression and its dysfunction is implicated in autism spectrum disorder (ASD). The eIF4E homologous protein (4EHP, also termed eIF4E2) binds to the mRNA 5' cap to repress translation. The stability of 4EHP is maintained through physical interaction with GRB10 interacting GYF protein 2 (GIGYF2). Gene-disruptive mutations in *GIGYF2* are linked to ASD, but causality is lacking. We hypothesized that *GIGYF2* mutations cause ASD by disrupting 4EHP function.

Methods: Since homozygous deletion of either gene is lethal, we generated a cell-type-specific knockout model where *Eif4e2* (the gene encoding 4EHP) is deleted in excitatory neurons of the forebrain (4EHP-eKO). In this model we investigated ASD-associated synaptic plasticity dysfunction, ASD-like behaviors, and global translational control. We also utilized mice lacking one copy of *Gigyf2*, *Eif4e2* or co-deletion of one copy of each gene to further investigate ASD-like behaviors.

Results: 4EHP is expressed in excitatory neurons and synaptosomes, and its amount increase during development. 4EHP-eKO mice display exaggerated mGluR-LTD, a phenotype frequently observed in mouse models of ASD. Consistent with synaptic plasticity dysfunction, the mice displayed social behavior impairments without being confounded by deficits in olfaction, anxiety, locomotion, or motor ability. Repetitive behaviors and vocal communication were not affected by loss of 4EHP in excitatory neurons. Heterozygous deletion of either *Gigyf2*, *Eif4e2*, or both genes in mice did not result in ASD-like behaviors (i.e. decreases in social behavior or increases

in marble burying). Interestingly, exaggerated mGluR-LTD and impaired social behaviors were not attributed to changes in hippocampal global protein synthesis, which suggests that 4EHP and GIGYF2 regulate the translation of specific mRNAs to mediate these effects.

Limitations: This study did not identify which genes are translationally regulated by 4EHP and GIGYF2. Identification of mistranslated genes in 4EHP-eKO mice might provide a mechanistic explanation for the observed impairment in social behavior and exaggerated LTD. Future experiments employing affinity purification of translating ribosomes and mRNA sequencing in 4EHP-eKO mice will address this relevant issue.

Conclusions: Together these results demonstrate an important role of 4EHP in regulating hippocampal plasticity and ASD-associated social behaviors, consistent with the link between mutations in *GIGYF2* and ASD.

Keywords: 4EHP, GIGYF2, long-term depression, social behavior, animal models

2.2. Background

Autism spectrum disorder (ASD) is a neurodevelopmental condition affecting 1-2% of the global population [228]. The fifth edition of the Diagnostic and Statistical Manual of Mental Disorders (DSM-5) defines ASD based on deficits in social interaction (including nonverbal social communication) and restrictive or repetitive patterns of behavior. Current medical practice relies primarily on behavioral assessment to diagnose ASD, and pharmaceutical treatment is often inadequate and does not target the underlying pathophysiology of the core deficits. This places precedence on the discovery of reliable biomarkers and more individualized medical interventions. In the case of idiopathic ASD, hundreds of gene mutations serve as potential biomarkers, but direct causal evidence is lacking. Understanding how these individual gene mutations contribute to ASD is paramount to the development of personalized medication.

The disruption of protein synthesis (mRNA translation or translation) in the brain by genetic perturbations of its regulators constitutes a known underlying etiology for ASD [124,229]. For most mRNAs, initiation of translation requires binding of initiation factors to their 5' end at a modified guanine nucleotide (m^7GpppN , where N is any nucleotide) termed the 5' cap [137]. The eukaryotic initiation factor (eIF) 4F complex is comprised of the cap binding protein eIF4E, an mRNA helicase eIF4A, and a molecular scaffold eIF4G. Together these proteins facilitate recruitment of the ribosomal 43S preinitiation complex to the mRNA. Overactivity of eIF4E in humans has been implicated in ASD [230,231] and ASD-like phenotypes in mice [144,145]. Indeed, disruption of the proteins regulating eIF4E activity, such as fragile X mental retardation protein (FMRP) [232], cytoplasmic FMR1 interacting protein 1 (CYFIP1) [170], and eIF4E-binding protein

2 (4E-BP2) [145–147], are implicated in ASD. It is therefore necessary to investigate the function of ASD-linked genes that encode for regulators of translation. Whole-genome sequencing of ASD patients has been invaluable in identifying these genes.

By inspecting these datasets, we identified 22 unique mutations in the gene encoding GRB10 interacting GYF protein 2 (GIGYF2) which have been associated with ASD [113–119] (Table 2.1). The nature of these mutations are gene disruptive, such as large deletions, premature termination, and loss of termination-codon mutations. Although its mechanism of action is not fully understood, GIGYF2 forms a complex with the eIF4E homologous protein (4EHP) which is required for the stable expression of both proteins (i.e. deletion of one results in reduced expression of the other) [14]. 4EHP, encoded by the gene *Eif4e2* in mice, binds to the mRNA 5' cap. Unlike eIF4E, 4EHP acts to repress translation [14] because it cannot recruit the scaffolding protein, eIF4G [4]. Instead, 4EHP requires interaction with GIGYF2 to repress translation of target mRNAs [68]. Therefore, loss of either GIGYF2 or 4EHP results in increased rates of protein synthesis [14,28]. We hypothesized that *GIGYF2* mutations disrupt the coordinated function of the 4EHP and GIGYF2 protein complex, resulting in impaired synaptic function and susceptibility to ASD. Here we investigated ASD-like phenotypes in various mutant mouse models for *Gigyf2* and *Eif4e2*. Our findings provide documentation of 4EHP expression in the brain and reveal an important role of 4EHP in excitatory neurons, namely in the regulation of synaptic plasticity and ASD-associated social behaviors. Together these findings are consistent with the genetic link between *GIGYF2* and ASD.

Table 2.1: Mutations in *GIGYF2* are linked to autism spectrum disorder

<i>GIGYF2</i> chromosome location	Genomic mutation	Amino acid change	Mutation type	Inheritance pattern	References
2:233612356	A to G	Thr25Ala	Missense	Maternal	Wang et al. 2016, <i>Nat Commun</i>
2:233612356	A to G	Thr25Ala	Missense	Paternal	Wang et al. 2016, <i>Nat Commun</i>
2:233612456	T to C	None	Splice donor	N.D	Wang et al. 2016, <i>Nat Commun</i>
2:233613755	C to T	Pro77Leu	Missense	Maternal	Wang et al. 2016, <i>Nat Commun</i>
2:233651280—233673273	Deletion	Unknown	Intron deletion	De novo	Gazzellone et al. 2014, <i>J Neurodev Disord</i>
2:233655527	A to G	Ile300Val	Missense	Maternal	Wang et al. 2016, <i>Nat Commun</i>
2:233655527	A to G	Ile300Val	Missense	Paternal	Wang et al. 2016, <i>Nat Commun</i>
2:233655615	T to G	Leu329Arg	Missense	Maternal	Wang et al. 2016, <i>Nat Commun</i>
2:233655745	G to T	Glu320Ter	Nonsense	De novo	Wang et al. 2016, <i>Nat Commun</i>
2:233656136	A to G	Lys442Arg	Missense	Maternal	Wang et al. 2016, <i>Nat Commun</i>
2:233656136	A to G	Lys442Arg	Missense	Paternal	Wang et al. 2016, <i>Nat Commun</i>
2:233659563	G to A	Arg484Gln	Missense	Paternal	Wang et al. 2016, <i>Nat Commun</i>
2:233671257	T to G	Ser587Ala	Missense	Maternal	Wang et al. 2016, <i>Nat Commun</i>
2:233671353	C to T	Pro619Ser	Missense	Maternal	Wang et al. 2016, <i>Nat Commun</i>
2:233675964	G to A	Ala658Thr	Missense	De novo	Wang et al. 2016, <i>Nat Commun</i>
2:233675982	C to T	Gln664Ter	Nonsense	De novo	Iossifov et al. 2014, <i>Nature</i> Lim et al. 2017, <i>Nat Neurosci</i> An et al. 2018, <i>Science</i>
2:233677147	G to A	Val706Ile	Missense	Paternal	Wang et al. 2016, <i>Nat Commun</i>
2:233684582	C to T	Arg827Ter	Nonsense	De novo	Lim et al. 2017, <i>Nat Neurosci</i>
2:233704609	G to C	Gln960His	Missense	Maternal	Wang et al. 2016, <i>Nat Commun</i>
2:233704659	G to A	Arg977Gln	Missense	De novo	De Rubeis et al. 2014, <i>Nature</i> Wang et al. 2016, <i>Nat Commun</i> Lim et al. 2017, <i>Nat Neurosci</i>
2:233709081 – 233709092	Deletion	Ser1035—His1038	Exon deletion	N.D	Wang et al. 2016, <i>Nat Commun</i>
2:233712060	C to A	Pro1176Thr	Missense	Maternal	Wang et al. 2016, <i>Nat Commun</i>
2:233712,061	C to G	Pro1176Arg	Missense	De novo	Krumm et al. 2015, <i>Nat Genet</i> An et al. 2018, <i>Science</i>
2:233721568	T to G	Ter to Gly	Stop lost	N.D	Wang et al. 2016, <i>Nat Commun</i>
2:233721568	T to A	Ter to Arg	Stop lost	N.D	Wang et al. 2016, <i>Nat Commun</i>

NCBI Gene Assembly GRCh37.p13

N.D not determined

2.3. Methods

2.3.1. Mice

Male mice on Jackson Laboratory C57BL/6J background aged postnatal day (P) 60-90 (i.e. young adults [233]) were used for experiments, unless otherwise specified. *Gigylf2^{+/-}* [50] and *Eif4e2^{+/-}* [14] were previously generated and characterized. Mice were weaned at P21 and housed by sex and mixed genotype (unless otherwise specified) in groups of 2-5 animals per cage under standard conditions: 20-22 °C, 12 h light/dark cycle (7:00-19:00 light period) with food and water access ad libitum. Mice were handled 3 times (once per day for 3 days) and habituated to the behavioral room for 20 min prior to behavioral testing. Behavioral experiments were conducted in an isolated, soundproof room between 9:00 and 16:00. All behavioral apparatuses were cleaned between animals. In the case where cohorts were evaluated in more than one behavioral assay, the testing order began with the least aversive test and ended in the most aversive (least – grooming, open field, elevated plus maze, marble burying, rotarod, three-chamber social interaction, and contextual fear conditioning – most). All other behavioral tests were conducted on separate cohorts aged P60-P90, unless otherwise specified. See below for detailed methods. The experimenter was blinded to mouse genotype during data acquisition, analysis and manual scoring. Mouse genotype was randomized throughout the day and across days in the case of multi-day experiments. Animal care, handling, and all experiments were performed according to the guidelines of the Canadian Council on Animal Care and approved by the McGill University Animal Care Committee.

2.3.2. Generating *Eif4e2* conditional knockout (KO) mice

To conditionally delete 4EHP in excitatory neurons, we crossed *Eif4e2^{flx/flx}* mice [14] with Emx1-IRES-Cre mice (glutamatergic forebrain neurons where Cre recombinase activity occurs at embryonic day (e) 10.5 [234], JAX stock no. 005628, on C57BL/6 background, backcrossed for 12 generations). *Eif4e2^{+/flx}:Emx1-Cre* mice were used to breed F2: *Eif4e2^{+/+}:Emx1-Cre* (referred to in the text as 4EHP-WT) and *Eif4e2^{flx/flx}:Emx1-Cre* (referred to in the text as 4EHP-eKO). F3 mice were used for experiments and housed according to genotype. Comparisons were made between these genotypes to normalize for any confounding effects generated by the presence of Cre recombinase alone.

2.3.3. Synaptic protein extraction

The hippocampus from mice (wildtype male on Jackson Laboratory C57BL/6J background, n=3) was dissected and homogenized in ice-cold Syn-PER Synaptic Protein Extraction Reagent (87793, Thermo) containing 1 tablet EDTA-free protease inhibitor mixture (4906845001, Roche), phosphatase inhibitor mixture 2 (P5726, Sigma) diluted 1:100, and phosphatase inhibitor mixture 3 (P0044, Sigma) diluted 1:100. Following the manufacturer's protocol, the samples were centrifuged at 1200 g for 10 min at 4°C and the supernatant was transferred to a new tube. A sample was taken for crude. The supernatant was then centrifuged at 15 000 g for 10 min at 4°C, and the supernatant (cytosol) was removed from the synaptosome pellet. The synaptosome pellet was then resuspended in Syn-PER Synaptic Protein Extraction Reagent for analysis. Samples were stored at -80° C until used for Western blotting.

2.3.4. Western blot

Soluble protein extracts were prepared by homogenizing brain tissue (from 3-8 mice, depending on the experiment) using a pestle mixer in ice-cold radioimmunoprecipitation assay (RIPA) buffer (R0278, Sigma) containing proteinase and phosphatase inhibitors. Samples were incubated on ice for 30 min. Lysate was then centrifuged at 16 000 g for 20 min at 4°C. The protein-containing supernatant was collected, and the pellet discarded. 25 µg of protein sample was loaded onto a polyacrylamide gel (final concentration: 12% Acrylamide/Bis Solution, 29:1, 375 mM Tris pH 8.8, 0.1% SDS, 0.1% TEMED, and 0.1% Ammonium Persulfate) and separated using a potential difference of 100 V. Protein was then electro transferred onto a nitrocellulose membrane in transfer buffer (25 mM Tris, 190 mM glycine, and 20% methanol, pH 8.3) at 25 V overnight at 4°C. Membranes were then blocked with 5% albumin (BSA) in Tris-Buffered Saline with Tween 20 (TBST, 20 mM Tris pH 7.5, 150 mM NaCl, 0.1% Tween 20) for 1-2 hr at room temperature (RT) to reduce non-specific binding. Membranes were then probed with one of the following primary antibodies at the indicated dilution: EIF4E2 (GTX103977, GeneTex, 1:500), GIGYF2 (A303-732A, Bethyl Laboratories, 1:500), PSD95 (75-028, NeuroMab, 1:5000), α -Tubulin (sc-23948, Santa Cruz, 1:5000), GAPDH (ab9482, Abcam, 1:40 000), β -actin (A5441, Sigma, 1:5000), diluted in TBST with 5% BSA overnight at 4°C (or 1 hr at RT for GAPDH and β -actin), then washed with fresh TBST 3 times for 10 min each at RT. Secondary antibody conjugated to horseradish peroxidase (HRP, anti-mouse and anti-rabbit, GE Healthcare) was diluted 1:5000 in TBST with 5% BSA and added to membranes for 1-2 hr at RT. Membranes were again washed with fresh TBST 3 times for 10 min each at RT. Enhanced chemiluminescence (Western Lighting® Plus ECL, ORT2655:ORT2755, Perkin Elmer) was then added to membranes for 1 min. Membranes were visualized on film. For re-probing, membranes were washed with double distilled water for 5 min, the antibody was

stripped with 0.2 M NaOH for 10 min, and membranes washed again with double distilled water for 5 min. Quantification of the band intensity was done using Image J software (NIH). For analysis of developmental expression of GIGYF2 and 4EHP (Fig. 2.1A-C), wildtype male mice on Jackson Laboratory C57BL/6J background were used at the indicated age (n=3 per age group).

2.3.5. Primary hippocampal neuron cultures

Hippocampi were dissected from wildtype e17.5 mouse brain on Jackson Laboratory C57BL/6J background in ice-cold Hank's Balanced Salt Solution (HBSS). Hippocampi were washed in ice-cold HBSS without calcium and magnesium twice and cells were dissociated by incubating in trypsin at 37°C. Trypsin digestion was stopped by adding fetal bovine serum (FBS). After washing twice with Dulbecco's Modified Eagle Medium (DMEM) containing 10% FBS, the dissociated cells were plated on dishes pre-coated with polyethyleneimine overnight in DMEM containing 10% FBS. 2 hr after plating, the media was removed and replaced by Neurobasal media containing B-27 supplement, GlutaMAX, and Penicillin/Streptomycin. After 2 d in vitro (DIV), cells were treated with mitotic inhibitor (5-Fluoro-2'-deoxyuridine) to prevent glial contamination. Half of the media was replaced with new media every 5 d until analysis.

2.3.6. Immunofluorescence on primary neuron cultures

DIV 14 primary hippocampal neurons were briefly washed with preheated phosphate-buffered saline (PBS) at 37°C. Cells were then fixed with preheated 4% paraformaldehyde (PFA) at 37°C for 10 min. After washing with PBS 3 times for 10 min, cells were permeabilized with 0.2% tritonX-100 in PBS at RT for 15 min. Cells were blocked in 1% BSA in PBS at RT for 1 hr. Blocking buffer

was then exchanged for the following primary antibodies: eIF4E2 (sc-100731, Santa Cruz), PSD95 (75-028, NeuroMab), diluted 1:100 in blocking buffer. Cells were incubated in primary antibody at 4°C overnight. Cells were washed with PBS 3 times for 10 min before adding secondary antibody diluted 1:1000 in blocking buffer for 1 hr at RT in the dark. Cells were washed with PBS 3 times for 10 min before being mounted on a microscope coverslip with DAKO. Cells were visualized using a ZEISS Laser Scanning Microscope 880 24 hr after mounting.

2.3.7. Immunofluorescence on brain slices

Mice were placed under isoflurane anesthetics until loss of pain reflex and transcardially perfused with filtered ice-cold PBS then 4% PFA. Brains were rapidly dissected and placed in ice-cold 4% PFA overnight at 4°C for post-fixation. Brains were then placed in 30% sucrose in PBS for 3 d at 4°C for cryoprotection. 20 µm coronal sections were prepared using a cryostat and adhered to glass coverslips (12-550-15, Fisher). Sections were washed 3 times in PBS for 5 min and placed in boiling 10 mM sodium citrate buffer, pH 6.0 for 20 min for antigen retrieval. Sections were washed 3 times with PBS for 5 min before placed in blocking solution (10% BSA and 0.5 % Tween 20 in PBS) for 1-2 hr at RT. Sections were then incubated in the following primary antibodies: eIF4E2 (sc-100731, Santa Cruz), EMX1 (PA5-35373, Thermo), PVALB (195004, Synaptic System), Somatostatin 28 (ab111912, Abcam), Laminin (L9393, Sigma), diluted 1:100 in blocking solution overnight at 4°C. After washing 3 times in PBS for 5 min, sections were incubated with Alexa-conjugated secondary antibodies (1:300) and Hoechst (1:1000) diluted in blocking buffer for 1-2 hr at RT in the dark. Sections were then washed 3 times with PBS for 5 min and then rinsed once

in double distilled water. Coverslips were mounted with DAKO. Samples were visualized 24 hr later with a ZEISS Laser Scanning Microscope 880.

2.3.8. Electrophysiological recordings

Transverse hippocampal slices (400 μm thick) were prepared from age-matched male mice (4-5 weeks of age) with a vibratome (Leica VT1200 S, Leica Biosystems Inc) at 4°C in artificial cerebrospinal fluid solution (ACSF, perfused with 95% O₂ and 5% CO₂) containing 124 mM NaCl, 5 mM KCl, 1.25 mM NaH₂PO₄•H₂O, 2 mM MgSO₄•7H₂O, 26 mM NaHCO₃, 2 mM CaCl₂•H₂O, and 10 mM Dextrose. Slices were recovered for at least 120 min before recording in an incubation chamber with ACSF at 32 °C. The slices were then transferred to the recording chamber and perfused with ACSF at a flow rate of 2 mL/min for 30 min prior to recording. Field excitatory postsynaptic potentials (fEPSPs) were recorded with ACSF-filled micropipettes and were elicited by bipolar stimulating electrodes placed in the CA1 stratum radiatum to excite the Schaffer collateral. Input-output curves were generated by increasing input current and recording fEPSP output. The intensity of the pulses was adjusted to evoke 40–50% of maximal response for subsequent recording. A stable baseline of responses was established for 30 min and metabotropic glutamate receptor-mediated long-term depression (mGluR-LTD) was induced by bath-application of 100 μM (*S*)-3,5-Dihydroxyphenylglycine (DHPG, 0805, Tocris Biosciences) for 10 min. Each data point represents the slope of fEPSP calculated with Clampfit 11.0.3 software. All data are presented as mean \pm s.e.m. and N refers to the number of mice (i.e. 1 recording from 1 slice from 1 mouse).

2.3.9. Measurement of global protein synthesis

The puromycin incorporation assay, also known as surface sensing of translation (SUnSET) [235], was performed on adult (P60-P90) hippocampal slices as previously described [159]. Briefly, 400 μm transverse hippocampal slices were prepared as indicated for electrophysiology experiments. Slices were recovered for a minimum of 3 hr in an incubation chamber with ACSF at 32 °C. Six slices were combined per animal and each N represents one animal. Puromycin Dihydrochloride (PUR333.10, BioShop) was added to the incubation chambers at a final concentration of 5 $\mu\text{g}/\text{mL}$. Slices were incubated in puromycin for 45 min and then either snap frozen and prepared for western blot or placed in 4% PFA in preparation for immunofluorescence. Puromycin incorporation was visualized using western blot or immunofluorescence with an anti-puromycin antibody, clone 12D10 (1:1000, MABE343, MilliporeSigma).

2.3.10. Three-chamber social interaction

An arena partitioned into three chambers containing doors to allow entry into each chamber was used to assess social interaction and preference for social novelty. Test mice were placed in the middle of the empty three-chambered arena and habituated for 10 min. After habituation, an unfamiliar mouse (stranger 1, age-matched male, C57BL/6J, and approximately the same size as the test mouse) was placed into one of the two side chambers and enclosed in a small holding device which only permitted social interaction to be initiated by the test mouse. An identical empty holding device was placed in the opposite chamber. During this time, the doors to the side chambers were blocked to prevent the test mouse from entering the chambers. The doors were then opened, and the test mouse could explore for 10 min. After 10 min, the doors were again

blocked and a new unfamiliar mouse (stranger 2, age-matched male, C57BL/6J, and approximately the same size as the test mouse) was placed in the previously empty holding device. The doors were opened again, and the test mouse freely explored for 10 min. The location of the holding device was counterbalanced between side chambers for different test mice to prevent chamber biases. Stranger 1 and 2 mice were from different home cages and counterbalanced for each side of the chamber. The time spent sniffing stranger 1, stranger 2 or the empty holding device was manually scored. Stranger mice were purchased from Charles River Laboratories (Sherbrooke, Canada).

2.3.11. Marble burying

An open field arena (50 cm by 50 cm by 30 cm) was filled with fresh bedding (i.e. sawdust, approximately 5 cm deep). 20 clean marbles were placed on the sawdust in a pre-arranged 5 by 4 grid. Mice were placed in the center of the field and allowed to bury the marbles for 20 min. After the test period, buried marbles (i.e. marbles that were at least 2/3 covered with sawdust) were counted manually.

2.3.12. Direct social interaction

The test mouse was placed in a new, clean cage and allowed to habituate for 5 min. A novel stranger mouse (age-matched male, C57BL/6J, and approximately the same size as the test mouse) was then placed in the cage and the mice interacted for 10 min. Activity and interaction was recorded using a camera placed vertically in front of the cage. Videos were scored manually to obtain the nose-to-anogenital sniffing time of the stranger mouse by the test mouse and total

interaction time, including nose-to-nose sniffing, nose-to-anogenital sniffing, following, chasing, mounting, and fighting during the 10 min interaction. Reciprocal interaction of the stranger mouse to test mouse was also included in the total interaction time.

2.3.13. Self-grooming

Clean home cages were filled with approximately 1 cm of fresh bedding material without nesting material. Mice were individually placed in a cage and recorded for 20 min using a video camera placed in front of the cage. Total grooming time was manually scored using a stopwatch.

2.3.14. Isolation-induced ultrasonic vocalizations

To induce USVs, mouse pups (P7) were gently separated from their mothers for 15 min (kept on a heating pad). Pups were then placed individually in an anechoic styrofoam chamber (recording chamber) containing a microphone (Avisoft Bioacoustics CM16/CMPA) fixed inside the top. The microphone was connected to an ultrasound recording interface (Avisoft Bioacoustics UltraSoundGate 116Hb) which detects USVs emitted by mouse pups and recorded using a digital recording system (Avisoft Bioacoustics RECORDER). USVs were recorded for 5 min. Recordings were analyzed manually using the Avisoft Bioacoustics SASLab Pro software. The number of calls per min and average call duration were analyzed.

2.3.15. Open field

Mice were placed in a white-colored square box (50 cm x 50 cm x 30 cm) with an open top and allowed to explore freely for 10 min while their locomotor activity was recorded with a camera

placed directly above the field. The center zone is defined as a square measuring 30 cm x 30 cm that is in the middle of the arena. Time spent in the center of the field, total distance travelled, and number of entries into the center were scored using Noldus EthoVision XT software.

2.3.16. Rotarod

Mice were first trained to walk on a 1¼ diameter rotating rod (Rotarod, IITC Life Science Inc, USA) with a constant rotation of 5 revolutions per min (rpm). The training period lasted for 3 min and mice that fell off were placed back on during this time. 1 hr after training, mice were placed on the rod which began rotating at 5 rpm and accelerated by 0.2 rpm per sec to a maximum speed of 40 rpm until either the mice fell off or 5 min passed. The latency to fall was recorded as a measure of motor function.

2.3.17. Olfactory preference

To test for intact olfaction in mice, either cinnamon extract (clear in color) or water was placed on a 2 cm by 2 cm patch of filter paper in a clean home cage. Mice were then placed in the cage for 5 min and observed for time spent sniffing the filter paper containing either cinnamon extract or water. Since novelty of the filter paper alone promotes sniffing and may mitigate any differences in time spent sniffing either water or an attractive odor, an aversive odor was chosen for this test.

2.3.18. Elevated plus maze

The testing apparatus consists of two black open arms and two black enclosed, protected arms that are both approximately 0.6 m above the floor, meeting at a center zone to form a plus shape. The open arms had open edges. The testing room was lit with 1200 lx. The total time spent in the open and closed arms was scored manually. A transition to another arm was defined as all four limbs entering either an open or a closed arm.

2.3.19. Contextual fear conditioning

Mice were placed in a sound-proof box containing an enclosed isolation chamber with an electric grid floor and overhead camera. Mice were recorded for 2 min before receiving a mild foot shock (0.7 mA, 1 sec). After 1 min, mice were removed and placed back in their home cage. After 24 hr, mice were placed back in the enclosure (context) and recorded for 4 min. The average percent freezing over 4 min was used as an assessment of long-term memory.

2.3.20. Statistical analysis

Statistical analysis was performed on GraphPad Prism 8. An unpaired t-test was used to compare one experimental parameter. Mixed design two-way ANOVA was used to compare two experimental parameters (i.e. genotype as an independent variable and arms in the elevated plus maze test as a repeated measure). Bonferroni test was used for pair-wise post-hoc analysis where there was a significant interaction in the data. A Welch's corrected t-test was used where the difference in variance between groups was significantly different according to the Levene's test. Data were expressed as mean \pm s.e.m. and p values < 0.05 were considered statistically significant. Details of all statistics used are listed in Supplementary Table S2.1.

2.4. Results

2.4.1. 4EHP is primarily expressed in neurons and synaptosomes and its amount increases during development

To study the effects of homozygous deletion of 4EHP in the brain, we employed Cre-Lox technology. We first investigated the expression of 4EHP to provide a basis for generating an appropriate model. In the cortex (Fig. 2.1A), hippocampus (Fig. 2.1B), and cerebellum (Fig. 2.1C), 4EHP expression increases through development. Interestingly, 4EHP is maximally expressed between P26 and P60. In the hippocampus, 4EHP protein expression is enriched in purified synaptosomes (Fig. 2.1D), but is also expressed in the cytosol, consistent with previous reports [12]. We confirmed synaptic expression of 4EHP in primary hippocampal neuron cultures by colocalization of the synaptic marker PSD95 (Fig. 2.1E). Lastly, we examined 4EHP expression in major cell types in the hippocampus. 4EHP was observed primarily in neurons, including excitatory neurons, labelled by empty spiracles homeobox 1 (EMX1, Fig. 2.1F), and inhibitory neurons, labelled by either parvalbumin (PV, Fig. 2.1G) or somatostatin (SST, Fig. 2.1H). We did not observe 4EHP in a non-neuron cell type, endothelial cells, labelled by laminin (LAMA1, Fig. 2.1I). Given these results, we opted to target 4EHP in EMX1-expressing cells to study its role in synaptic plasticity and ASD-like behaviors. We chose the EMX1-Cre model over the CaMKIIa-Cre model to delete 4EHP in excitatory neurons because EMX1-driven Cre recombinase activity was reported to occur by e10.5 [234] whereas CaMKIIa-driven Cre recombinase activity occurs postnatally [147,236,237].

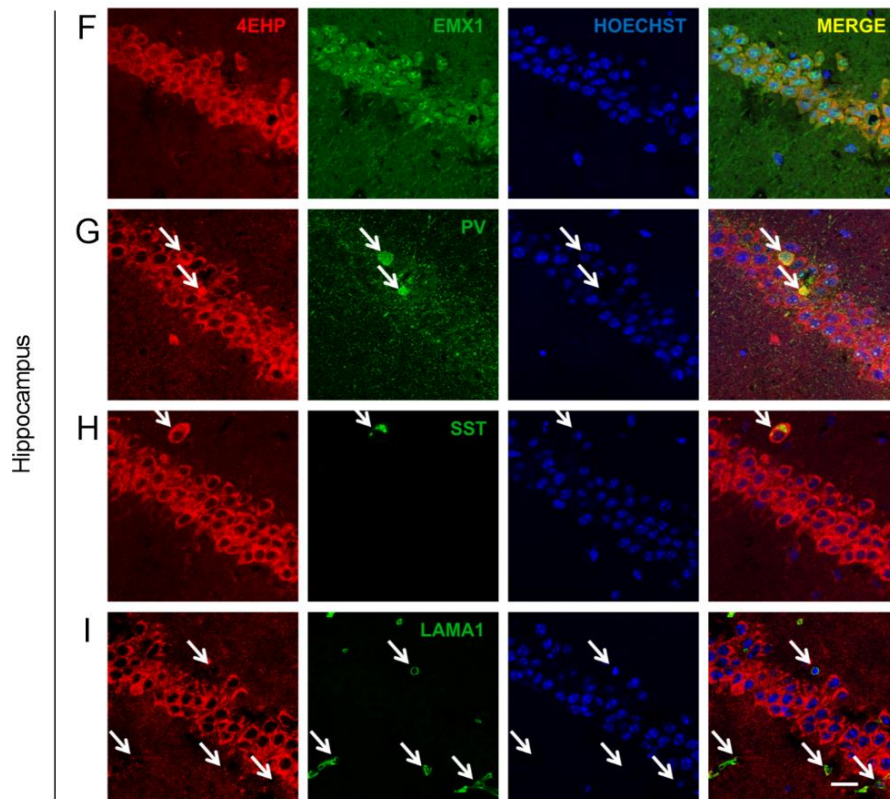
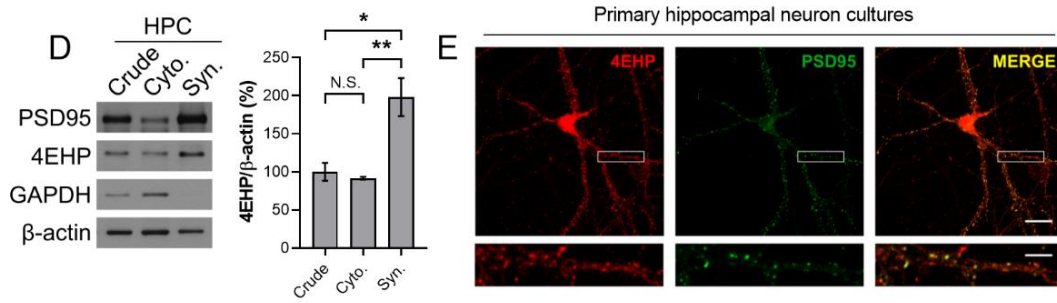
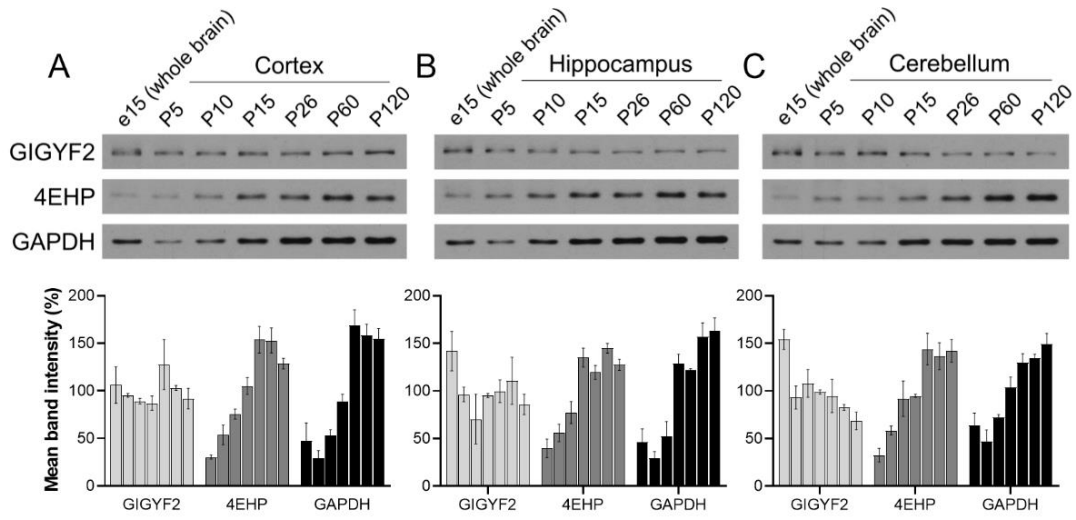


Figure 2.1. 4EHP expression in the brain.

A, B, and C Developmental expression of 4EHP, GIGYF2, and GAPDH in the cortex, hippocampus, and cerebellum, respectively, as measured by western blot. Quantification of A, B, and C (lower panel, n=3 per group, normalized to the average of all age points for each protein per membrane). **D** 4EHP expression in a synaptosome preparation (left panel). PSD95 was enriched in the synaptosome (Syn) as opposed to the cytosol (Cyto), demonstrating proper synaptosome preparation. GAPDH and β -actin were used as loading controls. Quantification of D (right panel, n=3). **E** Primary neurons were derived from the hippocampus of wildtype mice and cultured for 14 d. Immunofluorescent analysis confirmed 4EHP expression in the synapse by colocalization with PSD95 (merge). The scale bar represents 20 μ m in the upper panel of images and 5 μ m in the lower panel of images. The lower panel of images correspond to 4x zoom of the upper panel of images defined by the white box. Analysis of cell-type-specific expression of 4EHP by colocalization with **F** Empty Spiracles Homeobox 1 (EMX1, defining excitatory neurons), **G** parvalbumin (PV, defining a subset of inhibitory neurons), **H** somatostatin (SST, defining another subset of inhibitory neurons), and **I** laminin (LAMA1, defining endothelial cells) in the hippocampus of wildtype mice. 4EHP expression is colored in red, the cell type marker in green, and Hoechst-stained nucleus in blue. Arrows indicate a positive signal for the cell type marker. Scale bar represents 20 μ m.

2.4.2. 4EHP in excitatory neurons regulates hippocampal mGluR-LTD and is necessary for normal social behaviors

The generation and characterization of mice expressing Cre in EMX1-specific cell types was previously reported [234]. By crossing these mice with those expressing a floxed *Eif4e2* (*Eif4e2^{flx/flx}*), we generated an excitatory neuron-specific 4EHP knockout (4EHP-eKO) mouse model. Western blot analysis confirmed reduction of 4EHP expression in both the prefrontal cortex (Fig. 2.2A) and hippocampus (Fig. 2.2B). Loss of 4EHP expression in excitatory neurons was confirmed using immunofluorescence in both the prefrontal cortex (Fig. 2.2C) and hippocampus (Fig. 2.2D). We confirmed a reduction of both 4EHP and GIGYF2 expression in whole brain of P0 mice (Supplementary Fig. S2.1 A, B and C) and the hippocampus of P60 4EHP-eKO mice (Supplementary Fig. S2.1 D, E and F).

Given the hippocampal expression characteristics of 4EHP, we first investigated its role in hippocampal plasticity. Long-term depression (LTD) is a plasticity phenomenon that is exaggerated in mouse models of ASD with alterations in translational control [238,239]. Depression of hippocampal neuron activity is also known to be necessary for normal social behavior in freely-moving rats [240] and is exaggerated in rats raised in social isolation [241]. To measure LTD, we recorded fEPSPs from CA1 pyramidal neurons after stimulating CA3 Schaffer collaterals (Fig. 2.2E). Application of 100 μ M DHPG for 10 min resulted in a sustained reduction in the slope of fEPSPs (Fig. 2.2F). LTD was significantly exaggerated by 15.74% in 4EHP-eKO mice compared to 4EHP-WT (Fig. 2.2G). Given the correlation between normal hippocampal LTD and typical social behavior and the link between exaggerated mGluR pathway activation and ASD, we

next investigated social behavior in 4EHP-eKO mice. To this end, we subjected mice to the three-chamber social preference and social novelty test (Fig. 2.2H). In the social preference phase, 4EHP-eKO preferred S1 over E, comparable to 4EHP-WT mice, but had 27.79% less overall interaction time with both S1 and E (Fig. 2.2I). However, in the social novelty phase, 4EHP-eKO mice did not exhibit a normal preference of the novel stranger mouse (S2) over S1 (Fig. 2.2J). Similarly, when allowed to freely interact with a stranger mouse in the direct or reciprocal social interaction test (Fig. 2.2K), 4EHP-eKO mice spent 59.91% less time sniffing and 44.22% less time interacting with the stranger mouse compared to 4EHP-WT mice (Fig. 2.2 L and M). Together these results demonstrate an important role for 4EHP in mediating social behavior and regulating synaptic plasticity.

We next investigated global protein synthesis in 4EHP-eKO and 4EHP^{+/-} mice by measuring puromycin incorporation into nascent peptides of the hippocampus using the SUnSET assay [235]. We did not observe changes to global protein synthesis by western blot (Supplementary Fig. S2.2A) or immunofluorescence (Supplementary Fig. S2.2C) in 4EHP-eKO mice or 4EHP^{+/-} mice (Supplementary Fig. S2.2B) compared to controls. These findings suggest that 4EHP likely represses translation of specific mRNAs rather than global protein synthesis in the brain.

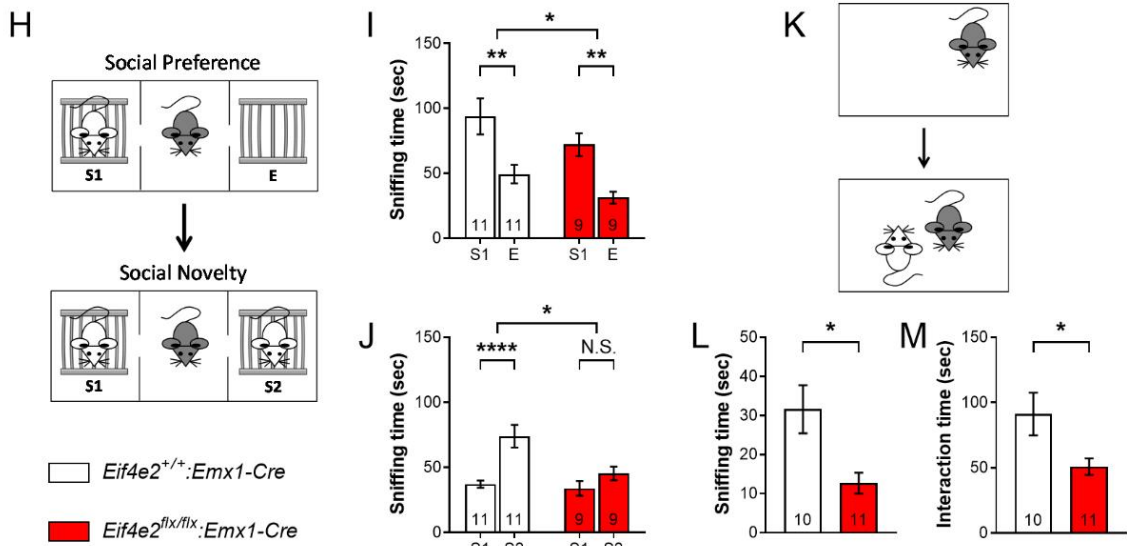
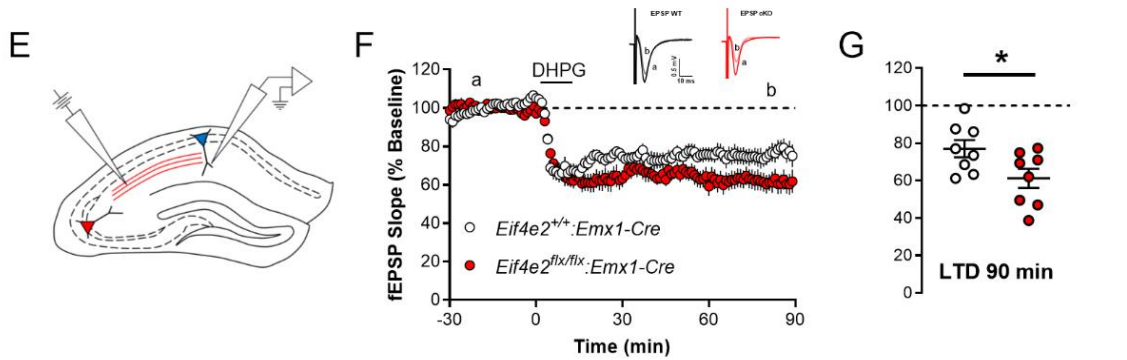
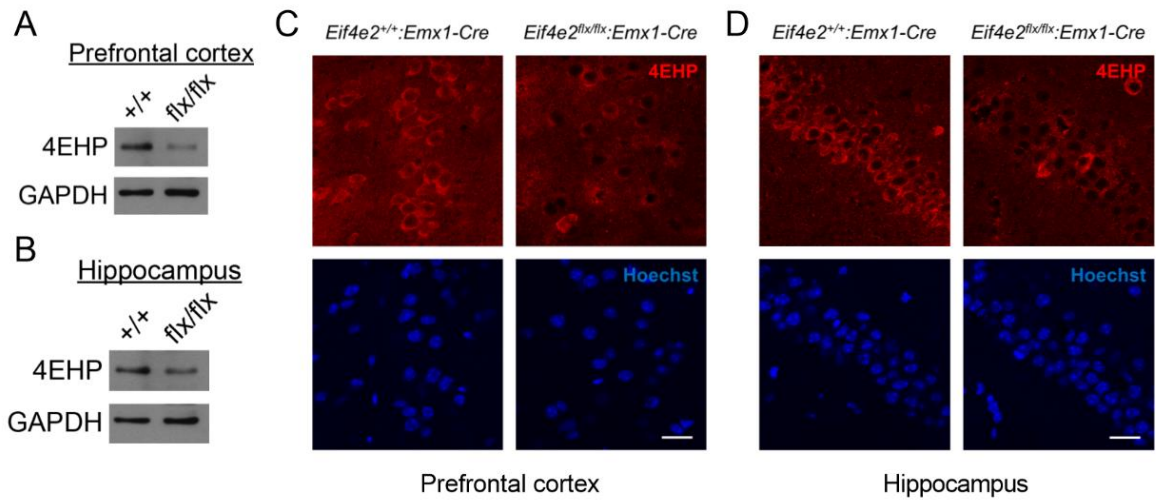


Figure 2.2. Loss of 4EHP in excitatory neurons exaggerates hippocampal mGluR-LTD and impairs social behavior.

A and B Confirmation of loss of 4EHP expression in the prefrontal cortex and hippocampus, respectively, of 4EHP-eKO (flx/flx) versus 4EHP-WT (+/+) mice using western blot. GAPDH was used as a loading control. **C and D** Confirmation of loss of 4EHP expression in excitatory neurons in the prefrontal cortex and hippocampus, respectively, of 4EHP-eKO versus 4EHP-WT mice using immunofluorescence microscopy. 4EHP expression is colored in red and Hoechst-stained nucleus in blue. Scale bar represents 20 μ m. **E** Schematic representation of stimulating (left) and recording (right) electrode position for measuring DHPG-induced long-term depression (mGluR-LTD) in the CA1 hippocampus. The red fibers represent CA3 pyramidal projections to the CA1 (Schaffer collaterals). **F** Field excitatory postsynaptic potential (fEPSP) recordings of CA1 pyramidal neurons during mGluR-LTD. Baseline was recorded for 30 min prior to adding mGluR1/5 agonist, DHPG (100 μ M), to slices for 10 min. LTD was recorded for 90 min. The inset is the average of all fEPSPs at time *a* and *b* for each genotype, n=8 per group. **G** Average of the last 10 min of recording. **H** Schematic representation of the three-chamber social preference and social novelty test. Mice were first habituated to the apparatus for 10 min. Two cages (mouse holding devices) were then placed in opposite corners of opposing chambers; one cage was empty (E) and one contained a conspecific stranger mouse (S1). After 10 min, a novel stranger mouse (S2) was added to E for the social novelty test lasting 10 min. **I** The amount of time the test mouse spent sniffing either S1 or E. **J** The amount of time the test mouse spent sniffing either S1 or S2. **K** Schematic representation of the direct (reciprocal) social interaction test. Test mice were first habituated to a clean home cage for 5 min. A novel stranger mouse was then added, and mice could freely interact for 10 min. **L** Nose-to-anogenital sniffing time of the stranger mouse by the test mouse. **M** Total interaction time including nose-to-nose sniffing, nose-to-anogenital sniffing, following, chasing, mounting, and fighting. Reciprocal interaction of the stranger mouse to test mouse was also included. Data are presented as mean \pm s.e.m.; *p<0.05, **p<0.01, ***p<0.0001, N.S., not significant; calculated by unpaired t-test or 2-way ANOVA with Bonferroni multiple comparisons test. Sample size is located within bar graphs. *Eif4e2* is the mouse gene encoding 4EHP.

2.4.3. ASD-like behavioral impairments in 4EHP-eKO mice are specific to social interaction and are not confounded by deficits in locomotion, motor function, olfaction, or anxiety

To further assess ASD-like behaviors in 4EHP-eKO mice, we investigated repetitive behaviors (marble burying and grooming) and ultrasonic vocalizations. 4EHP-eKO mice buried the same number of marbles (Fig. 2.3A) and self-groomed for the same duration (Fig. 2.3B) as 4EHP-WT mice. Ultrasonic vocalizations (USVs) were not different between 4EHP-eKO and 4EHP-WT mice (calls/min, Fig. 2.3C left panel; call duration, Fig. 2.3C right panel). As a measure of locomotion, distance travelled was not different between groups in an open field except during the last min of exploration where 4EHP-eKO mice travelled significantly further than 4EHP-WT mice (Fig. 2.3D left panel, $P=0.0128$). As a measure of gross motor function, the latency to fall off a rotating rod of increasing speed was also not different between groups (Fig. 2.3E). Olfaction was not different between groups (Fig. 2.3F) as determined by the difference in time spent sniffing a neutral scent (water) and a repulsive scent (cinnamon extract). The elevated plus maze and open field were used to assess general anxiety as anxious mice spend less time in the open arms or less time in the center of an open field, respectively [242,243]. We did not observe general anxiety in the 4EHP-eKO mice compared to 4EHP-WT in either the elevated plus maze (Fig. 2.3G) or in the open field (Fig. 2.3D middle and right panel). Since 4EHP was previously shown to regulate p-ERK [28], we measured hippocampal-dependent contextual fear memory in 4EHP-eKO mice, which requires activation of ERK [244–246]. Percent freezing 24 hr after receiving an adverse stimulus (foot shock) was not different between 4EHP-eKO and 4EHP-WT mice (Supplementary Fig. S2.3A). Consistently, we did not observe a significant difference in p-ERK levels in the hippocampus of 4EHP-eKO mice (Supplementary Fig. S2.3 B-E).

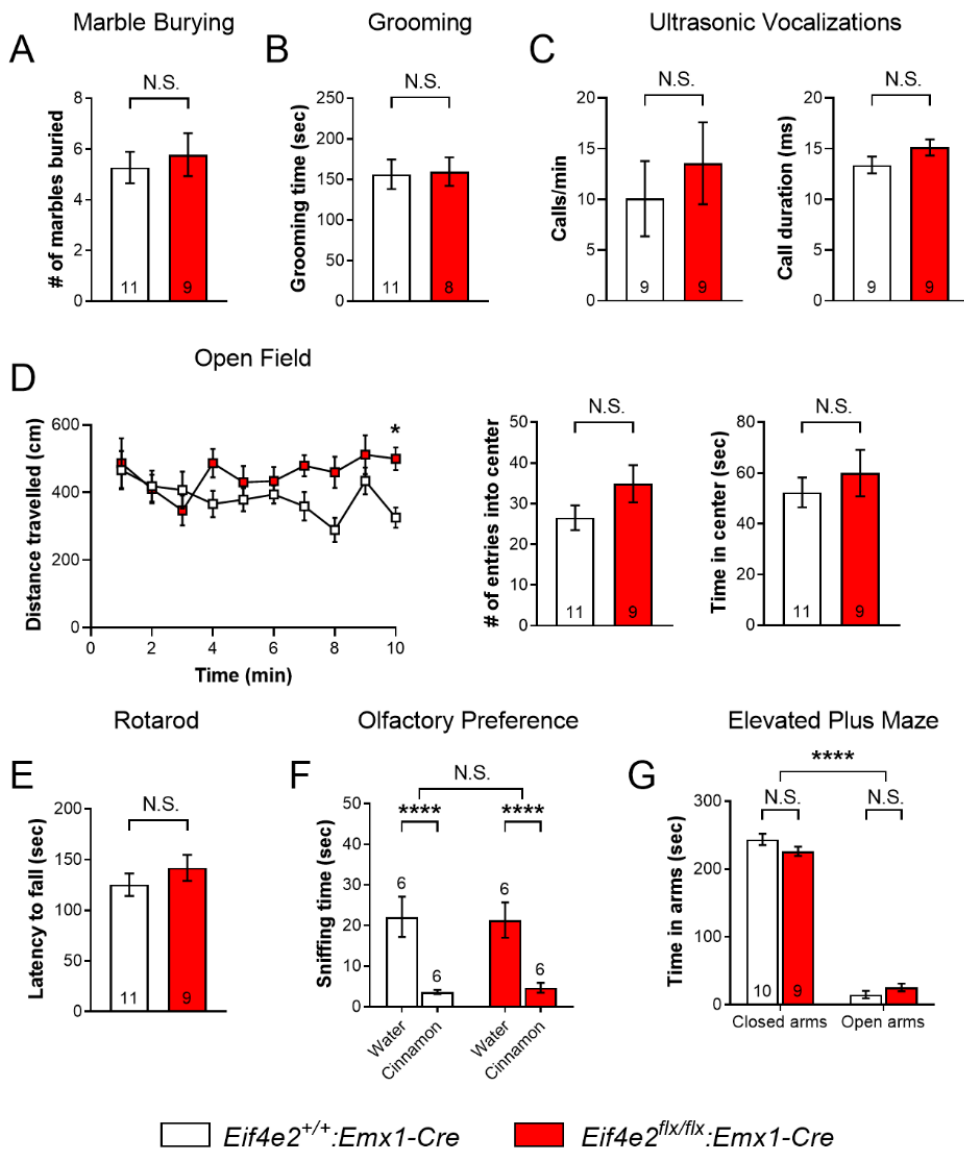


Figure 2.3. 4EHP-eKO mice do not present wide-spread behavioral alterations.

A To investigate repetitive behaviors, mice were analyzed in the marble burying assay. Mice were placed in an open field containing approximately 3 cm of fresh bedding material with 20 marbles in an evenly spaced 4 by 5 grid on the surface. Mice could bury marbles for 20 min. **B** Mice were placed in a clean home cage and total time spent grooming was recorded for 20 min. **C** P7 mice were separated from their mother and habituated for 15 min to induce vocalizations. The calls per min (left panel) and call duration (right panel) were recorded for 5 min. **D** Mice were placed into an open field for 10 min to assess locomotion and generalized anxiety. The distance travelled over time (left panel), number of entries into the center of the field (middle panel), and cumulative time spent in the center (right panel) were recorded; * $p < 0.05$, between groups at $t = 10$ min, calculated by 2-way ANOVA with Bonferroni multiple comparisons test. **E** Mice were placed on a rod rotating at a constant speed for 5 min for habituation. Mice were then placed back on the rod of increasing rotation speed until mice fell. The latency to fall was recorded as a measure of motor function. **F** To test olfaction, mice were placed into a clean home cage containing a piece of filter paper with a drop of either water or pure cinnamon extract. Time spent sniffing the filter paper was recorded for 5 min. **G** Generalized anxiety was assessed in the elevated plus maze by comparing time spent in an open versus closed arm for 5 min. Data are presented as mean \pm s.e.m.; ** $p < 0.01$, **** $p < 0.0001$, N.S., not significant; calculated by unpaired t-test or 2-way ANOVA with Bonferroni multiple comparisons test. Sample size is located within or above bar graphs.

2.4.4. GIGYF2 mutations are linked to ASD, but heterozygous deletion of *Gigylf2*, *Eif4e2*, or both in mice does not elicit ASD-like behaviors

Formation of a complex between 4EHP and GIGYF2 is required for the stability of both proteins [14] (Supplementary Fig. S2.1). As a translational repressing mechanism, disruption of this complex is a potential underlying cause of ASD (Fig. 2.5D). Various mutations in *GIGYF2* have been observed in ASD patients including truncations, large deletions, alternative splice donors, and loss of a stop codon (Table 2.1), with each having a potentially deleterious effect on GIGYF2 expression and function. To test whether loss of *Gigylf2* results in ASD-like behaviors in mice, we investigated social and repetitive behaviors in *Gigylf2*^{+/-} compared to *Gigylf2*^{+/+}, since homozygous deletion of *Gigylf2* is lethal [50]. We did not observe either impaired social interaction in the three-chamber social preference and social novelty test (Fig. 2.4 A and B) or exaggerated repetitive behaviors in the marble burying test (Fig. 2.4D). Similar to *Gigylf2* KO, homozygous deletion of *Eif4e2* is lethal in mice [14]. To determine whether loss of 4EHP alone or in concert with GIGYF2 results in ASD-like behaviors, we assessed social and repetitive behaviors in *Eif4e2*^{+/-} compared to *Eif4e2*^{+/+} mice and *Gigylf2*^{+/-}:*Eif4e2*^{+/-} compared to *Gigylf2*^{+/+}:*Eif4e2*^{+/+} mice. Consistent with findings in *Gigylf2*^{+/-} mice, heterozygous deletion of *Eif4e2* did not result in abnormal social preference (Fig. 2.4E), preference for social novelty (Fig. 2.4F) or increased marble burying (Fig. 2.4H). Heterozygous deletion of both *Gigylf2* and *Eif4e2* also did not result in impaired social behavior (Fig. 2.4 I and J), although *Gigylf2*^{+/-}:*Eif4e2*^{+/-} spent less time overall interacting with both stranger 1 (S1) and the empty cage (E) (Fig. 2.4I). The mice also did not present with differences in the number of marbles buried (Fig. 2.4L). As a measure of locomotion, distance travelled during the habituation phase of the three-chamber social interaction test, was

not different between groups (Fig. 2.4 C, G and K). Together these results indicate that heterozygous deletion of *Gigyl2*, *Eif4e2*, or both is not sufficient to cause ASD-like behaviors in mice (Fig. 2.5C).

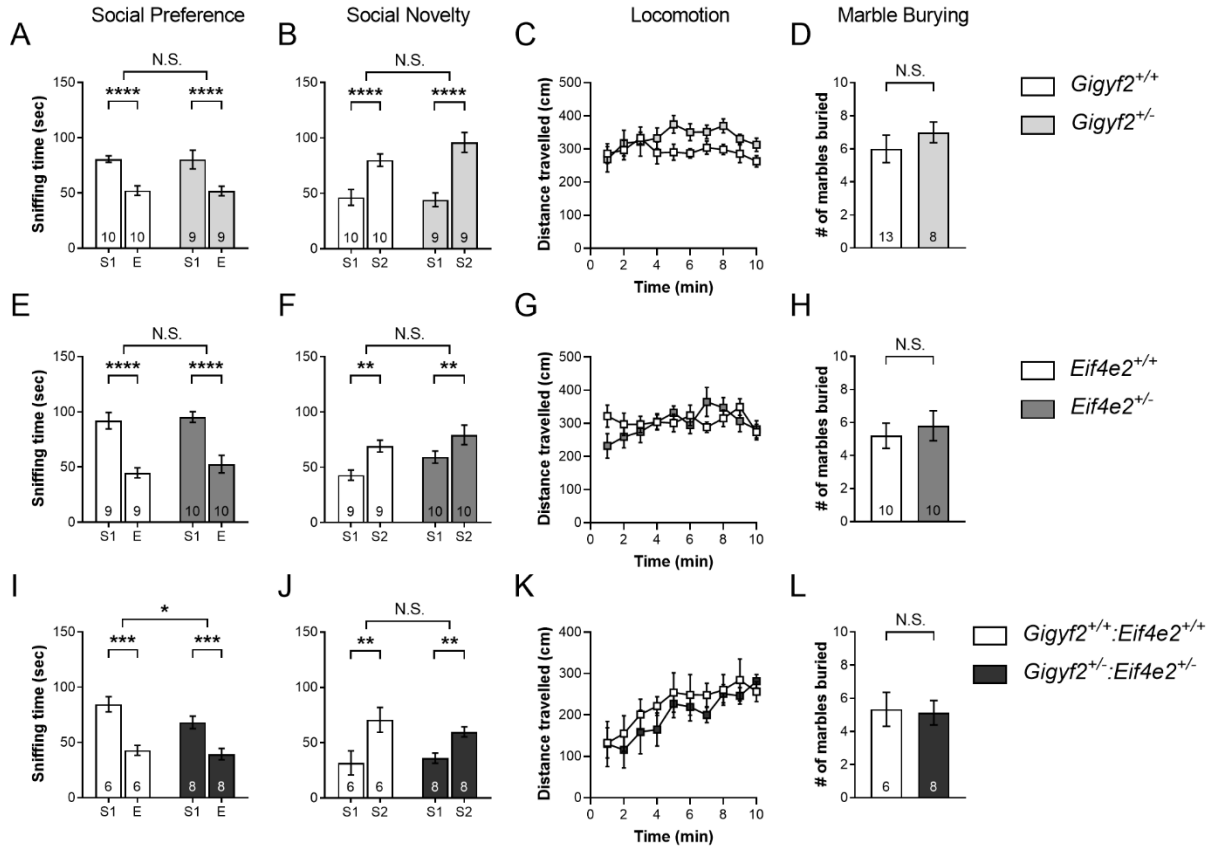


Figure 2.4. Heterozygous deletion of *Gigyl2*, *Eif4e2*, or both in mice does not result in ASD-like behavioral deficits.

A, E and I The amount of time the test mouse of the specified genotype spent sniffing either S1 or E. **B, F and J** The amount of time the test mouse of the specified genotype spent sniffing either S1 or S2. **D, H and L** The number of marbles buried by the specified genotypes in 20 min. **C, G and K** Distance travelled over time during the 10 min habituation phase of the three-chamber social interaction test by the specified genotypes. Data are presented as mean \pm s.e.m.; * $p < 0.05$, ** $p < 0.01$, *** $p < 0.001$, **** $p < 0.0001$, N.S., not significant; calculated by unpaired t-test or 2-way ANOVA with Bonferroni multiple comparisons test. Sample size is located within bar graphs.

2.5. Discussion

The behavioral deficits observed in 4EHP-eKO mice were specific to sociability, and not confounded by alterations in other behavioral domains. Impairments in either locomotion or motor activity may confound social interaction, since the mice are required to explore unhindered. The social behavior tests utilized here rely on intact olfaction as time spent sniffing is the dependent variable. Likewise, compounds that reduce general anxiety, such as the GABA_A receptor allosteric modulator ganaxolone, are known to have a confounding effect on social behavior [247]. We therefore tested and controlled for each of these potential confounding variables using the open field (Fig. 2.3D), rotarod (Fig. 2.3E), olfactory preference test (Fig. 2.3F), and the elevated plus maze (Fig. 2.3G), respectively. We conclude that 4EHP-eKO mice have specific social deficits.

In fact, the only behavioral phenotype relevant for ASD observed in 4EHP-eKO was impaired sociability. Both marble burying and self-grooming, which are used to assess repetitive behaviors, were unaltered in these mice. Since these behaviors are highly dependent on midbrain structures, such as the basal ganglia [248–250], restricted deletion of 4EHP in the forebrain of the eKO model [234] is not expected to affect these behaviors. Another possibility is that 4EHP activity in other cell types, such as inhibitory neurons, is mediating these behaviors. This is the case for 4E-BP2 conditional KO mice where 4E-BP2 deletion in inhibitory neurons resulted in impaired USVs, but not when it is deleted in excitatory neurons [147]. Consistent with these findings, USVs were not affected in 4EHP-eKO mice (Fig. 2.3C).

We confirmed social behavior deficits in two similar but distinct sociability tests: the three-chamber social interaction test and the direct or reciprocal interaction test. In the three-chamber social interaction test, 4EHP-eKO mice were not impaired in the first phase, which tests the animal's preference for social interaction over interaction with an inanimate object. However, in the second phase, which tests the animal's preference for social novelty, 4EHP-eKO mice did not prefer to interact with a novel stranger mouse over the one previously encountered. This phenotype is also observed in FMRP KO mice [251]. The reduction in nose-to-anogenital sniffing in 4EHP-eKO is also consistent with findings in other models of ASD, including in *Shank3* KO mice [252].

Long-term contextual fear memory was not affected by deletion of *Eif4e2* in excitatory neurons (Supplementary Fig. S2.3A). This finding was unexpected because 4EHP is known to regulate the levels of phospho-extracellular-signal-regulated kinase (p-ERK) via translational upregulation of dual-specificity phosphatase (DUSP) 6 in mouse embryonic fibroblasts (MEFs) [28]. Similarly, siRNA knockdown of GIGYF2 in human embryonic kidney (HEK) 293T cells decreased levels of p-ERK [72]. Since activation of ERK signaling is required for long-term memory [244–246], it is anticipated that loss of 4EHP in the hippocampus would result in long-term memory impairments. However, we did not observe changes to p-ERK levels in the hippocampus of 4EHP-eKO mice compared to controls (Supplementary Fig. S2.3 B-E). It is possible that in neurons, the molecular mechanism of 4EHP is different than in MEFs or HEK293T cells. Another possibility is that 4EHP regulates long-term memory in inhibitory neurons, since previous findings demonstrated the importance of translational control in SST neurons for long-term memory [148].

4EHP-eKO mice displayed exaggerated hippocampal mGluR-LTD together with impaired social behavior (Fig. 2.2). Field potential recordings in the hippocampus of freely moving rats have demonstrated that during normal social behavior, hippocampal responses are inhibited [240]. Similarly, rats that were socially isolated from P2-9 had exaggerated LTD in amygdalo-hippocampal synapses while undergoing social behavior [241]. Together these findings suggest that depression of synaptic responses in the hippocampus is necessary for normal social behavior, but excessive inhibition occurs during impaired social development. These findings are consistent with the mGluR theory of Fragile X Syndrome (FXS) which suggests that exaggerated mGluR-LTD is a hallmark feature of ASD animal models with dysregulated translation control [239]. This theory has been supported by numerous studies in the FXS mouse model [159,167,253,254] and other ASD mouse models where translational repressors are deleted, such as CYFIP1 [255] and 4E-BP2 [146]. We therefore conclude that 4EHP function in forebrain excitatory neurons is required for social behavior by regulating hippocampal long-term depression (Fig. 2.5B).

We did not observe changes in global protein synthesis in the hippocampus of either 4EHP-eKO or 4EHP^{+/-} mice. Since 4EHP^{+/-} do not have any behavioral impairments, these findings are not surprising and are likely due to haplosufficiency. In the 4EHP eKO mice, these observations are consistent with a role for 4EHP in regulating the translation of specific mRNAs via micro RNA silencing [18]. Future experiments employing cell-type-specific ribosome profiling (such as viral Translating Ribosome Affinity Purification, vTRAP [256]) and mRNA sequencing will be required to address this hypothesis. It is also possible that 4EHP regulates local translation, as we observed

its expression in synapses. In this case, changes to global protein synthesis may only be observed under stimulated conditions, such as upon activation of mGluRs, and would require more sensitive techniques than SUnSET.

There are currently no approved pharmaceutical treatments for the hallmark features of ASD and the available therapeutic options are limited to treating comorbidities. Together with its high prevalence rate, ASD poses a socio-economic burden across the globe. The complex genetic landscape of ASD creates further difficulty in effectively treating a heterogeneous population without reliable biomarkers. Understanding the pathophysiology of individual genetic aberrations is one step towards individualized medicine and more precise and targeted therapeutic interventions. This is reinforced by the unlikelihood of having a single treatment or therapy work for a variety of ASD patients [257,258]. To this end, much work has identified prospective therapeutics for treating ASD and other neurological disorders, such as metformin [112,259]. The data and models obtained from this work may provide a basis for preclinical pharmacogenetic studies to reverse ASD-like symptoms that could potentially benefit the health of individuals with ASD, particularly those harboring *GIGYF2* mutations (Fig. 2.5D).

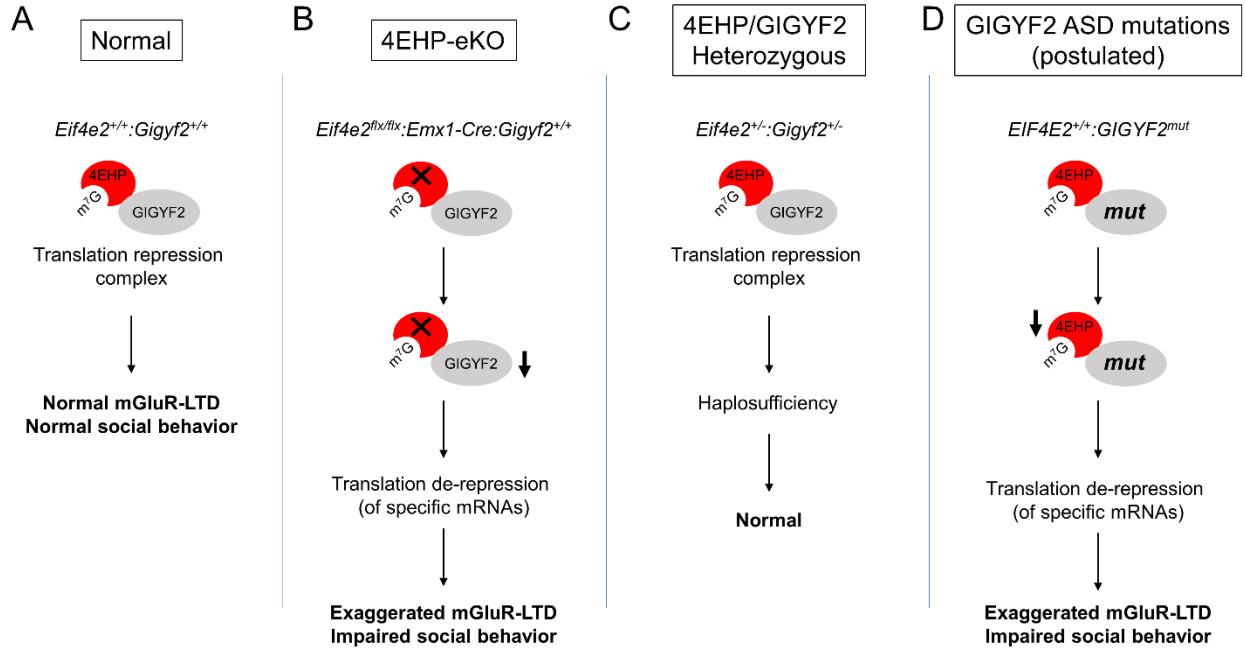


Figure 2.5. Proposed model.

A 4EHP binds to the 5' mRNA cap where its stable expression and function is maintained and reciprocated by physical interaction with GIGYF2. **B** Homozygous deletion of 4EHP in excitatory neurons of the forebrain (4EHP-eKO) results in reduced protein expression of GIGYF2, exaggerated mGluR-LTD, and impaired social behavior (possibly due to translation de-repression of specific mRNAs without affecting global protein synthesis). **C** Heterozygous deletion of *Gigyf2*, *Eif4e2*, or both does not result in ASD-like behaviors (possibly due to haplosufficiency). **D** Proposed model for the development of ASD in patients harboring *GIGYF2* mutations.

2.5.1. Limitations

In this study, we did not elucidate the molecular mechanism of 4EHP and GIGYF2 in the brain and how their dysregulation underlies the ASD-like phenotypes observed in 4EHP-eKO mice. To understand how 4EHP and GIGYF2 regulate ASD-like behaviors and LTD at the molecular level, future studies could employ viral Translating Ribosome Affinity Purification (vTRAP) to tag and capture mRNAs undergoing active translation [256]. This technique utilizes an adeno-associated virus (AAV) to express an eGFP-tagged ribosomal protein under the control of Cre recombinase. By purifying and sequencing ribosome-bound mRNAs, we can compare the translational efficiency (TE) of a gene across different treatment groups or genotypes [69]. This would allow for cell-type-specific and regionally selective gene expression analysis.

2.5.2. Conclusions

Here we describe a novel mouse model featuring established phenotypes of ASD, such as exaggerated hippocampal mGluR-LTD and social behavior deficits. Taken together, our findings provide evidence to support a link between human mutations in *GIGYF2* and the development of ASD via dysregulation of the 4EHP/GIGYF2 complex (Fig. 2.5).

2.6. Connecting text

The following text (section 2.6) is not included in the Wiebe et al. 2020 manuscript published in Mol Autism and exclusively serves to conceptually connect Chapter 2 to Chapter 3 and provide continuity for the overall theme of this thesis. First, de novo protein synthesis in neurons is unequivocally necessary for strengthening synaptic connections and storing memory long term. It was therefore pertinent to study the role of 4EHP in long-term memory. For the experiments in Chapter 3 we chose the *Camk2a*-driven Cre model because CaMKII α expression, and consequently expression of Cre, occurs at post-natal day 14 in excitatory cells of the forebrain [236] and thus limits developmental consequences of 4EHP deletion, as opposed to deletion following expression of EMX1. Second, we further developed an inhibitory neuron-specific 4EHP KO mouse model and characterized their learning and memory. This was necessary given that recent work has implicated the necessity of translation control in both excitatory and inhibitory neurons for long-term memory. Lastly, given the high co-morbidity of intellectual disability in ASD (>30%), we assessed the cell-type-specific role of 4EHP in cognitive ability using a working memory task.

**Chapter 3: Cell-type-specific translational control of spatial working memory
by the cap-binding protein 4EHP**

3.1. Abstract

The consolidation of learned information into long-lasting memories requires de novo protein synthesis and the strengthening of synaptic connections. Translation initiation factors play a cardinal role in gating the production of new proteins thereby regulating memory formation. Both positive and negative regulators of translation are necessary for optimal protein output during learning and memory consolidation. The eukaryotic initiation factor 4E (eIF4E) homologous protein (4EHP or eIF4E2) is an important negative regulator of translation but its role in learning and memory is unknown. To study 4EHP in learning and memory, we generated both excitatory (glutamatergic: CaMKII α -positive) and inhibitory (GABAergic: GAD65-positive) conditional knockout mouse models of 4EHP for analysis in various behavioral tasks. Knockout of 4EHP in *Camk2a*-expressing neurons (4EHP-cKO) did not impact long-term memory in either the contextual fear conditioning or Morris Water Maze task. Similarly, long-term spatial memory was not altered in *Gad2*-directed 4EHP knockout mice (4EHP-gKO). Surprisingly, when subjected to a short-term T-maze working memory task, both mouse models exhibited impaired cognition. We therefore tested if de novo protein synthesis has a direct role in working memory. However, mice treated with the protein synthesis inhibitor anisomycin prior to training did not present altered working memory. In attempts to understand how 4EHP mediates working memory, we discovered that phosphorylation of ribosomal protein S6, a measure of mTORC1 activity, is dramatically reduced in the CA1 hippocampus of 4EHP-cKO mice. Consistently, genetic reduction of mTORC1 activity alone in excitatory neurons is sufficient to impair working memory. Taken together these findings suggest that mTORC1 activity may be directly regulated by 4EHP to ultimately control expression of the underlying mechanisms necessary for working memory.

3.2. Background

Experiments from the 1960's established the first evidence for an essential role of protein synthesis in memory formation. Mice trained in a Y-maze shock avoidance task were unable to recall which arm of the Y-maze delivered the aversive shock 3 days after bilateral intracerebral injection of the protein synthesis inhibitor, puromycin [260]. This finding fueled interest in understanding exactly how protein synthesis is necessary for memory formation. One of the limiting factors in using bacterial toxins such as puromycin to block protein synthesis is that detailed insight into the biomolecular processes underlying memory cannot be achieved. For instance, one of the seminal discoveries elucidating translational control over memories was that preventing the phosphorylation of eukaryotic initiation factor (eIF)2 α , a molecular break mechanism for protein synthesis, increases general neural translation and enhances long-term memory (LTM) [178,217]. Protein synthesis is highly regulated at the initiation stage by a protein complex termed eIF4F which interacts directly with the mRNA 5' cap structure (m⁷GpppN cap, where N is any nucleotide and m is a methyl group). The components of eIF4F include a cap-binding protein eIF4E, a molecular scaffolding protein eIF4G, and a mRNA helicase eIF4A [137]. Disrupting the interaction between eIF4E and eIF4G using the 4EGI-1 inhibitor prevents LTM [261]. These findings, among many others, have elucidated key molecular components important in memory and thus warrant further research into how the translation machinery governs memory formation.

The eIF4E homolog 4EHP is a 5' cap-binding protein but does not stimulate translation [12]. 4EHP instead functions as a negative regulator of translation by employing the microRNA (miRNA) gene

silencing machinery [18,28], despite having a weaker cap-binding affinity than eIF4E [17]. Importantly, translational control via miRNA-induced mRNA silencing is known to play a critical role in synaptic plasticity and memory [262]. We therefore reasoned that 4EHP performs a critical function in the brain and hypothesize that it regulates translation of specific mRNAs important for plasticity-related events at the synapse, similar to eIF4E [261]. The implications of this would result in altered learning and memory. We therefore investigated the role of 4EHP in translational control of learning and memory. To this end, we generated 4EHP conditional knockout (KO) mice using the Cre-Lox system in both excitatory and inhibitory neurons. Unexpectedly, we did not observe alterations in long-term memory, but rather short-term working memory was impaired. In an effort to identify possible mechanisms underlying this phenotype, we discovered reduced levels of ribosomal protein S6 phosphorylation, a measure of mTORC1 activity, in the CA1 hippocampus of 4EHP-cKO mice. Our findings reveal an important cell-type-specific role of 4EHP in mediating working memory possibly through direct modulation of mTORC1 activity ultimately controlling translation of the mRNAs necessary for working memory.

3.3. Methods

3.3.1. Mice

Adult (i.e. postnatal day [P] 60-90 [233]) male mice on Jackson Laboratory C57BL/6J background were used for experiments. Mice were housed by sex and genotype after weaned at P21 in groups of 2-5 animals per cage. Mice were kept at standard room temperature (RT): 20-22 °C on a 12 h light/dark cycle (7:00-19:00 light period) with food and water access ad libitum. Behavioral experiments were conducted in a soundproof room between 8:00 and 16:00. All behavioral apparatuses were cleaned between animals. Mice were handled 2 times (once per day for 2 days) and habituated in the behavioral room for 20 min prior to behavioral testing. See below for detailed behavioral methods. For data acquisition, analysis and manual scoring, the experimenter was blind to mouse genotype which was randomized throughout the day and across days (in the case of multi-day experiments). Animal care, handling, and experiments were performed according to the guidelines of the Canadian Council on Animal Care and approved by the McGill University Animal Care Committee.

3.3.2. Generating conditional knockout (KO) mice

To conditionally delete 4EHP in excitatory neurons, we crossed *Eif4e2^{flx/flx}* mice [14] with CaMKII α -Cre mice (glutamatergic forebrain neurons where Cre recombinase activity has been reported to occur at postnatal day (P) 19 [236], JAX stock no. 005359, on C57BL/6 background). *Eif4e2^{+/flx}:Camk2a-Cre* mice were used to breed F2: *Eif4e2^{+/+}:Camk2a-Cre* (referred to in the text as 4EHP-WT) and *Eif4e2^{flx/flx}:Camk2a-Cre* (referred to in the text as 4EHP-cKO). F3 mice were used for experiments and housed according to genotype. The same breeding scheme was used to

generate *Eif4e2^{+/+}:Gad2-Cre* (referred to in the text as 4EHP-WT) and *Eif4e2^{flx/flx}:Gad2-Cre* (referred to in the text as 4EHP-gKO) using GAD65-Cre mice (GABAergic interneurons, where Cre recombinase activity occurs around embryonic day (e) 15 [263], JAX stock no. 010802, on C57BL/6 background). *Rptor^{flx/flx}:Camk2a-Cre* were used as previously characterized [264]. Comparisons were made between these genotypes to normalize for any confounding effects generated by the presence of Cre recombinase alone.

3.3.3. Genotyping

Mouse genotype was determined for each animal using PCR and gel electrophoresis. *Eif4e2* gene was amplified using 5'-TCAGAGCAAGAACAACCTTACAGGACCAAG forward and 5'-GGCCCAGCCTGCCTGGCATTCTAGTGG reverse primers. The PCR product was separated through a 1.5% agarose gel using a 150 V potential difference. WT bands were detected around 700 bp and floxed bands at 850 bp. To detect the presence of Cre (300 bp), the forward 5'-GATTGCTTATAACACCCTGTTACG and reverse 5'-GTAAATCAATCGATGAGTTGCTTCA primers were used.

3.3.4. Western blot

Soluble protein lysates were prepared by homogenizing brain tissue (from 7-9 mice, depending on the experiment) using a pestle grinder in radioimmunoprecipitation assay (RIPA) buffer (R0278, Sigma) on ice containing proteinase (05892970001, Roche) and phosphatase inhibitors (P5726 and P0044, Sigma). Samples were first incubated on ice for 30 min then centrifuged at 16 000 g for 20 min at 4°C. 25 µg of protein from the supernatant were loaded onto a polyacrylamide

gel (final concentration: 12% Acrylamide/Bis Solution, 29:1, 375 mM Tris pH 8.8, 0.1% SDS, 0.1% TEMED, and 0.1% Ammonium Persulfate) and separated using a potential difference of 100 V. Protein was then transferred onto a nitrocellulose membrane at 25 V overnight at 4°C in transfer buffer (25 mM Tris, 190 mM glycine, and 20% methanol, pH 8.3). Membranes were then incubated with 5% albumin (BSA) in Tris-Buffered Saline with Tween 20 (TBST, 20 mM Tris pH 7.5, 150 mM NaCl, 0.1% Tween 20) for 1-2 hr at RT to reduce non-specific binding. Membranes were then probed with one of the following primary antibodies at the indicated dilution: EIF4E2 (GTX103977, GeneTex, 1:500), GAPDH (ab9482, Abcam, 1:40 000), diluted in TBST with 5% BSA overnight at 4°C (or 1 hr at RT for GAPDH). Secondary antibody conjugated to horseradish peroxidase (HRP, anti-mouse and anti-rabbit, GE Healthcare) was diluted 1:5000 in TBST with 5% BSA and added to membranes for 1-2 hr at RT. Membranes were visualized on film after incubating in enhanced chemiluminescence (Western Lighting® Plus ECL, ORT2655:ORT2755, Perkin Elmer) for 1 min. Quantification of the band intensity was done using Image J software (NIH).

3.3.5. Immunofluorescence on brain slices

Mice were placed under general isoflurane anesthetics until loss of pain reflex. Mice were then transcardially perfused with filtered ice-cold PBS then ice-cold 4% PFA. Dissected brains were placed in ice-cold 4% PFA overnight at 4°C for post-fixation and then moved to 30% sucrose in PBS for 3 d at 4°C for cryoprotection. 20 µm coronal sections were prepared using a cryostat and adhered to glass coverslips (12-550-15, Fisher). Sections were placed in boiling 10 mM sodium citrate buffer, pH 6.0 for 20 min for antigen retrieval after being washed 3 times in PBS for 5 min.

Sections were placed in blocking solution (10% BSA and 0.5 % Tween 20 in PBS) for 1-2 hr at RT. The following primary antibodies were used to probe for: eIF4E2 (sc-100731, Santa Cruz), CaMKII α (sc-13141), GAD67 (ab213508, Abcam), Phospho-S6 Ribosomal Protein (Ser240/244) (D68F8) XP (5364, Cell Signaling Technology), EMX1 (PA5-35373, Thermo), PVALB (195004, Synaptic System), Somatostatin 28 (ab111912, Abcam), Laminin (L9393, Sigma) diluted 1:100 in blocking solution overnight at 4°C. Sections were incubated with Alexa-conjugated secondary antibodies (1:300) and Hoechst (1:1000) diluted in blocking buffer for 1-2 hr at RT in the dark. Coverslips were mounted with DAKO. Samples were visualized 24 hr later with a ZEISS Laser Scanning Microscope 880.

3.3.6. Administration of anisomycin

Anisomycin was first dissolved dropwise with 1M HCl. Saline was slowly added to make the stock solution of 15 mg/ml. Solution pH was adjusted to 7.4 by dropwise addition of 1M NaOH. Anisomycin was delivered to mice at 150 mg/kg via intraperitoneal injection prior to experiments as indicated. This dose of anisomycin was shown to inhibit protein synthesis in the hippocampus by around 90% 30 min after intraperitoneal injection in mice [265]. Inhibition was reduced to baseline after 6 hr.

3.3.7. Morris Water Maze

The Morris Water Maze (MWM) memory task was performed as previously described [266]. Mice were trained with either 1 trial per day (weak) or 3 trials per day (strong) over 5 consecutive days in a circular pool 1 m in diameter. Learning was determined manually by timing the latency to

locate the hidden (submerged) platform (i.e. escape latency). For probe trials on the following day (day 6), the platform was removed from the maze and the animals were given 60 s to navigate the maze. The percentage of time spent in each quadrant of the maze (quadrant occupancy) was recorded using an automated video tracking system (HVS Image, Buckingham, UK).

3.3.8. T-maze

The T-maze is a test to measure spatial working memory. The T-maze consists of a runway (stem) with a left and right arm choice at the end. The maze is enclosed by short walls so the animal can navigate using cues in the environment. Mice were individually placed at the bottom of the stem. For the training phase, one of the maze arms was closed and the animal was allowed to freely explore the other maze arm for 10 min. After one hour, the mouse was reintroduced to the maze with exception that the animal could enter the previously closed and unexplored arm. We used the animal's innate preference for novelty to probe their ability to alternate exploratory behavior of the previously unencountered T-maze arm. Each trial was recorded using an overhead camera and performance was quantified manually. Time spent in the familiar arm and novel arm were scored. From this data we further calculated discrimination index (DI, see equation below).

$$DI(\%) = \frac{\textit{novel arm} - \textit{familiar arm}}{\textit{total exploration time}} \times 100$$

3.3.9. Contextual fear conditioning

Mice were placed in a sound-proof box containing an enclosed isolation chamber with an electric grid floor and overhead camera. Mice were recorded for 2 min before receiving a mild foot shock

(0.7 mA, 1 sec). After 1 min, mice were removed and placed back in their home cage. After 24 hr, mice were placed back in the enclosure (context) and recorded for 4 min. The average percent freezing over 4 min was used as an assessment of LTM.

3.3.10. Statistical analysis

Statistical analysis was performed on GraphPad Prism 9. An unpaired t-test was used to compare one experimental parameter. Mixed design two-way ANOVA was used to compare two experimental parameters (i.e. genotype as an independent variable and arms in the elevated plus maze test as a repeated measure). Bonferroni test was used for pair-wise post-hoc analysis where there was a significant interaction in the data. A Welch's corrected t-test was used where the difference in variance between groups was significantly different according to the Levene's test. Data were expressed as mean \pm s.e.m. and p values < 0.05 were considered statistically significant. Details of all statistics used are listed in Supplementary Table S3.1.

3.4. Results

3.4.1. Conditional deletion of 4EHP in CaMKII α -positive excitatory neurons

We previously generated and characterized an excitatory neuron-specific 4EHP KO model which displayed impaired sociability, hyperactivity, and synaptic plasticity dysfunction which are reminiscent of autism spectrum disorder (ASD) [121]. We used EMX1 to drive Cre expression to excitatory neurons since EMX1 is expressed during embryonic development. Deleting 4EHP early in development was necessary to include the possibility of developmental effects which are characteristic of ASD. Here, we sought to preclude potential developmental effects of 4EHP on learning and memory by driving Cre expression under the CaMKII α promoter. Cre recombinase activity was originally reported to occur at P19 [236], although recent work has shown gene deletion as early as P14 [147,237]. To generate excitatory neuron-specific deletion of 4EHP, we crossed *Eif4e*^{2^{flx/flx}} with mice expressing Cre recombinase under the *Camk2a* promoter (Fig. 3.1A). Genotyping confirmed homozygous floxed alleles and the presence of Cre (Fig. 3.1B). Immunofluorescence imaging of the CA1 hippocampus using antibodies against 4EHP and CaMKII revealed cell-type-specific KO of 4EHP in excitatory neurons (Fig. 3.1C). We further confirmed that deletion of 4EHP occurs at P60 (Fig. 3.1 D and F) but not at P0 (Fig. 3.1 D and E) via western blotting.

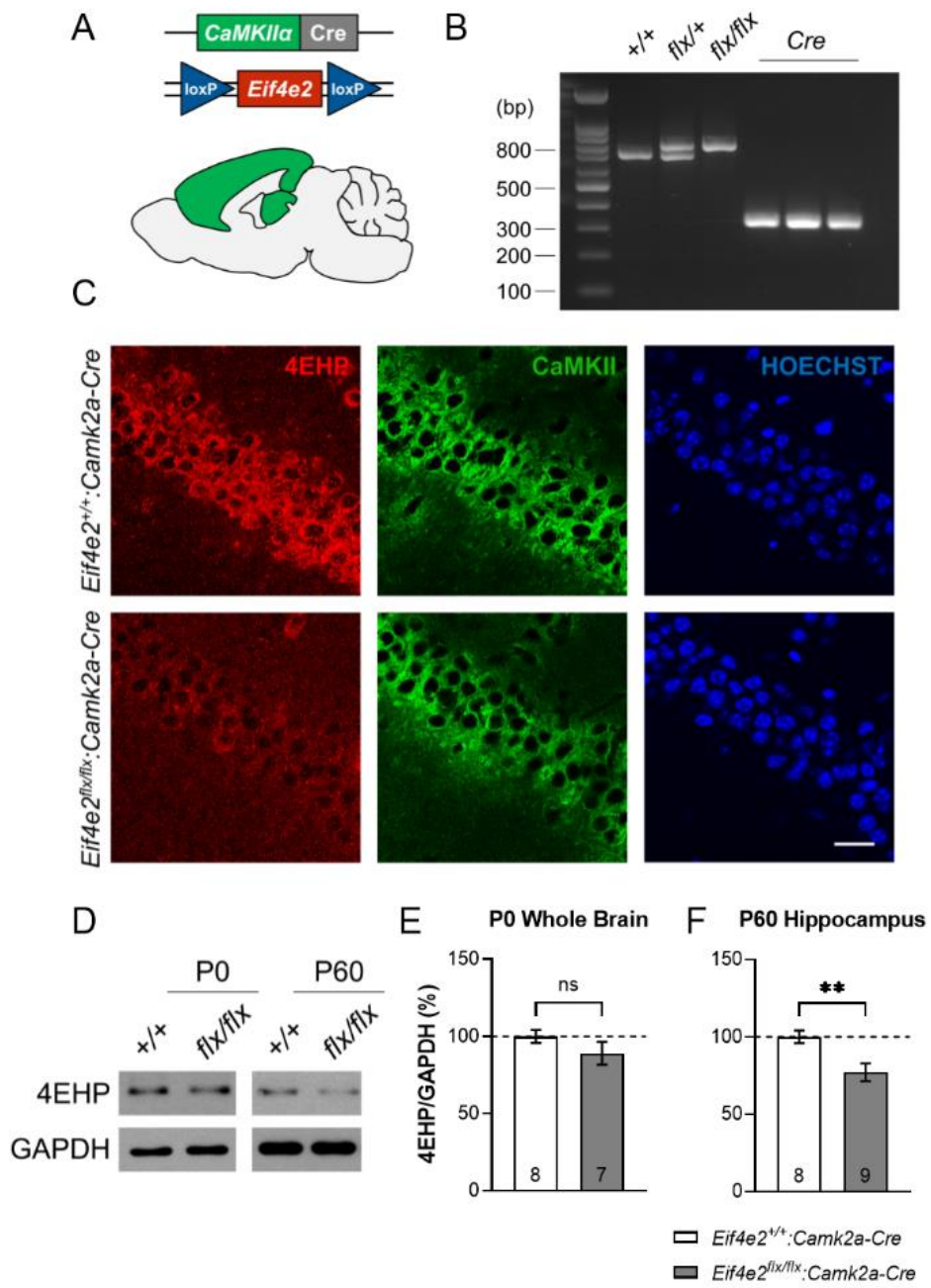


Figure 3.1. Conditional deletion of 4EHP in CaMKII α -positive excitatory neurons.

A Schematic depicting forebrain and hippocampal regions mainly (but not exclusively) targeted for Cre recombinase expression under the promoter of *Camk2a*. *Eif4e2* was flanked with loxP sites on both alleles. **B** Genotyping confirms WT or homozygous flx/flx mice with Cre recombinase. **C** Immunofluorescence analysis on the CA1 region of hippocampal coronal slices confirms specific deletion of 4EHP (red) in CaMKII-positive excitatory neurons (green). Hoechst-stained nuclei are in blue, scale bar represents 20 μ m. Images are representative of replicated independent experiments. **D** Western blot analysis further validates loss of 4EHP protein in the hippocampus of P60 mice (WT n=8, cKO n=9) but not in P0 whole brain (WT n=8, cKO n=7). **E** and **F** are quantifications of **D**. Data are presented as mean \pm s.e.m. **p<0.01; ns, not significant. P value calculated using an unpaired t-test. Sample size is located within the bar graph for each group.

3.4.2. 4EHP in excitatory neurons is not required for long-term memory

Given the necessity of de novo protein synthesis in LTM formation, we first tested 4EHP-cKO mice for contextual fear conditioned memory (Fig. 3.2A). Mice were placed in a context with an electric grid floor and scored for naïve freezing prior to receiving either a weak (0.3 mA) foot shock for 1 sec or a medium strength (0.7 mA) foot shock for 1 sec. LTM was assessed by freezing behavior 24 hr following the foot shock. Under both conditions, LTM was not changed in 4EHP-cKO mice (Fig. 3.2 B and C). Next, we subjected mice to the MWM spatial navigation learning and memory task (Fig. 3.2D). Mice were trained to locate a hidden platform over 5 days having been given a training protocol of either 1 trial per day (weak) or 3 trials per day (strong). With a weak training protocol, mice learned the task after 5 days (Fig. 3.2E) but did not show memory retention on the 6th day test where the hidden platform was removed and mouse quadrant occupancy was scored (Fig. 3.2F). Given a strong training protocol, 4EHP-cKO mice had a significantly increased latency to locate the hidden platform on training day 2 by 16 sec but were comparable to WT on days 3 to 5 (Fig. 3.2G). Both WT and 4EHP-cKO mice showed a similar preference for the target quadrant on the following test day (Fig. 3.2H). Together these data indicate that 4EHP in excitatory neurons does not mediate LTM.

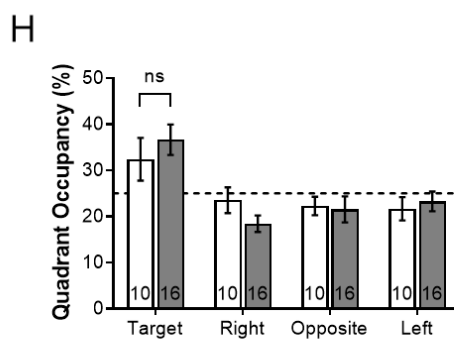
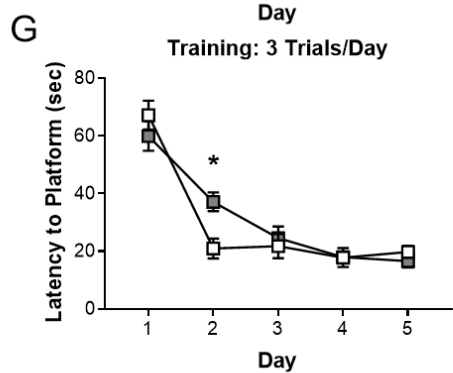
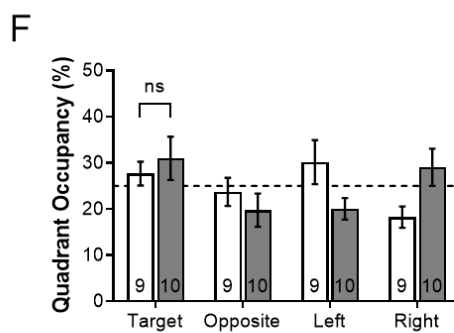
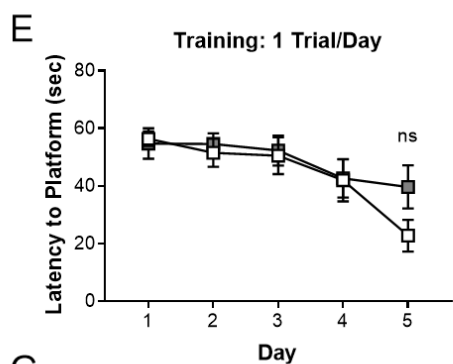
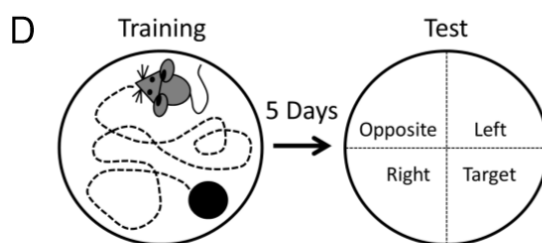
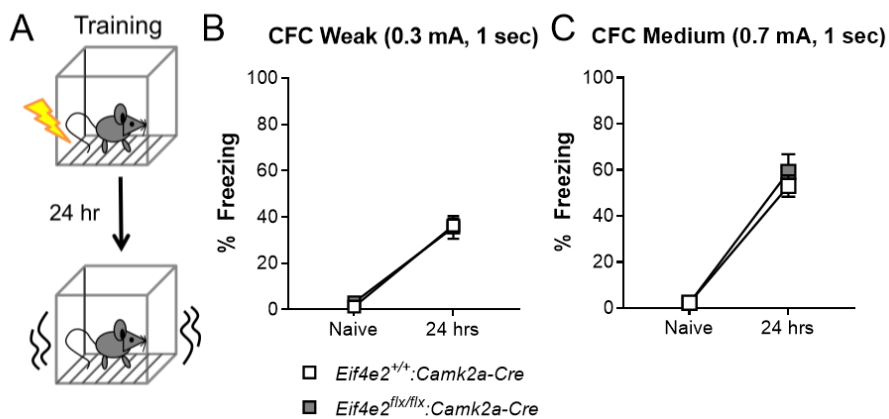


Figure 3.2. Long-term memory is normal in 4EHP-CaMKII α KO mice.

A Schematic depicting contextual fear conditioning (CFC) training and LTM test regime. **B** With weak CFC (0.3 mA, 1 sec) training, 4EHP cKO mice (n=10) show the same freezing behavior as WT (n=8) 24 hr after receiving a foot shock. **C** 24 hr freezing behavior is not altered in 4EHP-cKO mice (n=8) compared to WT (n=9) with a medium foot shock (0.7 mA, 1 sec) training. **D** Training and testing paradigm for assessing memory in the MWM. Mice were trained to locate a hidden platform in a water maze using spatial cues for 5 days. On the 6th day, the platform was removed, and mice were scored for time spent in each quadrant of the maze. **E** Learning curve graphed as latency to find platform on training days using a mild training protocol of 1 trial per day (WT n=9, cKO n=10). **F** Percent time mice spend in each quadrant. Dashed line at 25% indicates no learning. **G** Learning curve graphed as latency to find platform on training days using a stronger training protocol of 3 trials per day (WT n=10, cKO n=16). **H** Percent time mice spend in each quadrant. Dashed line at 25% indicates no learning. Data are presented as mean \pm s.e.m. *p<0.05; ns, not significant. P value calculated using 2-way ANOVA repeated measures with Bonferroni multiple comparisons test. Sample size is located within the bar graph for each group.

3.4.3. Spatial working memory requires 4EHP in both excitatory and inhibitory neurons.

Deletion of the translational repressor protein 4E-BP2 was previously shown to impair WM in mice [205]. This finding suggests that cap-dependent translation has a role in regulating working memory (WM), but the mechanistic details are completely unknown. We tested 4EHP-cKO and WT mice in a T-maze spatial WM task (Fig. 3.3C). Similar to 4E-BP2 KO mice, we observed robust WM impairment in 4EHP-cKO mice compared to WT controls (Fig. 3.3 D and E) without changes to total exploratory behavior (Fig. 3.3F). We next investigated WM in inhibitory neuron-specific 4EHP KO mice (4EHP-gKO). We first validated specific deletion of 4EHP in GABAergic (GAD67-positive) neurons by immunofluorescence (Fig. 3.4A) in the prefrontal cortex where 4EHP is primarily expressed in neuronal cell types (Fig. S3.1). Similar to 4EHP-cKO mice, 4EHP-gKO also demonstrate WM impairment (Fig. 3.4 B and C) without changes in total exploratory behavior (Fig. 3.4D) and do not show long-term CFC memory impairments (Fig. 3.4E). These memory impairments were specific to spatial WM, as short-term (1 hr, Fig. 3.3A) contextual fear memory was not impacted (Fig. 3.3B). We conclude that 4EHP in both excitatory and inhibitory neurons is necessary for intact spatial WM.

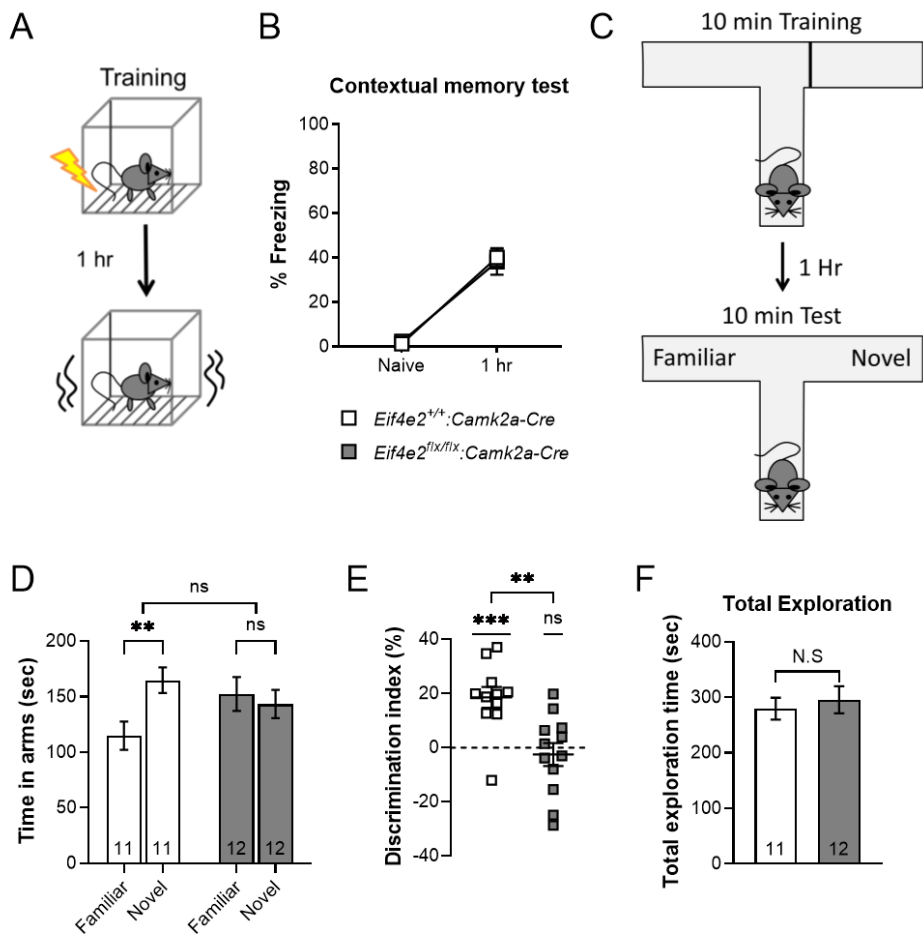


Figure 3.3. Working memory is impaired in 4EHP-CaMKII α KO mice.

A Schematic depicting contextual fear conditioning (CFC) training and short-term memory test regime. **B** CFC fear memory calculated by % freezing 1 hr after receiving a mild foot shock (0.3 mA, 1 sec) (WT n=10, cKO n=9). **C** Schematic depicting T-maze spatial WM test. Mice were placed in a T-maze facing away from the junction (starting point) with one of either arms blocked for 10 min. After 1 hr, mice were placed back in the maze with free access to both arms for 10 min of exploration. **D** Time spent in either the familiar or novel arm (WT n=11, cKO n=12). **E** Memory is shown as a discrimination index for novel vs. familiar arm where 0% means equal time spent in both arms. **F** Total exploration in either arm. Data are presented as mean \pm s.e.m. **p<0.01, ***p<0.001; ns, not significant. P value calculated using 2-way ANOVA repeated measures with Bonferroni multiple comparisons test, one sample t-test, or unpaired t-test. Sample size is located within the bar graph for each group.

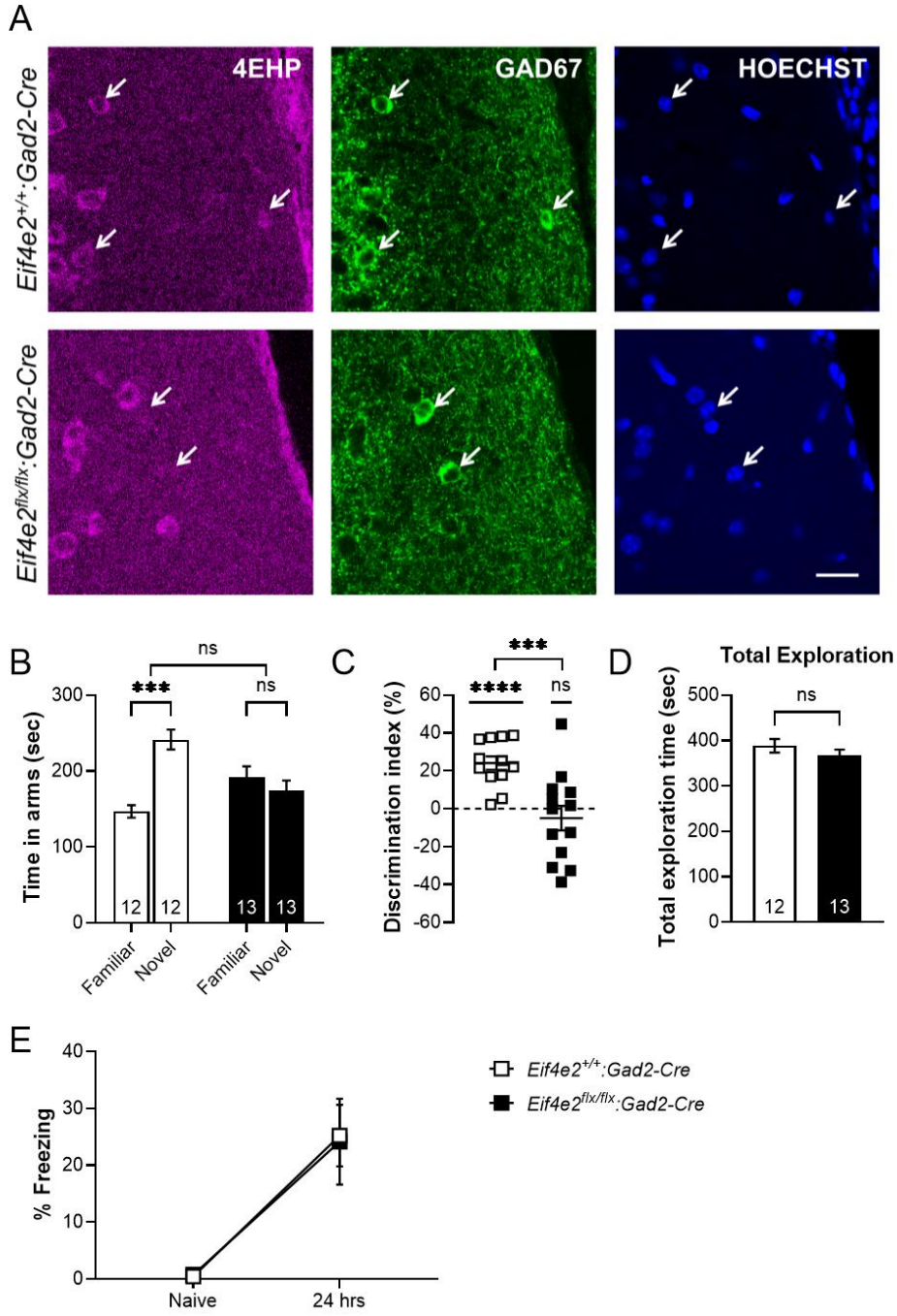


Figure 3.4. Working memory is impaired in 4EHP-GAD65 KO mice.

A Immunofluorescence analysis on prefrontal cortex coronal slices confirms specific deletion of 4EHP (purple) in GAD67-positive inhibitory neurons (green). Hoechst-stained nuclei are in blue, scale bar represents 20 μm . Images are representative of replicated independent experiments. **B** Time spent in either the familiar or novel arm of the T-maze during a working memory task (WT n=12, gKO n=13). **C** Memory is shown as a discrimination index for novel vs. familiar arm where 0% means equal time spent in both arms. **D** Total exploration in either arm. **E** With weak CFC (0.3 mA, 1 sec) training, 4EHP gKO mice (n=9) show same freezing behavior as WT (n=9) 24 hr after receiving the foot shock. Data are presented as mean \pm s.e.m. ***p<0.001, ****p<0.0001; ns, not significant. P value calculated using 2-way ANOVA repeated measures with Bonferroni multiple comparisons test, one sample t-test, or unpaired t-test. Sample size is located within the bar graph for each group.

3.4.4. Sustained, but not acute inhibition of translation impairs working memory

We next assessed if protein synthesis has a direct role in T-maze spatial WM. WT mice on C57Bl/6 background were injected (i.p.) with anisomycin (150 mg/kg) 1 hr prior to training and assessed for WM in the T-maze (Fig. 3.5A). This dose of anisomycin was shown to inhibit protein synthesis in the hippocampus by around 90% 30 min after i.p. injection in mice [265]. Compared with vehicle treatment, anisomycin had no effect on WM (Fig. 3.5 B-C), suggesting that de novo protein synthesis is not acutely necessary for WM. We next sought to elucidate how 4EHP mediates WM based on its known functions. We previously performed an unbiased ribosome profiling study where the translational efficiency (TE) of mRNAs in mouse embryonic fibroblasts (MEFs) lacking 4EHP expression were determined compared to WT [28]. In this study, the ERK1/2 signalling pathway was negatively regulated by 4EHP deletion via translational upregulation of the ERK1/2 phosphatase *Dusp6* [28]. However we did not previously observe changes in p-ERK1/2 in 4EHP KO brain [121]. Here we instead assessed the activity of the mTORC1 signalling pathway in the hippocampus of 4EHP-cKO mice using immunofluorescence analysis. We observed a 36.4% reduction in p-S6 (S240/44) signal in 4EHP-cKO excitatory neurons (Fig. 3.5 E-F), consistent with reduced mTORC1 activity. Furthermore, mice lacking the defining component of the mTORC1 complex (Raptor) in excitatory neurons (*Rptor^{flx/flx}:Camk2a-Cre*), which results in reduced p-S6 (S240/44) levels (Fig. 3.5G), have impaired working memory (Fig. 3.5H). Together these data suggest that WM does not require de novo protein synthesis but that prolonged attenuation of mTORC1 via loss of 4EHP circumvents WM.

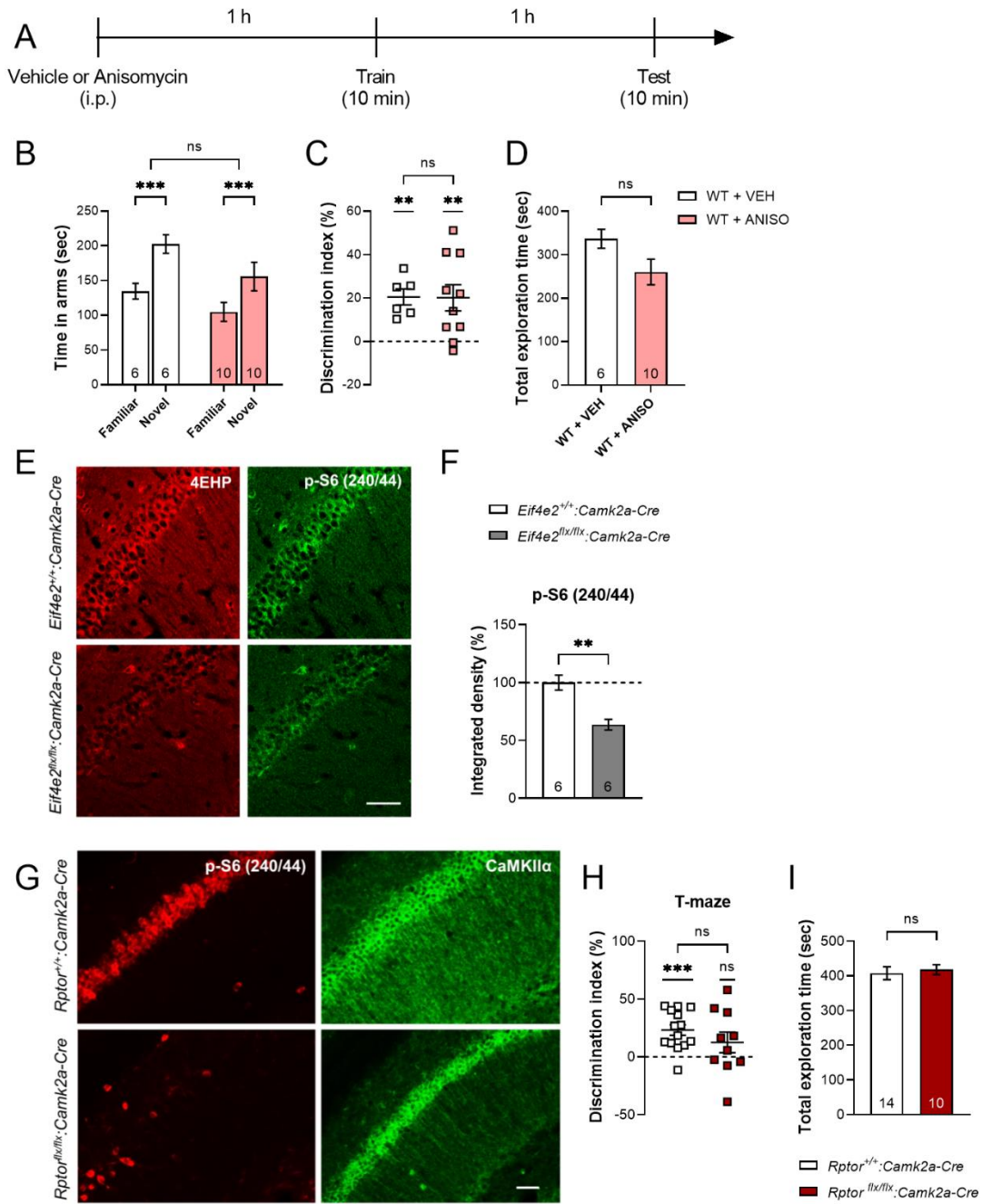


Figure 3.5. Working memory is impaired after sustained, but not acute inhibition of protein synthesis.

A Anisomycin or vehicle was administered via intraperitoneal injection (i.p.) 1 hr prior to training in a T-maze. Working memory was assessed 1 hr after training. Both training and testing sessions were 10 min. **B** Time spent in either the familiar or novel arm during the test. **C** Memory is shown as a discrimination index for novel vs. familiar arm where 0% means equal time spent in both arms. **D** Total exploration time of both maze arms was assessed as a potential confounding variable. **E** Immunofluorescence analysis of p-S6 (Ser240/244) in 4EHP-cKO vs. WT mouse hippocampus. **F** Quantification of p-S6 integrated density was performed on CA1 pyramidal neurons using image J. Scale bar represents 60 μm . **G** Immunofluorescence analysis of p-S6 (Ser240/244) in *Rptor^{flx/flx}:Camk2a-Cre* mouse hippocampus compared to *Rptor^{+/+}:Camk2a-Cre*. **H** Discrimination index for T-maze working memory in *Rptor^{flx/flx}:Camk2a-Cre* (n=14) compared to *Rptor^{+/+}:Camk2a-Cre* (n=10). **I** Total exploration time of both maze arms. Data are presented as mean \pm s.e.m.; **p<0.01; ***p<0.001; ns, not significant. P value calculated using 2-way ANOVA with repeated measures, one sample t-test, or unpaired t-test. Sample size is located within the bar graph for each group.

3.5. Discussion

Rapid de novo protein synthesis in neurons is required for memory consolidation [227]. Temporally inhibiting cap-dependent translation via eIF4E during consolidation prevents LTM formation [226]. Similarly, translational control via phosphorylation of eIF2 α on Ser 51 acts as a critical gatekeeper of LTM whereby the non-phosphorylatable Ser51Ala mutant mice have a lower threshold for L-LTP and enhanced LTM [178,217]. Given the necessity of de novo protein synthesis for LTMs and the emerging importance of microRNAs in synaptic plasticity and memory [262], we investigated 4EHP in LTM. To this end, we screened 4EHP conditional KO mice in a variety of LTM tests. First, using a classic conditioned memory paradigm (CFC), we tested 4EHP both in excitatory and inhibitory neurons for memory 24 hr post training. In both models, memory retention was comparable to WT controls (Fig. 3.2 B-C and Fig. 3.4E, respectively). We further assessed 4EHP-cKO mice in the MWM where we did not observe any changes to LTM given either a mild or strong training regime (Fig. 3.2 D-H). Given these results, we conclude that 4EHP in either excitatory or inhibitory neurons alone is sufficient to mediate LTM. Ablation of 4EHP in all neurons will be required to conclusively exclude a role for 4EHP in LTMs.

Protein synthesis has an unappreciated role in memories required for executive function, such as WM. This is likely because early studies demonstrated that short-term memories remain intact despite blocking protein synthesis with anisomycin or cycloheximide [267–270]. Furthermore, in vivo recordings have revealed an important role of prefrontal cortical neuron firing for a WM delayed-response task [271]. We can not exclude the possibility, however, that a properly regulated proteome is necessary to facilitate the mechanisms underlying short-term-like

memories. This is supported by studies showing WM impairments in mice lacking protein synthesis repressing proteins, such as 4E-BP2 [205] and PERK [206,272]. Here, we show that 4EHP in both excitatory and inhibitory neurons is necessary for WM (Fig. 3.3 D-F and Fig. 3.4 B-D). Since deletion of 4EHP in either cell type abolishes WM, we conclude that the coordinated function of excitatory and inhibitory neurons mediates WM, as opposed to each cell type being sufficiently able to orchestrate WM.

We previously showed that mice lacking 4EHP in excitatory neurons defined by EMX1 have impaired preference for social novelty in the 3-chamber sociability assay [121]. It can be argued that this impairment is mediated by a WM deficiency, rather than social interaction. However, 4EHP-EMX1 KO mice were also impaired in the direct/reciprocal social assay which is unlikely to be confounded by WM deficits. Furthermore, 4EHP-gKO mice, which have impaired working memory, do not show impairments in the 3-chamber sociability assay or exaggerated grooming behavior (Fig. S3.2). This raises an interesting possibility that 4EHP function is not only important for social behavior, but also for cognition. This is consistent with findings that executive functions, such as WM, are often affected in patients with ASD [273–275]. Together these studies on 4EHP provide not only another layer of mechanistic complexity mediating memory but offer a potential therapeutic avenue for treating neurodevelopmental disorders such as ASD.

In attempts to understand how 4EHP mediates working memory, we observed a reduction in p-S6 levels in 4EHP null excitatory neurons, consistent with attenuated activity of mTORC1 signalling. One possible explanation for this finding is that 4EHP translationally represses factors

that have direct roles in regulating this signalling pathway. This type of regulation was previously observed in an unbiased ribosome profiling study where the translational efficiency (TE) of mRNAs in mouse embryonic fibroblasts (MEFs) lacking 4EHP expression were determined compared to WT [28]. In this study, TE of the ERK1/2 phosphatase *Dusp6* was significantly upregulated in 4EHP KO MEFs which resulted in reduced p-ERK1/2 levels and impairments in cell proliferation and increased apoptosis [28]. In the list of top differentially translated genes, we found the N-Myc Downstream Regulated 1 (*Ndrp1*) gene as being significantly ($p=0.00069044$) translationally upregulated (KO/WT average TE=2.06588987) in 4EHP KO MEFs, without changes in transcript levels [28]. NDRG1 is a cytoplasmic protein that functions in regulating stress and hormone responses, cell growth, and cell differentiation [276]. Autosomal-recessive mutations in NDRG1 cause Charcot-Marie-Tooth disease, resulting in motor and sensory neuropathy [277,278]. NDRG1 overexpression was shown to suppress growth of glioblastoma cells by suppressing AKT and S6 cell signaling [279]. Future studies are required to determine if translational de-repression of NDRG1 is suppressing mTORC1 signalling in 4EHP null neurons. Together, our results suggest that sustained mTORC1-S6 activity, which may be modulated directly by 4EHP via translational control of factors such as NDRG1, is necessary to support working memory.

Chapter 4: General Discussion

4.1. Summary and integration of findings

Taken together, the work presented in this thesis provides the first characterization of 4EHP in the brain and implicates a novel role for 4EHP in ASD and memory. In summary, the expression of 4EHP increases throughout development across various brain regions. Both excitatory and inhibitory neurons express 4EHP, whereas endothelial cells do not. 4EHP localizes to synaptosomes but is also expressed in the cytosol. In 4EHP-eKO mice, expression of the critical 4EHP-binding partner GIGYF2 is reduced and the animals display impaired social interaction and exaggerated mGluR-LTD. 4EHP does not regulate global rates of de novo protein synthesis in the brain, suggesting that dysregulated translation of specific mRNAs may be causing these phenotypes. Despite the strong genetic link between mutations in *GIGYF2* and the development of ASD, both *Eif4e2* and *Gigyf2* are haplosufficient in mice. Working memory (WM), but not long-term memory, is impaired in both 4EHP-cKO and -gKO mice. Loss of 4EHP in excitatory neurons reduces mTORC1 activity, which is sufficient to impair to WM. The following sections will discuss the integration of these findings and their potential relevance to human health and disease.

4.1.1. How might *GIGYF2* mutations engender ASD?

GIGYF2 mutations in ASD patients are heterozygous as they are inherited either maternally or paternally, or arise from de novo mutations. Homozygous de novo mutations are known to occur, for example in the *C1NH* gene which causes hereditary angioedema [280], but are unlikely events. The lack of ASD-like phenotypes in *Gigyf2* heterozygous mice may suggest that *GIGYF2* in humans is also haplosufficient and therefore not linked to the development of ASD. However, this direct comparison between mouse and human does not take into consideration several important

factors. First, heterozygous mice were housed in mixed genotypes. It is known, for example in the *Cntnap2*^{-/-} (contactin associated protein 2) mouse model of neurodevelopmental disorders [281], that KO mice raised with WT littermates fail to present ASD-like behaviors that are present if they are otherwise raised with littermates of the same genotype. In the case of *Cntnap2*, the authors demonstrate that co-housing after weaning restores the microbiome profile in KO mice similar to WT controls [281]. Future experiments housing *Gigyf2*^{+/+} and heterozygous mice separately after weaning might provide insight into this possibility. Second, the biochemical nature of the *GIGYF2* mutations in humans is unknown. Despite being heterozygous, a dominant negative mutation, for example, could adversely affect the normal gene product within the same cell, thereby causing the ASD phenotypes. Further experiments are therefore necessary to specifically address the biochemical nature of ASD-linked *GIGYF2* mutations on protein function.

It is also possible that the effects of *GIGYF2* mutations in ASD patients are independent of 4EHP [282]. This would conversely suggest that the ASD-like phenotypes observed in 4EHP-eKO mice are independent of *GIGYF2* loss of function. However, given the close functional relationship between 4EHP and *GIGYF2*, it is more likely that the findings presented here are consistent with and support a causative role of *GIGYF2* mutations in ASD pathogenesis. For instance, the truncation mutations in *GIGYF2* most likely stimulate NMD mechanisms resulting in loss of protein levels and destabilization of 4EHP. To address this directly, one could create cell lines harboring the ASD-linked mutations in *GIGYF2* and perform the appropriate biochemical analysis on 4EHP. Such experiments would include a 5' cap pulldown assay to determine if 4EHP

association with the cap is changed and a proximity ligation assay to determine if interaction between 4EHP and GIGYF2 is reduced.

4.1.2. What is the link between working memory and ASD?

Given the role of 4EHP in translational repression, particularly as part of the miRNA gene silencing mechanism, we hypothesized that long-term memories are regulated by 4EHP. It was indeed unexpected to not only observe normal long-term memory in 4EHP conditional KO mice, but instead find an impairment in WM. Retrospectively, investigating WM in these models is a logical progression after the initial observation of ASD-like behaviors and synaptic plasticity dependency on 4EHP. The T-maze test used to assess WM is also useful for identifying a certain aspect of ASD behaviors, which is the insistence on sameness [283]. Numerous studies have identified WM impairments in patients with ASD, a consistent finding shown to be significant in a meta-analysis review [284]. For instance, in a study examining visuospatial working memory (VSWM) in ASD and ADHD (attention deficit/hyperactivity disorder), the ASD, but not ADHD group showed poorer performance in VSWM than control groups [285]. Furthermore, in a cross-sectional comparative study between participants with high-functioning ASD and those typically developing, it was found that in general, WM was impaired in the individuals with ASD [274].

Although WM is not specifically part of the diagnostic criteria for ASD, it is necessary for many aspects of human life, including intellectual ability and intelligence quotient (IQ). Intellectual disability (ID) is co-morbid in roughly 30% of patients with ASD [286]. In previous diagnostic criteria (i.e. according to the DSM IV), IQ cut-offs for ID were: 50-55 to 70 (mild), 35-40 to 50-55

(moderate), 20-25 to 35-40 (severe), and < 20-25 (profound) [287]. The current diagnostic criteria (i.e. according to the DSM-V) places less emphasis on IQ as a sole determinant for ID, and incorporates impairments in other domains such as conceptual, social, and practical abilities [288].

4.1.3. What are the implications of altered translation in working memory?

From the puromycin incorporation assay, we did not observe a change in global rates of de novo protein synthesis in 4EHP-eKO brain, despite previous findings in a cell model [14]. One explanation is that in a mouse, compensatory mechanisms are sufficient to balance the proteome from the loss of 4EHP. In this case, the compensation would be necessary for cell or organism survival. This argument has been proposed similarly against the hypothesis that an excitatory to inhibitory input (E/I) imbalance is the major driver of ASD phenotypes [289]. The authors of this study observed that in four different mutant mouse models of ASD, there was an increase in E/I conductance ratio, but feedforward spiking, synaptic depolarization, and spontaneous spiking were normal. In other words, the E/I imbalance is a result of compensatory mechanisms maintaining synaptic depolarization for cells near spike threshold and not the factor driving ASD phenotypes. The findings of reduced mTORC1 activity in cells lacking 4EHP could similarly be a compensatory mechanism to maintain proteostasis which would explain why global rates of de novo protein synthesis are not changed overall. However, reduction in mTORC1 activity itself can drive WM impairments, as deletion of Raptor alone was sufficient to impair WM. This suggests that mTORC1 activity regulates the expression of critical factors involved in WM. In this case, the WM impairments in 4EHP conditional KO mice are likely a direct consequence of reduced

mTORC1 activity by 4EHP-mediated translational control of factors regulating the mTORC1 pathway (see discussion in section 3.5).

Another mechanism which could compensate for the loss of 4EHP would be through activation of the ISR pathway and increased phosphorylation of eIF2 α . This possibility remains to be examined in our models. It was recently shown that in both iPSCs from Down syndrome (DS) patients and in a mouse model of DS, p-eIF2 α was increased [187]. Genetic or pharmacological inhibition of the ISR was sufficient to rescue the deficits in memory and synaptic plasticity in the DS mouse model. The authors argued that the “ISR-mediated maladapted regulation of protein synthesis may [be] a central molecular mechanism underlying the cognitive decline associated with DS” [187]. The authors go on to suggest that correcting the overall translation program may be more beneficial than targeting individually dysregulated genes. These findings argue against our claim that reduced activity of mTORC1 in 4EHP-cKO brains may be the underlying driver of WM impairments by insufficient translation of WM genes, since overall translation rates are unaffected.

4.1.4. What are the potential mechanisms of 4EHP in the brain?

4.1.4.1. Post translational modifications

The molecular mechanism of 4EHP in the brain (in any cell type) is currently unknown. There are, however, numerous possibilities to regulate 4EHP function. First, 4EHP was shown to undergo interferon-stimulated gene 15 (ISG15) modification which enhances the cap structure-binding activity of 4EHP [290]. This may have important implications for the role of 4EHP in antiviral

immunity [83]. There are also candidate 4EHP-binding proteins that may regulate its function. The Sonenberg lab previously identified 4E-T as a 4EHP-binding protein in a BioID proteomic screen using 4EHP as bait [18]. Direct interaction with 4E-T increases 4EHP cap-binding affinity by fourfold. Furthermore, a phosphoproteomic study identified the basophilic RxRxxS/T (R, arginine; S, serine; T, threonine; and x, any amino acid) [291] phosphorylation site motif in 4E-T which is sensitive to receptor tyrosine kinase inhibitors [292]. These phosphorylation events may have important implications for regulating the cap-binding affinity of 4EHP and miRNA-mediated translation repression.

4.1.4.2. Phase separation and biomolecular condensates

4E-T also colocalizes with mRNA decapping factors in processing bodies (P-bodies) [293,294], a type of biomolecular condensate [295]. There is a growing appreciation for the role of phase separation as one of the major driving forces behind biomolecular condensate formation [296]. For example, the translational repressor protein FMRP phase separates in the presence of RNA [297,298]. Furthermore, the components of the miRNA silencing machinery, including miRISC, condense into phase-separated droplets which is accompanied by accelerated deadenylation of target RNAs bound to Ago2 [299]. Based on predictive modeling, the 4EHP-interacting proteins GIGYF2 and 4E-T are highly likely to phase separate (PSPredictor scores [300]; GIGYF2: 0.97; 4E-T: 0.95; with 1 being the strongest prediction). 4EHP itself was previously shown to localize to stress granules upon heat shock [301]. Intriguingly, the ratio of 4EHP to eIF4E in cells shifts in favour of 4EHP at higher temperatures [302]. Given these observations, the function of 4EHP is

likely regulated by its interacting proteins, their post translational modification, and phase separation into biomolecular condensates.

4.1.5. Concluding remarks

Brain disorders affect hundreds of millions of individuals worldwide and constitute a major economic burden [303]. Clinically, neurological disorders are particularly difficult to diagnose and treat given the significant interpatient heterogeneity in symptom manifestation, even among patients harboring the same disease-causing genetic mutation [304]. As a result, patients are often treated for symptomatic resolution with only minor improvements in health outcome. The complexity of the brain has made research progress difficult and drug development slow. Of the neuropsychiatric drugs tested in clinical trials, only 9% succeed and become available for patient use [305]. Developing effective therapeutics for brain disorders is founded on a comprehensive understanding of the molecular mechanisms underlying brain function. Regulated mRNA translation is essential for proper brain development and function. Multiple mechanisms govern the rate, specificity, and localization of mRNA translation and their dysfunction constitute a risk factor for neuropathological conditions, such as ASD. Together the findings presented in this thesis provide the first insights into the neurobiological function of 4EHP with particular relevance for ASD and memory.

References

1. Pelletier J, Schmeing TM, Sonenberg N: **The multifaceted eukaryotic cap structure.** *Wiley Interdiscip Rev RNA* 2021, **12**:e1636.
2. Galloway A, Cowling VH: **mRNA cap regulation in mammalian cell function and fate.** *Biochim Biophys Acta Gene Regul Mech* 2019, **1862**:270–279.
3. Topisirovic I, Svitkin Y V, Sonenberg N, Shatkin AJ: **Cap and cap-binding proteins in the control of gene expression.** *Wiley Interdiscip Rev RNA* 2011, **2**:277–298.
4. Joshi B, Cameron A, Jagus R: **Characterization of mammalian eIF4E-family members.** *Eur J Biochem* 2004, **271**:2189–2203.
5. Zuberek J, Kuchta K, Hernández G, Sonenberg N, Ginalski K: **Diverse cap-binding properties of Drosophila eIF4E isoforms.** *Biochim Biophys Acta - Proteins Proteomics* 2016, **1864**:1292–1303.
6. Worch R, Jankowska-Anyszka M, Niedzwiecka A, Stepinski J, Mazza C, Darzynkiewicz E, Cusack S, Stolarski R: **Diverse role of three tyrosines in binding of the RNA 5' cap to the human nuclear cap binding complex.** *J Mol Biol* 2009, **385**:618–627.
7. Smith RWP, Anderson RC, Larralde O, Smith JWS, Gorgoni B, Richardson WA, Malik P, Graham S V, Gray NK: **Viral and cellular mRNA-specific activators harness PABP and eIF4G to promote translation initiation downstream of cap binding.** *Proc Natl Acad Sci U S A* 2017, **114**:6310–6315.
8. Alekhina OM, Terenin IM, Dmitriev SE, Vassilenko KS: **Functional Cyclization of Eukaryotic mRNAs.** *Int J Mol Sci* 2020, **21**.
9. Martineau Y, Derry MC, Wang X, Yanagiya A, Berlanga JJ, Shyu A-B, Imataka H, Gehring K, Sonenberg N: **Poly(A)-binding protein-interacting protein 1 binds to eukaryotic translation initiation factor 3 to stimulate translation.** *Mol Cell Biol* 2008, **28**:6658–6667.
10. Gingras AC, Raught B, Sonenberg N: **eIF4 initiation factors: effectors of mRNA recruitment to ribosomes and regulators of translation.** *Annu Rev Biochem* 1999, **68**:913–963.
11. Cho PF, Poulin F, Cho-Park YA, Cho-Park IB, Chicoine JD, Lasko P, Sonenberg N: **A new paradigm for translational control: inhibition via 5'-3' mRNA tethering by Bicoid and the eIF4E cognate 4EHP.** *Cell* 2005, **121**:411–423.

12. Rom E, Kim HC, Gingras A-C, Marcotrigiano J, Favre D, Olsen H, Burley SK, Sonenberg N: **Cloning and Characterization of 4EHP, a Novel Mammalian eIF4E-related Cap-binding Protein.** *J Biol Chem* 1998, **273**:13104–13109.
13. Christie M, Igreja C: **eIF4E-homologous protein (4EHP): a multifarious cap-binding protein.** *FEBS J* 2021, doi:10.1111/febs.16275.
14. Morita M, Ler LW, Fabian MR, Siddiqui N, Mullin M, Henderson VC, Alain T, Fonseca BD, Karashchuk G, Bennett CF, et al.: **A Novel 4EHP-GIGYF2 Translational Repressor Complex Is Essential for Mammalian Development.** *Mol Cell Biol* 2012, **32**:3585–3593.
15. Osborne MJ, Borden KLB: **The eukaryotic translation initiation factor eIF4E in the nucleus: taking the road less traveled.** *Immunol Rev* 2015, **263**:210–223.
16. Rosettani P, Knapp S, Vismara M-G, Rusconi L, Cameron AD: **Structures of the Human eIF4E Homologous Protein, h4EHP, in its m7GTP-bound and Unliganded Forms.** *J Mol Biol* 2007, **368**:691–705.
17. Zuberek J, Kubacka D, Jablonowska A, Jemielity J, Stepinski J, Sonenberg N, Darzynkiewicz E: **Weak binding affinity of human 4EHP for mRNA cap analogs.** *RNA* 2007, **13**:691–697.
18. Chapat C, Jafarnejad SM, Matta-Camacho E, Hesketh GG, Gelbart IA, Attig J, Gkogkas CG, Alain T, Stern-Ginossar N, Fabian MR, et al.: **Cap-binding protein 4EHP effects translation silencing by microRNAs.** *Proc Natl Acad Sci* 2017, **114**:5425–5430.
19. Hernández G, Altmann M, Sierra JM, Urlaub H, Diez del Corral R, Schwartz P, Rivera-Pomar R: **Functional analysis of seven genes encoding eight translation initiation factor 4E (eIF4E) isoforms in Drosophila.** *Mech Dev* 2005, **122**:529–543.
20. Holcik M, Sonenberg N: **Translational control in stress and apoptosis.** *Nat Rev Mol Cell Biol* 2005, **6**:318–327.
21. Holcik M, Yeh C, Korneluk RG, Chow T: **Translational upregulation of X-linked inhibitor of apoptosis (XIAP) increases resistance to radiation induced cell death.** *Oncogene* 2000, **19**:4174–4177.
22. Harding HP, Zhang Y, Bertolotti A, Zeng H, Ron D: **Perk is essential for translational regulation and cell survival during the unfolded protein response.** *Mol Cell* 2000, **5**:897–904.

23. Uniacke J, Holterman CE, Lachance G, Franovic A, Jacob MD, Fabian MR, Payette J, Holcik M, Pause A, Lee S: **An oxygen-regulated switch in the protein synthesis machinery.** *Nature* 2012, **486**:126–129.
24. Ho JJD, Wang M, Audas TE, Kwon D, Carlsson SK, Timpano S, Evagelou SL, Brothers S, Gonzalzo ML, Krieger JR, et al.: **Systemic Reprogramming of Translation Efficiencies on Oxygen Stimulus.** *Cell Rep* 2016, **14**:1293–1300.
25. Uniacke J, Perera JK, Lachance G, Francisco CB, Lee S: **Cancer cells exploit eIF4E2-directed synthesis of hypoxia response proteins to drive tumor progression.** *Cancer Res* 2014, **74**:1379–1389.
26. Yi T, Papadopoulos E, Hagner PR, Wagner G: **Hypoxia-inducible factor-1 α (HIF-1 α) promotes cap-dependent translation of selective mRNAs through up-regulating initiation factor eIF4E1 in breast cancer cells under hypoxia conditions.** *J Biol Chem* 2013, **288**:18732–18742.
27. Mayya VK, Flamand MN, Lambert AM, Jafarnejad SM, Wohlschlegel JA, Sonenberg N, Duchaine TF: **microRNA-mediated translation repression through GYF-1 and IFE-4 in *C. elegans* development.** *Nucleic Acids Res* 2021, **49**:4803–4815.
28. Jafarnejad SM, Chapat C, Matta-Camacho E, Gelbart IA, Hesketh GG, Arguello M, Garzia A, Kim S-H, Attig J, Shapiro M, et al.: **Translational control of ERK signaling through miRNA/4EHP-directed silencing.** *Elife* 2018, **7**:e35034.
29. Chen S, Gao G: **MicroRNAs recruit eIF4E2 to repress translation of target mRNAs.** *Protein Cell* 2017, **8**:750–761.
30. O'Brien J, Hayder H, Zayed Y, Peng C: **Overview of MicroRNA Biogenesis, Mechanisms of Actions, and Circulation.** *Front Endocrinol (Lausanne)* 2018, **9**:402.
31. Jonas S, Izaurralde E: **Towards a molecular understanding of microRNA-mediated gene silencing.** *Nat Rev Genet* 2015, **16**:421–433.
32. Braun JE, Huntzinger E, Fauser M, Izaurralde E: **GW182 proteins directly recruit cytoplasmic deadenylase complexes to miRNA targets.** *Mol Cell* 2011, **44**:120–133.
33. Ozgur S, Basquin J, Kamenska A, Filipowicz W, Standart N, Conti E: **Structure of a Human 4E-T/DDX6/CNOT1 Complex Reveals the Different Interplay of DDX6-Binding Proteins**

- with the CCR4-NOT Complex. *Cell Rep* 2015, **13**:703–711.**
34. Nishimura T, Padamsi Z, Fakim H, Milette S, Dunham WH, Gingras A-C, Fabian MR: **The eIF4E-Binding Protein 4E-T Is a Component of the mRNA Decay Machinery that Bridges the 5' and 3' Termini of Target mRNAs.** *Cell Rep* 2015, **11**:1425–1436.
 35. Kamenska A, Simpson C, Vindry C, Broomhead H, Bénard M, Ernoult-Lange M, Lee BP, Harries LW, Weil D, Standart N: **The DDX6-4E-T interaction mediates translational repression and P-body assembly.** *Nucleic Acids Res* 2016, **44**:6318–6334.
 36. Dostie J, Ferraiuolo M, Pause A, Adam SA, Sonenberg N: **A novel shuttling protein, 4E-T, mediates the nuclear import of the mRNA 5' cap-binding protein, eIF4E.** *EMBO J* 2000, **19**:3142–3156.
 37. Kubacka D, Kamenska A, Broomhead H, Minshall N, Darzynkiewicz E, Standart N: **Investigating the Consequences of eIF4E2 (4EHP) Interaction with 4E-Transporter on Its Cellular Distribution in HeLa Cells.** *PLoS One* 2013, **8**:e72761.
 38. Giovannone B, Lee E, Laviola L, Giorgino F, Cleveland KA, Smith RJ: **Two novel proteins that are linked to insulin-like growth factor (IGF-I) receptors by the Grb10 adapter and modulate IGF-I signaling.** *J Biol Chem* 2003, **278**:31564–31573.
 39. Wang L, Guo J, Zhang W, Xu Q, Zuo X, Shi C, Luo L, Liu J, Hu L, Hu Y, et al.: **Novel GIGYF2 gene variants in patients with Parkinson's disease in Chinese population.** *Neurosci Lett* 2010, **473**:131–135.
 40. Wang L, Guo J-F, Zhang W-W, Xu Q, Zuo X, Shi C-H, Luo L-Z, Liu J, Hu L, Hu Y-C, et al.: **Follow-up study of variants of the GIGYF2 gene in Chinese patients with Parkinson's disease.** *J Clin Neurosci Off J Neurosurg Soc Australas* 2011, **18**:1699–1701.
 41. Dai D, Wang Y, Zhou X, Tao J, Jiang D, Zhou H, Jiang Y, Pan G, Ru P, Ji H, et al.: **Meta-analyses of seven GIGYF2 polymorphisms with Parkinson's disease.** *Biomed reports* 2014, **2**:886–892.
 42. Ruiz-Martinez J, Krebs CE, Makarov V, Gorostidi A, Martí-Massó JF, Paisán-Ruiz C: **GIGYF2 mutation in late-onset Parkinson's disease with cognitive impairment.** *J Hum Genet* 2015, **60**:637–640.
 43. Zhang Y, Sun Q-Y, Yu R-H, Guo J-F, Tang B-S, Yan X-X: **The contribution of GIGYF2 to**

- Parkinson's disease: a meta-analysis.** *Neurol Sci Off J Ital Neurol Soc Ital Soc Clin Neurophysiol* 2015, **36**:2073–2079.
44. Gorostidi A, Martí-Massó JF, Bergareche A, Rodríguez-Oroz MC, López de Munain A, Ruiz-Martínez J: **Genetic Mutation Analysis of Parkinson's Disease Patients Using Multigene Next-Generation Sequencing Panels.** *Mol Diagn Ther* 2016, **20**:481–491.
 45. Huo Z, Luo X, Zhan X, Chu Q, Xu Q, Yao J, Pang H: **Genetic analysis of indel markers in three loci associated with Parkinson's disease.** *PLoS One* 2017, **12**:e0184269.
 46. Cristina T-P, Pablo M, Teresa PM, Lydia V-D, Irene A-R, Araceli A-C, Inmaculada B-B, Marta B-T, Dolores B-R, José C-AM, et al.: **A genetic analysis of a Spanish population with early onset Parkinson's disease.** *PLoS One* 2020, **15**:e0238098.
 47. Lautier C, Goldwurm S, Dürr A, Giovannone B, Tsiaras WG, Pezzoli G, Brice A, Smith RJ: **Mutations in the GIGYF2 (TNRC15) gene at the PARK11 locus in familial Parkinson disease.** *Am J Hum Genet* 2008, **82**:822–833.
 48. Guo Y, Jankovic J, Zhu S, Le W, Song Z, Xie W, Liao D, Yang H, Deng H: **GIGYF2 Asn56Ser and Asn457Thr mutations in Parkinson disease patients.** *Neurosci Lett* 2009, **454**:209–211.
 49. Zhang Y, Zheng L, Zhang T, Wang Y, Xiao Q, Fei Q-Z, Cui P-J, Cao L, Chen S-D: **GIGYF2 Asn56Ser mutation is rare in Chinese Parkinson's disease patients.** *Neurosci Lett* 2009, **463**:172–175.
 50. Giovannone B, Lautier C, Karashchuk G, Tsiaras WG, Smith RJ, de la Monte S, Klysik J, Goldwurm S: **GIGYF2 gene disruption in mice results in neurodegeneration and altered insulin-like growth factor signaling.** *Hum Mol Genet* 2009, **18**:4629–4639.
 51. Samaranch L, Lorenzo E, Pastor MA, Riverol M, Luquin MR, Rodríguez-Oroz MC, Obeso JA, Pastor P: **Analysis of the GIGYF2 gene in familial and sporadic Parkinson disease in the Spanish population.** *Eur J Neurol* 2010, **17**:321–325.
 52. Tan EK, Schapira AH: **Summary of GIGYF2 studies in Parkinson's disease: the burden of proof.** *Eur J Neurol* 2010, **17**:175–176.
 53. Lesage S, Condroyer C, Lohman E, Troiano A, Tison F, Viallet F, Damier P, Tranchant C, Vidhaillet M, Ouvrard-Hernandez A-M, et al.: **Follow-up study of the GIGYF2 gene in**

- French families with Parkinson's disease.** *Neurobiol Aging* 2010, **31**:1064–1069.
54. Cao L, Zhang T, Zheng L, Wang Y, Wang G, Zhang J, Fei QZ, Cui PJ, Wang XJ, Ma JF, et al.: **The GIGYF2 variants are not associated with Parkinson's disease in the mainland Chinese population.** *Parkinsonism Relat Disord* 2010, **16**:294–297.
55. Li L, Funayama M, Tomiyama H, Li Y, Yoshino H, Sasaki R, Kokubo Y, Kuzuhara S, Mizuno Y, Hattori N: **No evidence for pathogenic role of GIGYF2 mutation in Parkinson disease in Japanese patients.** *Neurosci Lett* 2010, **479**:245–248.
56. Dos Santos AV, Pestana CP, Diniz KR da S, Campos M, Abdalla-Carvalho CB, de Rosso ALZ, Pereira JS, Nicaretta DH, de Carvalho WL, Dos Santos JM, et al.: **Mutational analysis of GIGYF2, ATP13A2 and GBA genes in Brazilian patients with early-onset Parkinson's disease.** *Neurosci Lett* 2010, **485**:121–124.
57. Tian J, Guo J, Wang L, Sun Q, Yao L, Luo L, Shi C, Hu Y, Yan X, Tang B: **Mutation analysis of LRRK2, SCNA, UCHL1, HtrA2 and GIGYF2 genes in Chinese patients with autosomal dominant Parkinson's disease.** *Neurosci Lett* 2012, **516**:207–211.
58. Saini P, Rudakou U, Yu E, Ruskey JA, Asayesh F, Laurent SB, Spiegelman D, Fahn S, Waters C, Monchi O, et al.: **Association study of DNAJC13, UCHL1, HTRA2, GIGYF2, and EIF4G1 with Parkinson's disease.** *Neurobiol Aging* 2021, **100**:119.e7-119.e13.
59. Bras J, Simón-Sánchez J, Federoff M, Morgadinho A, Januario C, Ribeiro M, Cunha L, Oliveira C, Singleton AB: **Lack of replication of association between GIGYF2 variants and Parkinson disease.** *Hum Mol Genet* 2009, **18**:341–346.
60. Vilariño-Güell C, Ross OA, Soto AI, Farrer MJ, Haugarvoll K, Aasly JO, Uitti RJ, Wszolek ZK: **Reported mutations in GIGYF2 are not a common cause of Parkinson's disease.** *Mov Disord* 2009, **24**:619–620.
61. Zimprich A, Schulte C, Reinthaler E, Haubenberger D, Balzar J, Lichtner P, El Tawil S, Edris S, Foki T, Pirker W, et al.: **PARK11 gene (GIGYF2) variants Asn56Ser and Asn457Thr are not pathogenic for Parkinson's disease.** *Parkinsonism Relat Disord* 2009, **15**:532–534.
62. Sutherland GT, Siebert GA, Newman JRB, Silburn PA, Boyle RS, O'Sullivan JD, Mellick GD: **Haplotype analysis of the PARK 11 gene, GIGYF2, in sporadic Parkinson's disease.** *Mov Disord* 2009, **24**:449–452.

63. Meeus B, Nuytemans K, Crosiers D, Engelborghs S, Pals P, Pickut B, Peeters K, Mattheijssens M, Corsmit E, Cras P, et al.: **GIGYF2 has no major role in Parkinson genetic etiology in a Belgian population.** *Neurobiol Aging* 2011, **32**:308–312.
64. Tan E-K, Lin C-H, Tai C-H, Tan LC, Chen M-L, Li R, Lim H-Q, Pavanni R, Yuen Y, Prakash KM, et al.: **Non-synonymous GIGYF2 variants in Parkinson's disease from two Asian populations.** *Hum Genet* 2009, **126**:425–430.
65. Bonetti M, Ferraris A, Petracca M, Bentivoglio AR, Dallapiccola B, Valente EM: **GIGYF2 variants are not associated with Parkinson's disease in Italy.** *Mov Disord* 2009, **24**:1867–1869.
66. Di Fonzo A, Fabrizio E, Thomas A, Fincati E, Marconi R, Tinazzi M, Breedveld GJ, Simons EJ, Chien HF, Ferreira JJ, et al.: **GIGYF2 mutations are not a frequent cause of familial Parkinson's disease.** *Parkinsonism Relat Disord* 2009, **15**:703–705.
67. Nichols WC, Kissell DK, Pankratz N, Pauciulo MW, Elsaesser VE, Clark KA, Halter CA, Rudolph A, Wojcieszek J, Pfeiffer RF, et al.: **Variation in GIGYF2 is not associated with Parkinson disease.** *Neurology* 2009, **72**:1886–1892.
68. Peter D, Weber R, Sandmeir F, Wohlbold L, Helms S, Bawankar P, Valkov E, Igreja C, Izaurralde E: **GIGYF1/2 proteins use auxiliary sequences to selectively bind to 4EHP and repress target mRNA expression.** *Genes Dev* 2017, **31**:1147–1161.
69. Ingolia NT: **Ribosome profiling: new views of translation, from single codons to genome scale.** *Nat Rev Genet* 2014, **15**:205.
70. Aktas H, Cai H, Cooper GM: **Ras links growth factor signaling to the cell cycle machinery via regulation of cyclin D1 and the Cdk inhibitor p27KIP1.** *Mol Cell Biol* 1997, **17**:3850–3857.
71. Sun Y, Liu W-Z, Liu T, Feng X, Yang N, Zhou H-F: **Signaling pathway of MAPK/ERK in cell proliferation, differentiation, migration, senescence and apoptosis.** *J Recept Signal Transduct Res* 2015, **35**:600–604.
72. Higashi S, Iseki E, Minegishi M, Togo T, Kabuta T, Wada K: **GIGYF2 is present in endosomal compartments in the mammalian brains and enhances IGF-1-induced ERK1/2 activation.** *J Neurochem* 2010, **115**:423–437.

73. Fu R, Olsen MT, Webb K, Bennett EJ, Lykke-Andersen J: **Recruitment of the 4EHP-GYF2 cap-binding complex to tetraproline motifs of tristetraprolin promotes repression and degradation of mRNAs with AU-rich elements.** *RNA* 2016, **22**:373–382.
74. Tao X, Gao G: **Tristetraprolin Recruits Eukaryotic Initiation Factor 4E2 To Repress Translation of AU-Rich Element-Containing mRNAs.** *Mol Cell Biol* 2015, **35**:3921–3932.
75. Carballo E, Lai WS, Blackshear PJ: **Feedback inhibition of macrophage tumor necrosis factor-alpha production by tristetraprolin.** *Science* 1998, **281**:1001–1005.
76. Stoecklin G, Tenenbaum SA, Mayo T, Chittur S V, George AD, Baroni TE, Blackshear PJ, Anderson P: **Genome-wide analysis identifies interleukin-10 mRNA as target of tristetraprolin.** *J Biol Chem* 2008, **283**:11689–11699.
77. Brooks SA, Blackshear PJ: **Tristetraprolin (TTP): interactions with mRNA and proteins, and current thoughts on mechanisms of action.** *Biochim Biophys Acta* 2013, **1829**:666–679.
78. Lai WS, Kennington EA, Blackshear PJ: **Tristetraprolin and its family members can promote the cell-free deadenylation of AU-rich element-containing mRNAs by poly(A) ribonuclease.** *Mol Cell Biol* 2003, **23**:3798–3812.
79. Lykke-Andersen J, Wagner E: **Recruitment and activation of mRNA decay enzymes by two ARE-mediated decay activation domains in the proteins TTP and BRF-1.** *Genes Dev* 2005, **19**:351–361.
80. Sandler H, Kreth J, Timmers HTM, Stoecklin G: **Not1 mediates recruitment of the deadenylase Caf1 to mRNAs targeted for degradation by tristetraprolin.** *Nucleic Acids Res* 2011, **39**:4373–4386.
81. Fabian MR, Frank F, Rouya C, Siddiqui N, Lai WS, Karetnikov A, Blackshear PJ, Nagar B, Sonenberg N: **Structural basis for the recruitment of the human CCR4-NOT deadenylase complex by tristetraprolin.** *Nat Struct Mol Biol* 2013, **20**:735–739.
82. Qi M-Y, Wang Z-Z, Zhang Z, Shao Q, Zeng A, Li X-Q, Li W-Q, Wang C, Tian F-J, Li Q, et al.: **AU-rich-element-dependent translation repression requires the cooperation of tristetraprolin and RCK/P54.** *Mol Cell Biol* 2012, **32**:913–928.
83. Zhang X, Chapat C, Wang P, Choi J-H, Li Q, Luo J, Wiebe S, Kim S-H, Robichaud N, Karam IF, et al.: **microRNA-induced translational control of antiviral immunity by the cap-binding**

- protein 4EHP.** *Mol Cell* 2021, **81**:1187-1199.e5.
84. Rönnblom L: **The importance of the type I interferon system in autoimmunity.** *Clin Exp Rheumatol* 2016, **34**:21–24.
85. Muralidar S, Ambi SV, Sekaran S, Krishnan UM: **The emergence of COVID-19 as a global pandemic: Understanding the epidemiology, immune response and potential therapeutic targets of SARS-CoV-2.** *Biochimie* 2020, **179**:85–100.
86. Gordon DE, Jang GM, Bouhaddou M, Xu J, Obernier K, White KM, O’Meara MJ, Rezelj V V, Guo JZ, Swaney DL, et al.: **A SARS-CoV-2 protein interaction map reveals targets for drug repurposing.** *Nature* 2020, **583**:459–468.
87. Perrin-Cocon L, Diaz O, Jacquemin C, Barthel V, Ogire E, Ramière C, André P, Lotteau V, Vidalain P-O: **The current landscape of coronavirus-host protein-protein interactions.** *J Transl Med* 2020, **18**:319.
88. V’kovski P, Kratzel A, Steiner S, Stalder H, Thiel V: **Coronavirus biology and replication: implications for SARS-CoV-2.** *Nat Rev Microbiol* 2021, **19**:155–170.
89. Verba K, Gupta M, Azumaya C, Moritz M, Pourmal S, Diallo A, Merz G, Jang G, Bouhaddou M, Fossati A, et al.: **CryoEM and AI reveal a structure of SARS-CoV-2 Nsp2, a multifunctional protein involved in key host processes.** *Res Sq* 2021, doi:10.21203/rs.3.rs-515215/v1.
90. Doma MK, Parker R: **Endonucleolytic cleavage of eukaryotic mRNAs with stalls in translation elongation.** *Nature* 2006, **440**:561–564.
91. Klauer AA, van Hoof A: **Degradation of mRNAs that lack a stop codon: a decade of nonstop progress.** *Wiley Interdiscip Rev RNA* 2012, **3**:649–660.
92. Letzring DP, Wolf AS, Brule CE, Grayhack EJ: **Translation of CGA codon repeats in yeast involves quality control components and ribosomal protein L1.** *RNA* 2013, **19**:1208–1217.
93. Schuller AP, Green R: **Roadblocks and resolutions in eukaryotic translation.** *Nat Rev Mol Cell Biol* 2018, **19**:526–541.
94. Choe Y-J, Park S-H, Hassemer T, Körner R, Vincenz-Donnelly L, Hayer-Hartl M, Hartl FU: **Failure of RQC machinery causes protein aggregation and proteotoxic stress.** *Nature* 2016, **531**:191–195.

95. Brandman O, Hegde RS: **Ribosome-associated protein quality control.** *Nat Struct Mol Biol* 2016, **23**:7–15.
96. Joazeiro CAP: **Ribosomal Stalling During Translation: Providing Substrates for Ribosome-Associated Protein Quality Control.** *Annu Rev Cell Dev Biol* 2017, **33**:343–368.
97. Hickey KL, Dickson K, Cogan JZ, Replogle JM, Schoof M, D’Orazio KN, Sinha NK, Hussmann JA, Jost M, Frost A, et al.: **GIGYF2 and 4EHP Inhibit Translation Initiation of Defective Messenger RNAs to Assist Ribosome-Associated Quality Control.** *Mol Cell* 2020, **79**:950-962.e6.
98. Juszkiwicz S, Chandrasekaran V, Lin Z, Kraatz S, Ramakrishnan V, Hegde RS: **ZNF598 Is a Quality Control Sensor of Collided Ribosomes.** *Mol Cell* 2018, **72**:469-481.e7.
99. Juszkiwicz S, Hegde RS: **Initiation of Quality Control during Poly(A) Translation Requires Site-Specific Ribosome Ubiquitination.** *Mol Cell* 2017, **65**:743-750.e4.
100. Garzia A, Jafarnejad SM, Meyer C, Chapat C, Gogakos T, Morozov P, Amiri M, Shapiro M, Molina H, Tuschl T, et al.: **The E3 ubiquitin ligase and RNA-binding protein ZNF598 orchestrates ribosome quality control of premature polyadenylated mRNAs.** *Nat Commun* 2017, **8**:16056.
101. Sundaramoorthy E, Leonard M, Mak R, Liao J, Fulzele A, Bennett EJ: **ZNF598 and RACK1 Regulate Mammalian Ribosome-Associated Quality Control Function by Mediating Regulatory 40S Ribosomal Ubiquitylation.** *Mol Cell* 2017, **65**:751-760.e4.
102. Juszkiwicz S, Slodkowicz G, Lin Z, Freire-Pritchett P, Peak-Chew S-Y, Hegde RS: **Ribosome collisions trigger cis-acting feedback inhibition of translation initiation.** *Elife* 2020, **9**.
103. Sinha NK, Ordureau A, Best K, Saba JA, Zinshteyn B, Sundaramoorthy E, Fulzele A, Garshott DM, Denk T, Thoms M, et al.: **EDF1 coordinates cellular responses to ribosome collisions.** *Elife* 2020, **9**.
104. Zinshteyn B, Sinha NK, Enam SU, Koleske B, Green R: **Translational repression of NMD targets by GIGYF2 and EIF4E2.** *PLoS Genet* 2021, **17**:e1009813.
105. Weber R, Chung M-Y, Keskeny C, Zinnall U, Landthaler M, Valkov E, Izaurralde E, Igreja C: **4EHP and GIGYF1/2 Mediate Translation-Coupled Messenger RNA Decay.** *Cell Rep* 2020, **33**:108262.

106. Notaras M, Allen M, Longo F, Volk N, Toth M, Li Jeon N, Klann E, Colak D: **UPF2 leads to degradation of dendritically targeted mRNAs to regulate synaptic plasticity and cognitive function.** *Mol Psychiatry* 2020, **25**:3360–3379.
107. Johnson JL, Stoica L, Liu Y, Zhu PJ, Bhattacharya A, Buffington SA, Huq R, Eissa NT, Larsson O, Porse BT, et al.: **Inhibition of Upf2-Dependent Nonsense-Mediated Decay Leads to Behavioral and Neurophysiological Abnormalities by Activating the Immune Response.** *Neuron* 2019, **104**:665-679.e8.
108. Jaffrey SR, Wilkinson MF: **Nonsense-mediated RNA decay in the brain: emerging modulator of neural development and disease.** *Nat Rev Neurosci* 2018, **19**:715–728.
109. Gulsuner S, Walsh T, Watts AC, Lee MK, Thornton AM, Casadei S, Rippey C, Shahin H, Nimgaonkar VL, Go RCP, et al.: **Spatial and temporal mapping of de novo mutations in schizophrenia to a fetal prefrontal cortical network.** *Cell* 2013, **154**:518–529.
110. Tarpey PS, Raymond FL, Nguyen LS, Rodriguez J, Hackett A, Vandeleur L, Smith R, Shoubridge C, Edkins S, Stevens C, et al.: **Mutations in UPF3B, a member of the nonsense-mediated mRNA decay complex, cause syndromic and nonsyndromic mental retardation.** *Nat Genet* 2007, **39**:1127–1133.
111. Mefford HC, Sharp AJ, Baker C, Itsara A, Jiang Z, Buysse K, Huang S, Maloney VK, Crolla JA, Baralle D, et al.: **Recurrent rearrangements of chromosome 1q21.1 and variable pediatric phenotypes.** *N Engl J Med* 2008, **359**:1685–1699.
112. Wiebe S, Nagpal A, Sonenberg N: **Dysregulated translational control in brain disorders: from genes to behavior.** *Curr Opin Genet Dev* 2020, **65**:34–41.
113. Wang T, Guo H, Xiong B, Stessman HAF, Wu H, Coe BP, Turner TN, Liu Y, Zhao W, Hoekzema K, et al.: **De novo genic mutations among a Chinese autism spectrum disorder cohort.** *Nat Commun* 2016, **7**:13316.
114. Gazzellone MJ, Zhou X, Lionel AC, Uddin M, Thiruvahindrapuram B, Liang S, Sun C, Wang J, Zou M, Tammimies K, et al.: **Copy number variation in Han Chinese individuals with autism spectrum disorder.** *J Neurodev Disord* 2014, **6**:34.
115. Iossifov I, O’Roak BJ, Sanders SJ, Ronemus M, Krumm N, Levy D, Stessman HA, Witherspoon KT, Vives L, Patterson KE, et al.: **The contribution of de novo coding**

- mutations to autism spectrum disorder.** *Nature* 2014, **515**:216–221.
116. Lim ET, Uddin M, De Rubeis S, Chan Y, Kamumbu AS, Zhang X, D’Gama AM, Kim SN, Hill RS, Goldberg AP, et al.: **Rates, distribution and implications of postzygotic mosaic mutations in autism spectrum disorder.** *Nat Neurosci* 2017, **20**:1217–1224.
117. An J-Y, Lin K, Zhu L, Werling DM, Dong S, Brand H, Wang HZ, Zhao X, Schwartz GB, Collins RL, et al.: **Genome-wide de novo risk score implicates promoter variation in autism spectrum disorder.** *Science* 2018, **362**:eaat6576.
118. De Rubeis S, He X, Goldberg AP, Poultney CS, Samocha K, Ercument Cicek A, Kou Y, Liu L, Fromer M, Walker S, et al.: **Synaptic, transcriptional and chromatin genes disrupted in autism.** *Nature* 2014, **515**:209–215.
119. Krumm N, Turner TN, Baker C, Vives L, Mohajeri K, Witherspoon K, Raja A, Coe BP, Stessman HA, He Z-X, et al.: **Excess of rare, inherited truncating mutations in autism.** *Nat Genet* 2015, **47**:582–588.
120. Satterstrom FK, Kosmicki JA, Wang J, Breen MS, De Rubeis S, An J-Y, Peng M, Collins R, Grove J, Klei L, et al.: **Large-Scale Exome Sequencing Study Implicates Both Developmental and Functional Changes in the Neurobiology of Autism.** *Cell* 2020, **180**:568-584.e23.
121. Wiebe S, Meng XQ, Kim S-H, Zhang X, Lacaille J-C, Aguilar-Valles A, Sonenberg N: **The eIF4E homolog 4EHP (eIF4E2) regulates hippocampal long-term depression and impacts social behavior.** *Mol Autism* 2020, **11**:92.
122. Tahmasebi S, Khoutorsky A, Mathews MB, Sonenberg N: **Translation deregulation in human disease.** *Nat Rev Mol Cell Biol* 2018, **19**:791–807.
123. Laplante M, Sabatini DM: **MTOR signaling in growth control and disease.** *Cell* 2012, **149**:274–293.
124. Sossin WS, Costa-Mattioli M: **Translational control in the brain in health and disease.** *Cold Spring Harb Perspect Biol* 2019, **11**:a032912.
125. Costa-Mattioli M, Monteggia LM: **mTOR complexes in neurodevelopmental and neuropsychiatric disorders.** *Nat Neurosci* 2013, **16**:1537–1543.
126. Huber KM, Klann E, Costa-Mattioli M, Zukin RS: **Dysregulation of Mammalian Target of**

- Rapamycin Signaling in Mouse Models of Autism.** *J Neurosci* 2015, **35**:13836 LP – 13842.
127. Zhou J, Parada LF: **PTEN signaling in autism spectrum disorders.** *Curr Opin Neurobiol* 2012, **22**:873–879.
 128. Ehninger D, Han S, Shilyansky C, Zhou Y, Li W, Kwiatkowski DJ, Ramesh V, Silva AJ: **Reversal of learning deficits in a Tsc2+/- mouse model of tuberous sclerosis.** *Nat Med* 2008, **14**:843–848.
 129. Carson RP, Van Nielen DL, Winzenburger PA, Ess KC: **Neuronal and glia abnormalities in Tsc1-deficient forebrain and partial rescue by rapamycin.** *Neurobiol Dis* 2012, **45**:369–380.
 130. Ehninger D, Silva AJ: **Rapamycin for treating Tuberous sclerosis and Autism spectrum disorders.** *Trends Mol Med* 2011, **17**:78–87.
 131. Chen CJ, Sgritta M, Mays J, Zhou H, Lucero R, Park J, Wang IC, Park JH, Kaipparattu BA, Stoica L, et al.: **Therapeutic inhibition of mTORC2 rescues the behavioral and neurophysiological abnormalities associated with Pten-deficiency.** *Nat Med* 2019, **25**:1684–1690.
 132. Tang J, Xue W, Xia B, Ren L, Tao W, Chen C, Zhang H, Wu R, Wang Q, Wu H, et al.: **Involvement of normalized NMDA receptor and mTOR-related signaling in rapid antidepressant effects of Yueju and ketamine on chronically stressed mice.** *Sci Rep* 2015, **5**:13573.
 133. Li N, Lee B, Liu RJ, Banasr M, Dwyer JM, Iwata M, Li XY, Aghajanian G, Duman RS: **mTOR-dependent synapse formation underlies the rapid antidepressant effects of NMDA antagonists.** *Science (80-)* 2010, **329**:959–964.
 134. Autry AE, Adachi M, Nosyreva E, Na ES, Los MF, Cheng PF, Kavalali ET, Monteggia LM: **NMDA receptor blockade at rest triggers rapid behavioural antidepressant responses.** *Nature* 2011, **475**:91–96.
 135. Sengupta S, Giaime E, Narayan S, Hahm S, Howell J, O'Neill D, Vlasuk GP, Saiah E: **Discovery of NV-5138, the first selective Brain mTORC1 activator.** *Sci Rep* 2019, **9**:4107.
 136. Kato T, Pothula S, Liu R-J, Duman CH, Terwilliger R, Vlasuk GP, Saiah E, Hahm S, Duman RS: **Sestrin modulator NV-5138 produces rapid antidepressant effects via direct mTORC1**

- activation.** *J Clin Invest* 2019, **129**:2542–2554.
137. Hinnebusch AG, Ivanov IP, Sonenberg N: **Translational control by 5'-untranslated regions of eukaryotic mRNAs.** *Science (80-)* 2016, **352**:1413–1416.
138. Joshi B, Cai AL, Keiper BD, Minich WB, Mendez R, Beach CM, Stepinski J, Stolarski R, Darzynkiewicz E, Rhoads RE: **Phosphorylation of eukaryotic protein synthesis initiation factor 4E at Ser-209.** *J Biol Chem* 1995, **270**:14597–14603.
139. Ueda T, Watanabe-Fukunaga R, Fukuyama H, Nagata S, Fukunaga R: **Mnk2 and Mnk1 are essential for constitutive and inducible phosphorylation of eukaryotic initiation factor 4E but not for cell growth or development.** *Mol Cell Biol* 2004, **24**:6539–6549.
140. Bramham CR, Jensen KB, Proud CG: **Tuning Specific Translation in Cancer Metastasis and Synaptic Memory: Control at the MNK–eIF4E Axis.** *Trends Biochem Sci* 2016, **41**:847–858.
141. Aguilar-Valles A, Haji N, De Gregorio D, Matta-Camacho E, Eslamizade MJ, Popic J, Sharma V, Cao R, Rummel C, Tanti A, et al.: **Translational control of depression-like behavior via phosphorylation of eukaryotic translation initiation factor 4E.** *Nat Commun* 2018, **9**:2459.
142. Amorim IS, Kedia S, Kouloulia S, Simbriger K, Gantois I, Jafarnejad SM, Li Y, Kampaite A, Pooters T, Romanò N, et al.: **Loss of eIF4E phosphorylation engenders depression-like behaviors via selective mRNA translation.** *J Neurosci* 2018, **38**:2118–2133.
143. Sonenberg N, Hinnebusch AG: **Regulation of Translation Initiation in Eukaryotes: Mechanisms and Biological Targets.** *Cell* 2009, **136**:731–745.
144. Santini E, Huynh TN, MacAskill AF, Carter AG, Pierre P, Ruggero D, Kaphzan H, Klann E: **Exaggerated translation causes synaptic and behavioural aberrations associated with autism.** *Nature* 2013, **493**:411–415.
145. Gkogkas CG, Khoutorsky A, Ran I, Rampakakis E, Nevarko T, Weatherill DB, Vasuta C, Yee S, Truitt M, Dallaire P, et al.: **Autism-related deficits via dysregulated eIF4E-dependent translational control.** *Nature* 2013, **493**:371.
146. Aguilar-Valles A, Matta-Camacho E, Khoutorsky A, Gkogkas C, Nader K, Lacaille J-C, Sonenberg N: **Inhibition of Group I Metabotropic Glutamate Receptors Reverses Autistic-Like Phenotypes Caused by Deficiency of the Translation Repressor eIF4E Binding Protein 2.** *J Neurosci* 2015, **35**:11125–11132.

147. Wiebe S, Nagpal A, Truong VT, Park J, Skalecka A, He AJ, Gamache K, Khoutorsky A, Gantois I, Sonenberg N: **Inhibitory interneurons mediate autism-associated behaviors via 4E-BP2.** *Proc Natl Acad Sci U S A* 2019, **116**:18060–18067.
148. Artinian J, Jordan A, Khlaifia A, Honore E, La Fontaine A, Racine A-S, Laplante I, Lacaille J-C: **Regulation of Hippocampal Memory by mTORC1 in Somatostatin Interneurons.** *J Neurosci* 2019, **39**:8439–8456.
149. Goel A, Cantu DA, Guilfoyle J, Chaudhari GR, Newadkar A, Todisco B, de Alba D, Kourdougli N, Schmitt LM, Pedapati E, et al.: **Impaired perceptual learning in a mouse model of Fragile X syndrome is mediated by parvalbumin neuron dysfunction and is reversible.** *Nat Neurosci* 2018, **21**:1404–1411.
150. Lozano R, Azarang A, Wilaisakditipakorn T, Hagerman RJ: **Fragile X syndrome: A review of clinical management.** *Intractable rare Dis Res* 2016, **5**:145–157.
151. Napoli I, Mercaldo V, Boyl PP, Eleuteri B, Zalfa F, De Rubeis S, Di Marino D, Mohr E, Massimi M, Falconi M, et al.: **The Fragile X Syndrome Protein Represses Activity-Dependent Translation through CYFIP1, a New 4E-BP.** *Cell* 2008, **134**:1042–1054.
152. Das Sharma S, Metz JB, Li H, Hobson BD, Hornstein N, Sulzer D, Tang G, Sims PA: **Widespread Alterations in Translation Elongation in the Brain of Juvenile Fmr1 Knockout Mice.** *Cell Rep* 2019, **26**:3313–3322.
153. Thomson SR, Seo SS, Barnes SA, Louros SR, Muscas M, Dando O, Kirby C, Wyllie DJA, Hardingham GE, Kind PC, et al.: **Cell-Type-Specific Translation Profiling Reveals a Novel Strategy for Treating Fragile X Syndrome.** *Neuron* 2017, **95**:550–563.
154. Bowling H, Bhattacharya A, Zhang G, Alam D, Lebowitz JZ, Bohm-Levine N, Lin D, Singha P, Mamcarz M, Puckett R, et al.: **Altered steady state and activity-dependent de novo protein expression in fragile X syndrome.** *Nat Commun* 2019, **10**:1–13.
155. Sawicka K, Hale CR, Park CY, Fak JJ, Gresack JE, Van Driesche SJ, Kang JJ, Darnell JC, Darnell RB: **FMRP has a cell-type-specific role in CA1 pyramidal neurons to regulate autism-related transcripts and circadian memory.** *Elife* 2019, **8**:e46919.
156. Stoppel LJ, Auerbach BD, Senter RK, Preza AR, Lefkowitz RJ, Bear MF: **β -Arrestin2 Couples Metabotropic Glutamate Receptor 5 to Neuronal Protein Synthesis and Is a Potential**

- Target to Treat Fragile X.** *Cell Rep* 2017, **18**:2807–2814.
157. Osterweil EK, Chuang S-C, Chubykin AA, Sidorov M, Bianchi R, Wong RKS, Bear MF: **Lovastatin corrects excess protein synthesis and prevents epileptogenesis in a mouse model of fragile X syndrome.** *Neuron* 2013, **77**:243–250.
 158. Muscas M, Louros SR, Osterweil EK: **Lovastatin, not simvastatin, corrects core phenotypes in the fragile X mouse model.** *eNeuro* 2019, **6**:1–12.
 159. Gantois I, Khoutorsky A, Popic J, Aguilar-Valles A, Freemantle E, Cao R, Sharma V, Pooters T, Nagpal A, Skalecka A, et al.: **Metformin ameliorates core deficits in a mouse model of fragile X syndrome.** *Nat Med* 2017, **23**:674–677.
 160. Gross C, Banerjee A, Tiwari D, Longo F, White AR, Allen AG, Schroeder-Carter LM, Krzeski JC, Elsayed NA, Puckett R, et al.: **Isoform-selective phosphoinositide 3-kinase inhibition ameliorates a broad range of fragile X syndrome-associated deficits in a mouse model.** *Neuropsychopharmacology* 2019, **44**:324–333.
 161. Berry-Kravis EM, Lindemann L, Jønch AE, Apostol G, Bear MF, Carpenter RL, Crawley JN, Curie A, Des Portes V, Hossain F, et al.: **Drug development for neurodevelopmental disorders: Lessons learned from fragile X syndrome.** *Nat Rev Drug Discov* 2018, **17**:280–298.
 162. Berry-Kravis E, Hagerman R, Visootsak J, Budimirovic D, Kaufmann WE, Cherubini M, Zarevics P, Walton-Bowen K, Wang P, Bear MF, et al.: **Arbaclofen in fragile X syndrome: Results of phase 3 trials.** *J Neurodev Disord* 2017, **9**:1–18.
 163. Asiminas A, Jackson AD, Louros SR, Till SM, Spano T, Dando O, Bear MF, Chattarji S, Hardingham GE, Osterweil EK, et al.: **Sustained correction of associative learning deficits after brief, early treatment in a rat model of Fragile X Syndrome.** *Sci Transl Med* 2019, **11**:1–11.
 164. Schenck A, Bardoni B, Langmann C, Harden N, Mandel JL, Giangrande A: **CYFIP/Sra-1 controls neuronal connectivity in Drosophila and links the Rac1 GTPase pathway to the fragile X protein.** *Neuron* 2003, **38**:887–898.
 165. De Rubeis S, Pasciuto E, Li KW, Fernandez E, Di Marino D, Buzzi A, Ostroff LE, Klann E, Zwartkruis FJT, Komiyama NH, et al.: **CYFIP1 coordinates mRNA translation and**

- cytoskeleton remodeling to ensure proper dendritic spine formation.** *Neuron* 2013, **79**:1169–1182.
166. Ronesi JA, Collins KA, Hays SA, Tsai N-P, Guo W, Birnbaum SG, Hu J-H, Worley PF, Gibson JR, Huber KM: **Disrupted Homer scaffolds mediate abnormal mGluR5 function in a mouse model of fragile X syndrome.** *Nat Neurosci* 2012, **15**:431–40, S1.
167. Santini E, Huynh TN, Longo F, Koo SY, Mojica E, D'Andrea L, Bagni C, Klann E: **Reducing eIF4E-eIF4G interactions restores the balance between protein synthesis and actin dynamics in fragile X syndrome model mice.** *Sci Signal* 2017, **10**:41–46.
168. Woo YJ, Kanellopoulos AK, Hemati P, Kirschen J, Nebel RA, Wang T, Bagni C, Abrahams BS: **Domain-Specific Cognitive Impairments in Humans and Flies With Reduced CYFIP1 Dosage.** *Biol Psychiatry* 2019, **86**:306–314.
169. Zhao Q, Li T, Zhao X, Huang K, Wang T, Li Z, Ji J, Zeng Z, Zhang Z, Li K, et al.: **Rare CNVs and tag SNPs at 15q11.2 are associated with schizophrenia in the Han Chinese population.** *Schizophr Bull* 2013, **39**:712–719.
170. Wang J, Tao Y, Song F, Sun Y, Ott J, Saffen D: **Common Regulatory Variants of CYFIP1 Contribute to Susceptibility for Autism Spectrum Disorder (ASD) and Classical Autism.** *Ann Hum Genet* 2015, **79**:329–340.
171. Davenport EC, Szulc BR, Drew J, Taylor J, Morgan T, Higgs NF, López-Doménech G, Kittler JT: **Autism and Schizophrenia-Associated CYFIP1 Regulates the Balance of Synaptic Excitation and Inhibition.** *Cell Rep* 2019, **26**:2037-2051.e6.
172. Fricano-Kugler C, Gordon A, Shin G, Gao K, Nguyen J, Berg J, Starks M, Geschwind DH: **CYFIP1 overexpression increases fear response in mice but does not affect social or repetitive behavioral phenotypes.** *Mol Autism* 2019, **10**:1–16.
173. Domínguez-Iturza N, Lo AC, Shah D, Armendáriz M, Vannelli A, Mercaldo V, Trusel M, Li KW, Gastaldo D, Santos AR, et al.: **The autism- and schizophrenia-associated protein CYFIP1 regulates bilateral brain connectivity and behaviour.** *Nat Commun* 2019, **10**:1–13.
174. Silva AI, Haddon JE, Ahmed Syed Y, Trent S, Lin T-CE, Patel Y, Carter J, Haan N, Honey RC, Humby T, et al.: **Cyfp1 haploinsufficient rats show white matter changes, myelin thinning, abnormal oligodendrocytes and behavioural inflexibility.** *Nat Commun* 2019, **10**:3455.

175. Siekierka J, Mauser L, Ochoa S: **Mechanism of polypeptide chain initiation in eukaryotes and its control by phosphorylation of the alpha subunit of initiation factor 2.** *Proc Natl Acad Sci U S A* 1982, **79**:2537–2540.
176. Wek RC: **Role of eIF2 α kinases in translational control and adaptation to cellular stress.** *Cold Spring Harb Perspect Biol* 2018, **10**:a032870.
177. Costa-Mattioli M, Gobert D, Harding H, Herdy B, Azzi M, Bruno M, Bidinosti M, Ben Mamou C, Marcinkiewicz E, Yoshida M, et al.: **Translational control of hippocampal synaptic plasticity and memory by the eIF2 α kinase GCN2.** *Nature* 2005, **436**:1166–1170.
178. Costa-Mattioli M, Gobert D, Stern E, Gamache K, Colina R, Cuello C, Sossin W, Kaufman R, Pelletier J, Rosenblum K, et al.: **eIF2 α Phosphorylation Bidirectionally Regulates the Switch from Short- to Long-Term Synaptic Plasticity and Memory.** *Cell* 2007, **129**:195–206.
179. Zhu PJ, Huang W, Kalikulov D, Yoo JW, Placzek AN, Stoica L, Zhou H, Bell JC, Friedlander MJ, Krnjević K, et al.: **Suppression of PKR promotes network excitability and enhanced cognition by interferon- γ -mediated disinhibition.** *Cell* 2011, **147**:1384–1396.
180. Stern E, Chinnakkaruppan A, David O, Sonenberg N, Rosenblum K: **Blocking the eIF2 α kinase (PKR) enhances positive and negative forms of cortex-dependent taste memory.** *J Neurosci* 2013, **33**:2517–2525.
181. Di Prisco GV, Huang W, Buffington SA, Hsu CC, Bonnen PE, Placzek AN, Sidrauski C, Krnjević K, Kaufman RJ, Walter P, et al.: **Translational control of mGluR-dependent long-term depression and object-place learning by eIF2 α .** *Nat Neurosci* 2014, **17**:1073–1082.
182. Sidrauski C, Acosta-Alvear D, Khoutorsky A, Vedantham P, Hearn BR, Li H, Gamache K, Gallagher CM, Ang KKH, Wilson C, et al.: **Pharmacological brake-release of mRNA translation enhances cognitive memory.** *Elife* 2013, **2**:e00498.
183. Jiang Z, Belforte JE, Lu Y, Yabe Y, Pickel J, Smith CB, Je HS, Lu B, Nakazawa K: **eIF2 α phosphorylation-dependent translation in CA1 pyramidal cells impairs hippocampal memory consolidation without affecting general translation.** *J Neurosci* 2010, **30**:2582–2594.
184. Ohno M: **PERK as a hub of multiple pathogenic pathways leading to memory deficits and**

- neurodegeneration in Alzheimer's disease.** *Brain Res Bull* 2018, **141**:72–78.
185. Hetz C, Mollereau B: **Disturbance of endoplasmic reticulum proteostasis in neurodegenerative diseases.** *Nat Rev Neurosci* 2014, **15**:233–249.
186. Halliday M, Radford H, Zents KAM, Molloy C, Moreno JA, Verity NC, Smith E, Ortori CA, Barrett DA, Bushell M, et al.: **Repurposed drugs targeting eIF2 α -P-mediated translational repression prevent neurodegeneration in mice.** *Brain* 2017, **140**:1768–1783.
187. Zhu PJ, Khatiwada S, Cui Y, Reineke LC, Dooling SW, Kim JJ, Li W, Walter P, Costa-Mattioli M: **Activation of the ISR mediates the behavioral and neurophysiological abnormalities in Down syndrome.** *Science (80-)* 2019, **366**:843–849.
188. Dierssen M: **Down syndrome: The brain in trisomic mode.** *Nat Rev Neurosci* 2012, **13**:844–858.
189. Baddeley A: **Working memory.** *Science* 1992, **255**:556–559.
190. Camina E, Güell F: **The Neuroanatomical, Neurophysiological and Psychological Basis of Memory: Current Models and Their Origins.** *Front Pharmacol* 2017, **8**:438.
191. Goelet P, Castellucci VF, Schacher S, Kandel ER: **The long and the short of long-term memory[mdash]a molecular framework.** *Nature* 1986, **322**:419–422.
192. Banko JL, Klann E: **Cap-dependent translation initiation and memory.** *Prog Brain Res* 2008, **169**:59–80.
193. Kats IR, Klann E: **Translating from cancer to the brain: regulation of protein synthesis by eIF4F.** *Learn Mem* 2019, **26**:332–342.
194. Squire LR, Zola-Morgan S: **The medial temporal lobe memory system.** *Science* 1991, **253**:1380–1386.
195. Malenka RC, Nicoll and RA: **Long-Term Potentiation--A Decade of Progress?** *Science (80-)* 1999, **285**:1870 LP – 1874.
196. Kennedy MB: **The postsynaptic density at glutamatergic synapses.** *Trends Neurosci* 1997, **20**:264–268.
197. Díaz-Alonso J, Nicoll RA: **AMPA receptor trafficking and LTP: Carboxy-termini, amino-termini and TARPs.** *Neuropharmacology* 2021, **197**:108710.
198. Nestler EJ, Hyman SE, Holtzman DM, Malenka RC: **Higher Cognitive Function and**

- Behavioral Control.** In *Molecular Neuropharmacology: A Foundation for Clinical Neuroscience, 3e.* . McGraw-Hill Education; 2015.
199. Diamond A: **Executive functions.** *Annu Rev Psychol* 2013, **64**:135–168.
 200. Vorhees C V, Williams MT: **Assessing spatial learning and memory in rodents.** *ILAR J* 2014, **55**:310–332.
 201. Fuster JM: **Unit activity in prefrontal cortex during delayed-response performance: neuronal correlates of transient memory.** *J Neurophysiol* 1973, **36**:61–78.
 202. Spellman T, Rigotti M, Ahmari SE, Fusi S, Gogos JA, Gordon JA: **Hippocampal-prefrontal input supports spatial encoding in working memory.** *Nature* 2015, **522**:309–314.
 203. Bizon JL, Foster TC, Alexander GE, Glisky EL: **Characterizing cognitive aging of working memory and executive function in animal models.** *Front Aging Neurosci* 2012, **4**:19.
 204. Touzani K, Puthanveettil S V, Kandel ER: **Consolidation of learning strategies during spatial working memory task requires protein synthesis in the prefrontal cortex.** *Proc Natl Acad Sci U S A* 2007, **104**:5632–5637.
 205. Banko JL, Merhav M, Stern E, Sonenberg N, Rosenblum K, Klann E: **Behavioral alterations in mice lacking the translation repressor 4E-BP2.** *Neurobiol Learn Mem* 2007, **87**:248–256.
 206. Zhu S, Henninger K, McGrath BC, Cavener DR: **PERK Regulates Working Memory and Protein Synthesis-Dependent Memory Flexibility.** *PLoS One* 2016, **11**:e0162766.
 207. Roesler R, McGaugh JL: **Memory Consolidation.** *Encycl Behav Neurosci* 2010, doi:10.1016/B978-0-08-045396-5.00147-0.
 208. Santini E, Huynh TN, Klann E: **Chapter Five - Mechanisms of Translation Control Underlying Long-Lasting Synaptic Plasticity and the Consolidation of Long-Term Memory.** In *Molecular Basis of Memory.* Edited by Khan ZU, Muly ECBT-P in MB and TS. Academic Press; 2014:131–167.
 209. Bontempi B, Frankland PW: **Memory Consolidation: Cerebral Cortex.** *Encycl Neurosci* 2009, doi:10.1016/B978-008045046-9.00771-3.
 210. SCOVILLE WB, MILNER B: **Loss of recent memory after bilateral hippocampal lesions.** *J Neurol Neurosurg Psychiatry* 1957, **20**:11–21.
 211. PENFIELD W, MILNER B: **Memory deficit produced by bilateral lesions in the hippocampal**

- zone. *AMA Arch Neurol Psychiatry* 1958, **79**:475–497.
212. Costa-Mattioli M, Sossin WS, Klann E, Sonenberg N: **Translational Control of Long-Lasting Synaptic Plasticity and Memory.** *Neuron* 2009, **61**:10–26.
213. Santini E, Klann E: **Dysregulated mTORC1-Dependent Translational Control: From Brain Disorders to Psychoactive Drugs.** *Front Behav Neurosci* 2011, **5**:76.
214. Klann E, Dever TE: **Biochemical mechanisms for translational regulation in synaptic plasticity.** *Nat Rev Neurosci* 2004, **5**:931–942.
215. Batista G, Johnson JL, Dominguez E, Costa-Mattioli M, Pena JL: **Translational control of auditory imprinting and structural plasticity by eIF2 α .** *Elife* 2016, **5**.
216. Sidrauski C, McGeachy AM, Ingolia NT, Walter P: **The small molecule ISRIB reverses the effects of eIF2 α phosphorylation on translation and stress granule assembly.** *Elife* 2015, **4**.
217. Sharma V, Sood R, Khlaifia A, Eslamizade MJ, Hung T-Y, Lou D, Asgarihafshejani A, Lalzar M, Kiniry SJ, Stokes MP, et al.: **eIF2 α controls memory consolidation via excitatory and somatostatin neurons.** *Nature* 2020, **586**:412–416.
218. Krukowski K, Nolan A, Frias ES, Boone M, Ureta G, Grue K, Paladini M-S, Elizarraras E, Delgado L, Bernales S, et al.: **Small molecule cognitive enhancer reverses age-related memory decline in mice.** *Elife* 2020, **9**.
219. Ryan B, Joilin G, Williams JM: **Plasticity-related microRNA and their potential contribution to the maintenance of long-term potentiation.** *Front Mol Neurosci* 2015, **8**:4.
220. Bredy TW, Lin Q, Wei W, Baker-Andresen D, Mattick JS: **MicroRNA regulation of neural plasticity and memory.** *Neurobiol Learn Mem* 2011, **96**:89–94.
221. Lugli G, Larson J, Martone ME, Jones Y, Smalheiser NR: **Dicer and eIF2c are enriched at postsynaptic densities in adult mouse brain and are modified by neuronal activity in a calpain-dependent manner.** *J Neurochem* 2005, **94**:896–905.
222. Lugli G, Larson J, Demars MP, Smalheiser NR: **Primary microRNA precursor transcripts are localized at post-synaptic densities in adult mouse forebrain.** *J Neurochem* 2012, **123**:459–466.
223. Pichardo-Casas I, Goff LA, Swerdel MR, Athie A, Davila J, Ramos-Brossier M, Lapid-Volosin

- M, Friedman WJ, Hart RP, Vaca L: **Expression profiling of synaptic microRNAs from the adult rat brain identifies regional differences and seizure-induced dynamic modulation.** *Brain Res* 2012, **1436**:20–33.
224. Konopka W, Schütz G, Kaczmarek L: **The microRNA contribution to learning and memory.** *Neurosci a Rev J bringing Neurobiol Neurol psychiatry* 2011, **17**:468–474.
225. Gu Q-H, Yu D, Hu Z, Liu X, Yang Y, Luo Y, Zhu J, Li Z: **miR-26a and miR-384-5p are required for LTP maintenance and spine enlargement.** *Nat Commun* 2015, **6**:6789.
226. Shrestha P, Shan Z, Mamcarz M, Ruiz KSA, Zerihoun AT, Juan C-Y, Herrero-Vidal PM, Pelletier J, Heintz N, Klann E: **Amygdala inhibitory neurons as loci for translation in emotional memories.** *Nature* 2020, doi:10.1038/s41586-020-2793-8.
227. Shrestha P, Ayata P, Herrero-Vidal P, Longo F, Gastone A, LeDoux JE, Heintz N, Klann E: **Cell-type-specific drug-inducible protein synthesis inhibition demonstrates that memory consolidation requires rapid neuronal translation.** *Nat Neurosci* 2020, **23**:281–292.
228. Lai M-C, Lombardo M V, Baron-Cohen S: **Autism.** *Lancet* 2014, **383**:896–910.
229. Santini E, Klann E: **Reciprocal signaling between translational control pathways and synaptic proteins in autism spectrum disorders.** *Sci Signal* 2014, **7**:re10.
230. Neves-Pereira M, Müller B, Massie D, Williams JHG, O'Brien PCM, Hughes A, Shen S-B, Clair DS, Miedzybrodzka Z: **Deregulation of EIF4E: a novel mechanism for autism.** *J Med Genet* 2009, **46**:759–765.
231. Lombardo M V, Moon HM, Su J, Palmer TD, Courchesne E, Pramparo T: **Maternal immune activation dysregulation of the fetal brain transcriptome and relevance to the pathophysiology of autism spectrum disorder.** *Mol Psychiatry* 2017, **23**:1001–1013.
232. Abbeduto L, Thurman AJ, McDuffie A, Klusek J, Feigles RT, Ted Brown W, Harvey DJ, Adayev T, LaFauci G, Dobkins C, et al.: **ASD Comorbidity in Fragile X Syndrome: Symptom Profile and Predictors of Symptom Severity in Adolescent and Young Adult Males.** *J Autism Dev Disord* 2019, **49**:960–977.
233. Shoji H, Takao K, Hattori S, Miyakawa T: **Age-related changes in behavior in C57BL/6J mice from young adulthood to middle age.** *Mol Brain* 2016, **9**:11.

234. Gorski JA, Talley T, Qiu M, Puellas L, Rubenstein JLR, Jones KR: **Cortical Excitatory Neurons and Glia, But Not GABAergic Neurons, Are Produced in the Emx1-Expressing Lineage.** *J Neurosci* 2002, **22**:6309–6314.
235. Schmidt EK, Clavarino G, Ceppi M, Pierre P: **SUnSET, a nonradioactive method to monitor protein synthesis.** *Nat Meth* 2009, **6**:275–277.
236. Tsien JZ, Chen DF, Gerber D, Tom C, Mercer EH, Anderson DJ, Mayford M, Kandel ER, Tonegawa S: **Subregion- and Cell Type–Restricted Gene Knockout in Mouse Brain.** *Cell* 1996, **87**:1317–1326.
237. Hoeffler CA, Tang W, Wong H, Santillan A, Patterson RJ, Martinez LA, Tejada-Simon M V, Paylor R, Hamilton SL, Klann E: **Removal of FKBP12 enhances mTOR-Raptor interactions, LTP, memory, and perseverative/repetitive behavior.** *Neuron* 2008, **60**:832–845.
238. Kelleher RJ, Bear MF: **The Autistic Neuron: Troubled Translation?** *Cell* 2008, **135**:401–406.
239. Bear MF, Huber KM, Warren ST: **The mGluR theory of fragile X mental retardation.** *Trends Neurosci* 2004, **27**:370–377.
240. Garritano J, Martinez C, Grossman K, Intemann P, Merritt K, Pfoff R, Smock T: **The output of the hippocampus is inhibited during social behavior in the male rat.** *Exp brain Res* 1996, **111**:35–40.
241. Blaise JH, Koranda JL, Chow U, Haines KE, Dorward EC: **Neonatal isolation stress alters bidirectional long-term synaptic plasticity in amygdalo-hippocampal synapses in freely behaving adult rats.** *Brain Res* 2008, **1193**:25–33.
242. Walf AA, Frye CA: **The use of the elevated plus maze as an assay of anxiety-related behavior in rodents.** *Nat Protoc* 2007, **2**:322–328.
243. Seibenhener ML, Wooten MC: **Use of the Open Field Maze to measure locomotor and anxiety-like behavior in mice.** *J Vis Exp* 2015, doi:10.3791/52434.
244. Blum S, Moore AN, Adams F, Dash PK: **A mitogen-activated protein kinase cascade in the CA1/CA2 subfield of the dorsal hippocampus is essential for long-term spatial memory.** *J Neurosci* 1999, **19**:3535–3544.
245. Adams JP, Sweatt JD: **Molecular psychology: roles for the ERK MAP kinase cascade in memory.** *Annu Rev Pharmacol Toxicol* 2002, **42**:135–163.

246. Kelly A, Laroche S, Davis S: **Activation of mitogen-activated protein kinase/extracellular signal-regulated kinase in hippocampal circuitry is required for consolidation and reconsolidation of recognition memory.** *J Neurosci* 2003, **23**:5354–5360.
247. Kazdoba TM, Hagerman RJ, Zolkowska D, Rogawski MA, Crawley JN: **Evaluation of the neuroactive steroid ganaxolone on social and repetitive behaviors in the BTBR mouse model of autism.** *Psychopharmacology (Berl)* 2016, **233**:309–323.
248. Friend DM, Kravitz A V: **Working together: basal ganglia pathways in action selection.** *Trends Neurosci* 2014, **37**:301–303.
249. Aldridge JW, Berridge KC, Rosen AR: **Basal ganglia neural mechanisms of natural movement sequences.** *Can J Physiol Pharmacol* 2004, **82**:732–739.
250. Jin X, Tecuapetla F, Costa RM: **Basal ganglia subcircuits distinctively encode the parsing and concatenation of action sequences.** *Nat Neurosci* 2014, **17**:423–430.
251. Sorensen EM, Bertelsen F, Weikop P, Skovborg MM, Banke T, Drasbek KR, Scheel-Kruger J: **Hyperactivity and lack of social discrimination in the adolescent Fmr1 knockout mouse.** *Behav Pharmacol* 2015, **26**:733–740.
252. Dhamne SC, Silverman JL, Super CE, Lammers SHT, Hameed MQ, Modi ME, Copping NA, Pride MC, Smith DG, Rotenberg A, et al.: **Replicable in vivo physiological and behavioral phenotypes of the Shank3B null mutant mouse model of autism.** *Mol Autism* 2017, **8**:26.
253. Auerbach BD, Osterweil EK, Bear MF: **Mutations causing syndromic autism define an axis of synaptic pathophysiology.** *Nature* 2011, **480**:63–68.
254. Huber KM, Gallagher SM, Warren ST, Bear MF: **Altered synaptic plasticity in a mouse model of fragile X mental retardation.** *Proc Natl Acad Sci U S A* 2002, **99**:7746–7750.
255. Bozdagi O, Sakurai T, Dorr N, Pilorge M, Takahashi N, Buxbaum JD: **Haploinsufficiency of Cyfip1 produces fragile X-like phenotypes in mice.** *PLoS One* 2012, **7**:e42422.
256. Nectow AR, Moya M V, Ekstrand MI, Mousa A, McGuire KL, Sferrazza CE, Field BC, Rabinowitz GS, Sawicka K, Liang Y, et al.: **Rapid Molecular Profiling of Defined Cell Types Using Viral TRAP.** *Cell Rep* 2017, **19**:655–667.
257. Van der Paelt S, Warreyn P, Roeyers H: **Effect of community interventions on social-communicative abilities of preschoolers with autism spectrum disorder.** *Dev*

- Neurorehabil* 2016, **19**:162–174.
258. Beversdorf DQ: **Phenotyping, Etiological Factors, and Biomarkers: Toward Precision Medicine in Autism Spectrum Disorders.** *J Dev Behav Pediatr* 2016, **37**:659–673.
259. Gantois I, Popic J, Khoutorsky A, Sonenberg N: **Metformin for Treatment of Fragile X Syndrome and Other Neurological Disorders.** *Annu Rev Med* 2019, **70**:167–181.
260. Flexner JB, Flexner LB, Stellar E: **Memory in Mice as Affected by Intracerebral Puromycin.** *Science (80-)* 1963, **141**:57 LP – 59.
261. Hoeffler CA, Cowansage KK, Arnold EC, Banko JL, Moerke NJ, Rodriguez R, Schmidt EK, Klosi E, Chorev M, Lloyd RE, et al.: **Inhibition of the interactions between eukaryotic initiation factors 4E and 4G impairs long-term associative memory consolidation but not reconsolidation.** *Proc Natl Acad Sci* 2011, **108**:3383–3388.
262. Wei C-W, Luo T, Zou S-S, Wu A-S: **Research progress on the roles of microRNAs in governing synaptic plasticity, learning and memory.** *Life Sci* 2017, **188**:118–122.
263. Taniguchi H, He M, Wu P, Kim S, Paik R, Sugino K, Kvitsani D, Fu Y, Lu J, Lin Y, et al.: **A Resource of Cre Driver Lines for Genetic Targeting of GABAergic Neurons in Cerebral Cortex.** *Neuron* 2011, **71**:995–1013.
264. De Gregorio D, Popic J, Enns JP, Inserra A, Skalecka A, Markopoulos A, Posa L, Lopez-Canul M, Qianzi H, Lafferty CK, et al.: **Lysergic acid diethylamide (LSD) promotes social behavior through mTORC1 in the excitatory neurotransmission.** *Proc Natl Acad Sci USA* 2021, **118**.
265. Wanisch K, Wotjak CT: **Time course and efficiency of protein synthesis inhibition following intracerebral and systemic anisomycin treatment.** *Neurobiol Learn Mem* 2008, **90**:485–494.
266. Morris RG, Garrud P, Rawlins JN, O’Keefe J: **Place navigation impaired in rats with hippocampal lesions.** *Nature* 1982, **297**:681–683.
267. Schwartz JH, Castellucci VF, Kandel ER: **Functioning of identified neurons and synapses in abdominal ganglion of Aplysia in absence of protein synthesis.** *J Neurophysiol* 1971, **34**:939–953.
268. Davis HP, Spanis CW, Squire LR: **Inhibition of cerebral protein synthesis: performance at different times after passive avoidance training.** *Pharmacol Biochem Behav* 1976, **4**:13–

- 16.
269. Montarolo PG, Goelet P, Castellucci VF, Morgan J, Kandel ER, Schacher S: **A critical period for macromolecular synthesis in long-term heterosynaptic facilitation in Aplysia.** *Science* 1986, **234**:1249–1254.
270. Davis HP, Rosenweig MR, Jones OW, Bennett EL: **Inhibition of cerebral protein synthesis does not prolong short-term memory.** *J Comp Physiol Psychol* 1981, **95**:556–564.
271. Goldman-Rakic PS: **Cellular basis of working memory.** *Neuron* 1995, **14**:477–485.
272. Trinh MA, Kaphzan H, Wek RC, Pierre P, Cavener DR, Klann E: **Brain-specific disruption of the eIF2 α kinase PERK decreases ATF4 expression and impairs behavioral flexibility.** *Cell Rep* 2012, **1**:676–688.
273. Friedman L, Sterling A: **A Review of Language, Executive Function, and Intervention in Autism Spectrum Disorder.** *Semin Speech Lang* 2019, **40**:291–304.
274. Rabiee A, Vasaghi-Gharamaleki B, Samadi SA, Amiri-Shavaki Y, Alaghband-Rad J: **Working Memory Deficits and its Relationship to Autism Spectrum Disorders.** *Iran J Med Sci* 2020, **45**:100–109.
275. Funabiki Y, Shiwa T: **Weakness of visual working memory in autism.** *Autism Res* 2018, **11**:1245–1252.
276. Melotte V, Qu X, Ongenaert M, van Criekinge W, de Bruïne AP, Baldwin HS, van Engeland M: **The N-myc downstream regulated gene (NDRG) family: diverse functions, multiple applications.** *FASEB J Off Publ Fed Am Soc Exp Biol* 2010, **24**:4153–4166.
277. Tazir M, Bellatache M, Nouioua S, Vallat J-M: **Autosomal recessive Charcot-Marie-Tooth disease: from genes to phenotypes.** *J Peripher Nerv Syst* 2013, **18**:113–129.
278. Dubourg O, Azzedine H, Verny C, Durosier G, Birouk N, Gouider R, Salih M, Bouhouche A, Thiam A, Grid D, et al.: **Autosomal-recessive forms of demyelinating Charcot-Marie-Tooth disease.** *Neuromolecular Med* 2006, **8**:75–86.
279. Ito H, Watari K, Shibata T, Miyamoto T, Murakami Y, Nakahara Y, Izumi H, Wakimoto H, Kuwano M, Abe T, et al.: **Bidirectional Regulation between NDRG1 and GSK3 β Controls Tumor Growth and Is Targeted by Differentiation Inducing Factor-1 in Glioblastoma.** *Cancer Res* 2020, **80**:234–248.

280. Bafunno V, Divella C, Sessa F, Tiscia GL, Castellano G, Gesualdo L, Margaglione M, Montinaro V: **De novo homozygous mutation of the C1 inhibitor gene in a patient with hereditary angioedema.** *J Allergy Clin Immunol* 2013, **132**:748-750.e3.
281. Buffington SA, Dooling SW, Sgritta M, Noecker C, Murillo OD, Felice DF, Turnbaugh PJ, Costa-Mattioli M: **Dissecting the contribution of host genetics and the microbiome in complex behaviors.** *Cell* 2021, **184**:1740-1756.e16.
282. Amaya Ramirez CC, Hubbe P, Mandel N, Béthune J: **4EHP-independent repression of endogenous mRNAs by the RNA-binding protein GIGYF2.** *Nucleic Acids Res* 2018, **46**:5792–5808.
283. Crawley JN: **Mouse behavioral assays relevant to the symptoms of autism.** *Brain Pathol* 2007, **17**:448–459.
284. Wang Y, Zhang Y-B, Liu L-L, Cui J-F, Wang J, Shum DHK, van Amelsvoort T, Chan RCK: **A Meta-Analysis of Working Memory Impairments in Autism Spectrum Disorders.** *Neuropsychol Rev* 2017, **27**:46–61.
285. Wang Z, Jing J, Igarashi K, Fan L, Yang S, Li Y, Jin Y: **Executive function predicts the visuospatial working memory in autism spectrum disorder and attention-deficit/hyperactivity disorder.** *Autism Res* 2018, **11**:1148–1156.
286. Miot S, Akbaraly T, Michelon C, Couderc S, Crepiat S, Loubersac J, Picot M-C, Pernon É, Gonnier V, Jeandel C, et al.: **Comorbidity Burden in Adults With Autism Spectrum Disorders and Intellectual Disabilities-A Report From the EFAAR (Frailty Assessment in Ageing Adults With Autism Spectrum and Intellectual Disabilities) Study.** *Front psychiatry* 2019, **10**:617.
287. Hoffenberg SE: **Mental Retardation.** In *Encyclopedia of Child Behavior and Development.* Edited by Goldstein S, Naglieri JA. Springer US; 2011:941–943.
288. Papazoglou A, Jacobson LA, McCabe M, Kaufmann W, Zabel TA: **To ID or not to ID? Changes in classification rates of intellectual disability using DSM-5.** *Intellect Dev Disabil* 2014, **52**:165–174.
289. Antoine MW, Langberg T, Schnepel P, Feldman DE: **Increased Excitation-Inhibition Ratio Stabilizes Synapse and Circuit Excitability in Four Autism Mouse Models.** *Neuron* 2019,

- 101:648-661.e4.**
290. Okumura F, Zou W, Zhang D-E: **ISG15 modification of the eIF4E cognate 4EHP enhances cap structure-binding activity of 4EHP.** *Genes Dev* 2007, **21**:255–260.
291. Manning BD, Cantley LC: **AKT/PKB signaling: navigating downstream.** *Cell* 2007, **129**:1261–1274.
292. Moritz A, Li Y, Guo A, Villén J, Wang Y, MacNeill J, Kornhauser J, Sprott K, Zhou J, Possemato A, et al.: **Akt-RSK-S6 kinase signaling networks activated by oncogenic receptor tyrosine kinases.** *Sci Signal* 2010, **3**:ra64.
293. Ferraiuolo MA, Basak S, Dostie J, Murray EL, Schoenberg DR, Sonenberg N: **A role for the eIF4E-binding protein 4E-T in P-body formation and mRNA decay.** *J Cell Biol* 2005, **170**:913–924.
294. Räsch F, Weber R, Izaurralde E, Igreja C: **4E-T-bound mRNAs are stored in a silenced and deadenylated form.** *Genes Dev* 2020, **34**:847–860.
295. Youn J-Y, Dyakov BJA, Zhang J, Knight JDR, Vernon RM, Forman-Kay JD, Gingras A-C: **Properties of Stress Granule and P-Body Proteomes.** *Mol Cell* 2019, **76**:286–294.
296. Alberti S, Gladfelter A, Mittag T: **Considerations and Challenges in Studying Liquid-Liquid Phase Separation and Biomolecular Condensates.** *Cell* 2019, **176**:419–434.
297. Tsang B, Arsenault J, Vernon RM, Lin H, Sonenberg N, Wang L-Y, Bah A, Forman-Kay JD: **Phosphoregulated FMRP phase separation models activity-dependent translation through bidirectional control of mRNA granule formation.** *Proc Natl Acad Sci U S A* 2019, **116**:4218–4227.
298. Kim TH, Tsang B, Vernon RM, Sonenberg N, Kay LE, Forman-Kay JD: **Phospho-dependent phase separation of FMRP and CAPRIN1 recapitulates regulation of translation and deadenylation.** *Science* 2019, **365**:825–829.
299. Sheu-Gruttadauria J, MacRae IJ: **Phase Transitions in the Assembly and Function of Human miRISC.** *Cell* 2018, **173**:946-957.e16.
300. Sun T, Li Q, Xu Y, Zhang Z, Lai L, Pei J: **Prediction of liquid-liquid phase separation proteins using machine learning.** *bioRxiv* 2019, doi:10.1101/842336.
301. Frydryskova K, Masek T, Borcin K, Mrvova S, Venturi V, Pospisek M: **Distinct recruitment**

- of human eIF4E isoforms to processing bodies and stress granules.** *BMC Mol Biol* 2016, **17**:21.
302. Ptushkina M, Berthelot K, von der Haar T, Geffers L, Warwicker J, McCarthy JE: **A second eIF4E protein in Schizosaccharomyces pombe has distinct eIF4G-binding properties.** *Nucleic Acids Res* 2001, **29**:4561–4569.
303. Collaborators G 2016 N: **Global, regional, and national burden of neurological disorders, 1990-2016: a systematic analysis for the Global Burden of Disease Study 2016.** *Lancet Neurol* 2019, **18**:459–480.
304. McClellan J, King M-C: **Genetic Heterogeneity in Human Disease.** *Cell* 2010, **141**:210–217.
305. Hay M, Thomas DW, Craighead JL, Economides C, Rosenthal J: **Clinical development success rates for investigational drugs.** *Nat Biotechnol* 2014, **32**:40–51.

Appendix A: Supplementary tables and figures

Table S2.1: Details of statistical analyses for Chapter 2

Fig. 2.1D	ANOVA summary		Brown-Forsythe test			
	F	13.68	F (DFn, DFd)	0.7629 (2, 6)		
	P value	0.0058	P value	0.5067		
	P value summary	**	P value summary	ns		
	Significant diff. among means (P < 0.05)?	Yes	Are SDs significantly different (P < 0.05)?	No		
	R squared	0.8202				
	ANOVA table	SS	DF	MS	F (DFn, DFd)	P value
	Treatment (between columns)	20971	2	10486	F (2, 6) = 13.68	P=0.0058
	Residual (within columns)	4598	6	766.3		
	Total	25569	8			
Fig. 2.2G	Tukey's multiple comparisons test	Mean Diff.	95.00% CI of diff.	Significant ?	Summary	Adjusted P Value
	Crude vs. Cyto.	8.355	-61.00 to 77.71	No	ns	0.9283
	Crude vs. Syn.	-97.97	-167.3 to -28.62	Yes	*	0.0116
	Cyto. vs. Syn.	-106.3	-175.7 to -36.97	Yes	**	0.0079
	Unpaired t test		How big is the difference?		F test to compare variances	
P value	0.0376	<i>Eif4e2^{+/+};Emx1-Cre</i>	76.95	F, DFn, Dfd	1.232, 7, 7	
P value summary	*	<i>Eif4e2^{flx/flx};Emx1-Cre</i>	61.21	P value	0.7902	
Significantly different (P < 0.05)?	Yes	Difference between means (B - A) ± SEM	-15.74 ± 6.856	P value summary	ns	
One- or two-tailed P value?	Two-tailed	95% confidence interval	-30.45 to -1.036	Significantly different (P < 0.05)?	No	
t, df	t=2.296, df=14	R squared (eta squared)	0.2735			
Fig. 2.2I	Two-way RM ANOVA		Matching:			
		Stacked				
	Assume sphericity?	Yes				
	Alpha	0.05				
	Source of Variation	% of total variation	P value	P value summary	Significant?	
	Chamber x Genotype	0.05365	0.8762	ns	No	
	Chamber	32.13	0.0011	**	Yes	
	Genotype	6.99	0.0266	*	Yes	
	Subject	21.57	0.8874	ns	No	
	ANOVA table	SS	DF	MS	F (DFn, DFd)	P value
	Chamber x Genotype	30.08	1	30.08	F (1, 18) = 0.02497	P=0.8762
	Chamber	18012	1	18012	F (1, 18) = 14.95	P=0.0011
	Genotype	3919	1	3919	F (1, 18) = 5.833	P=0.0266
	Subject	12094	18	671.9	F (18, 18) = 0.5578	P=0.8874
	Residual	21681	18	1205		
	Difference between row means		Difference between column means		Interaction CI	
	Mean of S1	82.99	Mean of <i>Eif4e2^{+/+};Emx1-Cre</i>	71.61	Mean diff, A1 - B1	21.64
	Mean of E	40.33	Mean of <i>Eif4e2^{flx/flx};Emx1-Cre</i>	51.71	Mean diff, A2 - B2	18.15
	Difference between means	42.65	Difference between means	19.9	(A1 - B1) - (A2 - B2)	3.486
	SE of difference	11.03	SE of difference	8.238	95% CI of difference	-42.86 to 49.83

	95% CI of difference	19.48 to 65.83	95% CI of difference	2.590 to 37.20	(B1 - A1) - (B2 - A2)	-3.486
					95% CI of difference	-49.83 to 42.86
Fig. 2.2J	Two-way RM ANOVA	Matching: Stacked				
	Assume sphericity?	Yes				
	Alpha	0.05				
	Source of Variation	% of total variation	P value	P value summary	Significant?	
	Chamber x Genotype	6.663	0.0235	*	Yes	
	Chamber	24.21	0.0002	***	Yes	
	Genotype	10.54	0.0342	*	Yes	
	Subject	36.12	0.1021	ns	No	
	ANOVA table	SS	DF	MS	F (DFn, DFd)	P value
	Chamber x Genotype	1591	1	1591	F (1, 18) = 6.121	P=0.0235
	Chamber	5781	1	5781	F (1, 18) = 22.24	P=0.0002
	Genotype	2516	1	2516	F (1, 18) = 5.253	P=0.0342
	Subject	8623	18	479.1	F (18, 18) = 1.843	P=0.1021
	Residual	4678	18	259.9		
	Difference between row means		Difference between column means		Interaction CI	
	Mean of S1	35.55	Mean of <i>Eif4e2^{+/+}:Emx1-Cre</i>	55.61	Mean diff, A1 - B1	3.267
	Mean of S2	59.72	Mean of <i>Eif4e2^{flx/flx}:Emx1-Cre</i>	39.67	Mean diff, A2 - B2	28.62
	Difference between means	-24.16	Difference between means	15.94	(A1 - B1) - (A2 - B2)	-25.35
	SE of difference	5.124	SE of difference	6.956	95% CI of difference	-46.88 to -3.823
	95% CI of difference	-34.93 to -13.40	95% CI of difference	1.329 to 30.56	(B1 - A1) - (B2 - A2)	25.35
					95% CI of difference	3.823 to 46.88
	Bonferroni's multiple comparisons test	Predicted (LS) mean diff.	95.00% CI of diff.	Significant ?	Summary	Adjusted P Value
	S1 - S2					
	<i>Eif4e2^{+/+}:Emx1-Cre</i>	-36.84	-53.65 to -20.03	Yes	****	<0.0001
	<i>Eif4e2^{flx/flx}:Emx1-Cre</i>	-11.49	-30.07 to 7.094	No	ns	0.296
Fig. 2.2L	Unpaired t test with Welch's correction		How big is the difference?		F test to compare variances	
	P value	0.0154	<i>Eif4e2^{+/+}:Emx1-Cre</i>	31.58	F, DFn, Dfd	4.774, 9, 10
	P value summary	*	<i>Eif4e2^{flx/flx}:Emx1-Cre</i>	12.65	P value	0.0226
	Significantly different (P < 0.05)?	Yes	Difference between means (B - A) ± SEM	-18.92 ± 6.733	P value summary	*
	One- or two-tailed P value?	Two-tailed	95% confidence interval	-33.54 to -4.297	Significantly different (P < 0.05)?	Yes
	Welch-corrected t, df	t=2.810, df=12.35	R squared (eta squared)	0.39		
Fig. 2.2M	Unpaired t test with Welch's correction		How big is the difference?		F test to compare variances	
	P value	0.0404	<i>Eif4e2^{+/+}:Emx1-Cre</i>	91.21	F, DFn, Dfd	6.058, 9, 10
	P value summary	*	<i>Eif4e2^{flx/flx}:Emx1-Cre</i>	50.87	P value	0.0094
	Significantly different (P < 0.05)?	Yes	Difference between means (B - A) ± SEM	-40.34 ± 17.50	P value summary	**
	One- or two-tailed P value?	Two-tailed	95% confidence interval	-78.59 to -2.085	Significantly different (P < 0.05)?	Yes
	Welch-corrected t, df	t=2.305, df=11.67	R squared (eta squared)	0.3129		

Fig. 2.3A	Unpaired t test		How big is the difference?		F test to compare variances		
	P value	0.6284	<i>Eif4e2^{+/+}:Emx1-Cre</i>	5.273	F, DFn, Dfd	1.528, 8, 10	
	P value summary	ns	<i>Eif4e2^{flx/flx}:Emx1-Cre</i>	5.778	P value	0.5208	
	Significantly different (P < 0.05)?	No	Difference between means (B - A) ± SEM	0.5051 ± 1.026	P value summary	ns	
	One- or two-tailed P value?	Two-tailed	95% confidence interval	-1.650 to 2.660	Significantly different (P < 0.05)?	No	
t, df	t=0.4924, df=18	R squared (eta squared)	0.01329				
Fig. 2.3B	Unpaired t test		How big is the difference?		F test to compare variances		
	P value	0.897	<i>Eif4e2^{+/+}:Emx1-Cre</i>	156.3	F, DFn, Dfd	1.465, 10, 7	
	P value summary	ns	<i>Eif4e2^{flx/flx}:Emx1-Cre</i>	159.7	P value	0.6292	
	Significantly different (P < 0.05)?	No	Difference between means (B - A) ± SEM	3.433 ± 26.13	P value summary	ns	
	One- or two-tailed P value?	Two-tailed	95% confidence interval	-51.70 to 58.57	Significantly different (P < 0.05)?	No	
t, df	t=0.1314, df=17	R squared (eta squared)	0.001014				
Fig. 2.3C	Table Analyzed						
	Unpaired t test		How big is the difference?		F test to compare variances		
	P value	0.5341	<i>Eif4e2^{+/+}:Emx1-Cre</i>	10.07	F, DFn, Dfd	1.178, 8, 8	
	P value summary	ns	<i>Eif4e2^{flx/flx}:Emx1-Cre</i>	13.56	P value	0.8227	
	Significantly different (P < 0.05)?	No	Difference between means (B - A) ± SEM	3.489 ± 5.491	P value summary	ns	
One- or two-tailed P value?	Two-tailed	95% confidence interval	-8.151 to 15.13	Significantly different (P < 0.05)?	No		
t, df	t=0.6354, df=16	R squared (eta squared)	0.02461				
	Table Analyzed						
	Unpaired t test		How big is the difference?		F test to compare variances		
	P value	0.15	<i>Eif4e2^{+/+}:Emx1-Cre</i>	13.39	F, DFn, Dfd	1.074, 8, 8	
	P value summary	ns	<i>Eif4e2^{flx/flx}:Emx1-Cre</i>	15.12	P value	0.9221	
	Significantly different (P < 0.05)?	No	Difference between means (B - A) ± SEM	1.736 ± 1.148	P value summary	ns	
	One- or two-tailed P value?	Two-tailed	95% confidence interval	-0.6977 to 4.171	Significantly different (P < 0.05)?	No	
	t, df	t=1.512, df=16	R squared (eta squared)	0.1251			
Fig. 2.3D	Two-way RM ANOVA		Matching: Stacked				
	Assume sphericity?	No					
	Alpha	0.05					
	Source of Variation		% of total variation	P value	P value summary	Significant?	Geisser-Greenhouse's epsilon
	Time x Genotype	6.203	0.0144	*	Yes		
	Time	4.82	0.1487	ns	No	0.3282	
	Genotype	5.813	0.1069	ns	No		
	Subject	36.32	<0.0001	****	Yes		
	ANOVA table		SS	DF	MS	F (DFn, DFd)	P value
	Time x Genotype	262418	9	29158	F (9, 162) = 2.391	P=0.0144	
	Time	203893	9	22655	F (2.954, 53.17) = 1.858	P=0.1487	
	Genotype	245893	1	245893	F (1, 18) = 2.881	P=0.1069	
	Subject	1536462	18	85359	F (18, 162) = 7.001	P<0.0001	

	Residual	1975187	162	12193		
	Difference between column means					
	Mean of <i>Eif4e2^{+/+};Emx1-Cre</i>	384				
	Mean of <i>Eif4e2^{flx/flx};Emx1-Cre</i>	454.5				
	Difference between means	-70.48				
	SE of difference	41.53				
	95% CI of difference	-157.7 to 16.76				
	Bonferroni's multiple comparisons test	Mean Diff.	95.00% CI of diff.	Significant ?	Summary	Adjusted P Value
	<i>Eif4e2^{+/+};Emx1-Cre</i> - <i>Eif4e2^{flx/flx};Emx1-Cre</i>					
	Row 1	-20.31	-322.3 to 281.7	No	ns	>0.9999
	Row 2	8.453	-192.3 to 209.2	No	ns	>0.9999
	Row 3	60.69	-164.5 to 285.8	No	ns	>0.9999
	Row 4	-120.5	-304.7 to 63.58	No	ns	0.5034
	Row 5	-51.68	-244.7 to 141.3	No	ns	>0.9999
	Row 6	-39.27	-204.6 to 126.1	No	ns	>0.9999
	Row 7	-120	-286.9 to 47.02	No	ns	0.3357
	Row 8	-170.6	-359.6 to 18.43	No	ns	0.097
	Row 9	-77.65	-307.8 to 152.5	No	ns	>0.9999
	Row 10	-174	-319.5 to -28.43	Yes	*	0.0128
	Table Analyzed					
	Center Entries					
	Unpaired t test		How big is the difference?		F test to compare variances	
	P value	0.1342	<i>Eif4e2^{+/+};Emx1-Cre</i>	26.55	F, DFn, Dfd	1.850, 8, 10
	P value summary	ns	<i>Eif4e2^{flx/flx};Emx1-Cre</i>	34.89	P value	0.3573
	Significantly different (P < 0.05)?	No	Difference between means (B - A) ± SEM	8.343 ± 5.320	P value summary	ns
	One- or two-tailed P value?	Two-tailed	95% confidence interval	-2.833 to 19.52	Significantly different (P < 0.05)?	No
	t, df	t=1.568, df=18	R squared (eta squared)	0.1202		
	Table Analyzed					
	Time in center					
	Unpaired t test		How big is the difference?		F test to compare variances	
	P value	0.4769	<i>Eif4e2^{+/+};Emx1-Cre</i>	52.32	F, DFn, Dfd	2.009, 8, 10
	P value summary	ns	<i>Eif4e2^{flx/flx};Emx1-Cre</i>	59.94	P value	0.2985
	Significantly different (P < 0.05)?	No	Difference between means (B - A) ± SEM	7.616 ± 10.48	P value summary	ns
	One- or two-tailed P value?	Two-tailed	95% confidence interval	-14.41 to 29.64	Significantly different (P < 0.05)?	No
	t, df	t=0.7265, df=18	R squared (eta squared)	0.02849		
Fig. 2.3E	Unpaired t test		How big is the difference?		F test to compare variances	
	P value	0.3408	<i>Eif4e2^{+/+};Emx1-Cre</i>	125.3	F, DFn, Dfd	1.090, 8, 10
	P value summary	ns	<i>Eif4e2^{flx/flx};Emx1-Cre</i>	141.8	P value	0.8806
	Significantly different (P < 0.05)?	No	Difference between means (B - A) ± SEM	16.51 ± 16.87	P value summary	ns
	One- or two-tailed P value?	Two-tailed	95% confidence interval	-18.93 to 51.94	Significantly different (P < 0.05)?	No
	t, df	t=0.9785, df=18	R squared (eta squared)	0.05051		
Fig. 2.3F	Two-way ANOVA					
	Ordinary					
	Alpha	0.05				
	Source of Variation	% of total variation	P value	P value summary	Significant?	
	Interaction	0.1542	0.7895	ns	No	
	Treatment	57.73	<0.0001	****	Yes	
	Genotype	0.00324	0.9691	ns	No	

	ANOVA table	SS (Type III)	DF	MS	F (DFn, DFd)	P value
	Interaction	4.95	1	4.95	F (1, 20) = 0.07322	P=0.7895
	Treatment	1854	1	1854	F (1, 20) = 27.42	P<0.0001
	Genotype	0.104	1	0.104	F (1, 20) = 0.001539	P=0.9691
	Residual	1352	20	67.61		
	Difference between column means		Difference between row means		Interaction CI	
	Predicted (LS) mean of <i>Eif4e2^{+/+}:Emx1-Cre</i>	12.9	Predicted (LS) mean of Water	21.75	Mean diff, A1 - B1	0.7767
	Predicted (LS) mean of <i>Eif4e2^{flx/flx}:Emx1-Cre</i>	13.03	Predicted (LS) mean of Cinnamon	4.177	Mean diff, A2 - B2	-1.04
	Difference between predicted means	-0.1317	Difference between predicted means	17.58	(A1 - B1) - (A2 - B2)	1.817
	SE of difference	3.357	SE of difference	3.357	95% CI of difference	-12.19 to 15.82
	95% CI of difference	-7.134 to 6.870	95% CI of difference	10.57 to 24.58	(B1 - A1) - (B2 - A2)	-1.817
					95% CI of difference	-15.82 to 12.19
Fig. 2.3G	Two-way RM ANOVA	Matching: Stacked				
	Assume sphericity?	Yes				
	Alpha	0.05				
	Source of Variation	% of total variation	P value	P value summary	Significant?	
	Arms x Genotype	0.4062	0.1431	ns	No	
	Arms	95.45	<0.0001	****	Yes	
	Genotype	0.02507	0.225	ns	No	
	Subject	0.2687	>0.9999	ns	No	
	ANOVA table	SS	DF	MS	F (DFn, DFd)	P value
	Arms x Genotype	1860	1	1860	F (1, 17) = 2.358	P=0.1431
	Arms	437149	1	437149	F (1, 17) = 554.0	P<0.0001
	Genotype	114.8	1	114.8	F (1, 17) = 1.586	P=0.2250
	Subject	1231	17	72.4	F (17, 17) = 0.09175	P>0.9999
	Residual	13415	17	789.1		
	Difference between row means		Difference between column means		Interaction CI	
	Mean of Closed arms	234.9	Mean of <i>Eif4e2^{+/+}:Emx1-Cre</i>	129.3	Mean diff, A1 - B1	17.49
	Mean of Open arms	20.11	Mean of <i>Eif4e2^{flx/flx}:Emx1-Cre</i>	125.8	Mean diff, A2 - B2	-10.53
	Difference between means	214.8	Difference between means	3.481	(A1 - B1) - (A2 - B2)	28.03
	SE of difference	9.127	SE of difference	2.764	95% CI of difference	-10.48 to 66.54
	95% CI of difference	195.6 to 234.1	95% CI of difference	-2.351 to 9.314	(B1 - A1) - (B2 - A2)	-28.03
					95% CI of difference	-66.54 to 10.48
Fig. 2.4A	Two-way RM ANOVA	Matching: Stacked				
	Assume sphericity?	Yes				
	Alpha	0.05				
	Source of Variation	% of total variation	P value	P value summary	Significant?	
	Chamber x Genotype	0.0002477	0.9889	ns	No	
	Chamber	46.09	<0.0001	****	Yes	
	Genotype	0.008138	0.9489	ns	No	
	Subject	32.76	0.184	ns	No	

	ANOVA table	SS	DF	MS	F (DFn, DFd)	P value
	Chamber x Genotype	0.04148	1	0.04148	F (1, 17) = 0.0002005	P=0.9889
	Chamber	7718	1	7718	F (1, 17) = 37.32	P<0.0001
	Genotype	1.363	1	1.363	F (1, 17) = 0.004223	P=0.9489
	Subject	5487	17	322.7	F (17, 17) = 1.560	P=0.1840
	Residual	3516	17	206.8		
	Difference between row means		Difference between column means		Interaction CI	
	Mean of S1	80.57	Mean of <i>Gigyf2^{+/+}</i>	66.49	Mean diff, A1 - B1	0.4454
	Mean of E	52.03	Mean of <i>Gigyf2^{-/-}</i>	66.11	Mean diff, A2 - B2	0.3131
	Difference between means	28.54	Difference between means	0.3793	(A1 - B1) - (A2 - B2)	0.1323
	SE of difference	4.672	SE of difference	5.837	95% CI of difference	-19.58 to 19.85
	95% CI of difference	18.68 to 38.40	95% CI of difference	-11.94 to 12.69	(B1 - A1) - (B2 - A2)	-0.1323
					95% CI of difference	-19.85 to 19.58
Fig. 2.4B	Two-way RM ANOVA	Matching: Stacked				
	Assume sphericity?	Yes				
	Alpha	0.05				
	Source of Variation	% of total variation	P value	P value summary	Significant?	
	Chamber x Genotype	2.258	0.1805	ns	No	
	Chamber	50.59	<0.0001	****	Yes	
	Genotype	1.315	0.3767	ns	No	
	Subject	27.14	0.2573	ns	No	
	ANOVA table	SS	DF	MS	F (DFn, DFd)	P value
	Chamber x Genotype	770.7	1	770.7	F (1, 17) = 1.950	P=0.1805
	Chamber	17270	1	17270	F (1, 17) = 43.71	P<0.0001
	Genotype	448.9	1	448.9	F (1, 17) = 0.8238	P=0.3767
	Subject	9264	17	544.9	F (17, 17) = 1.379	P=0.2573
	Residual	6717	17	395.1		
	Difference between row means		Difference between column means		Interaction CI	
	Mean of S1	45.26	Mean of <i>Gigyf2^{+/+}</i>	63.17	Mean diff, A1 - B1	2.135
	Mean of S2	87.96	Mean of <i>Gigyf2^{-/-}</i>	70.05	Mean diff, A2 - B2	-15.9
	Difference between means	-42.7	Difference between means	-6.884	(A1 - B1) - (A2 - B2)	18.04
	SE of difference	6.458	SE of difference	7.584	95% CI of difference	-9.213 to 45.29
	95% CI of difference	-56.32 to -29.07	95% CI of difference	-22.89 to 9.118	(B1 - A1) - (B2 - A2)	-18.04
					95% CI of difference	-45.29 to 9.213
Fig. 2.4C	Two-way RM ANOVA	Matching: Stacked				
	Assume sphericity?	No				
	Alpha	0.05				
	Source of Variation	% of total variation	P value	P value summary	Significant?	Geisser-Greenhouse's epsilon
	Time x Genotype	3.565	0.344	ns	No	

	Time	4.697	0.2236	ns	No	0.3716
	Genotype	5.743	0.1017	ns	No	
	Subject	32.62	<0.0001	****	Yes	
	ANOVA table	SS	DF	MS	F (DFn, DFd)	P value
	Time x Genotype	46770	9	5197	F (9, 153) = 1.131	P=0.3440
	Time	61617	9	6846	F (3.345, 56.86) = 1.490	P=0.2236
	Genotype	75332	1	75332	F (1, 17) = 2.993	P=0.1017
	Subject	427852	17	25168	F (17, 153) = 5.479	P<0.0001
	Residual	702780	153	4593		
	Difference between column means					
	Mean of Gigyf2 +/+	293.2				
	Mean of Gigyf2 +/-	333.1				
	Difference between means	-39.88				
	SE of difference	23.05				
	95% CI of difference	-88.51 to 8.753				
Fig. 2.4D	Unpaired t test		How big is the difference?		F test to compare variances	
	P value	0.4055	Gigyf2 +/+	6	F, DFn, Dfd	2.864, 12, 7
	P value summary	ns	Gigyf2 +/-	7	P value	0.1704
	Significantly different (P < 0.05)?	No	Difference between means (B - A) ± SEM	1.000 ± 1.175	P value summary	ns
	One- or two-tailed P value?	Two-tailed	95% confidence interval	-1.460 to 3.460	Significantly different (P < 0.05)?	No
	t, df	t=0.8508, df=19	R squared (eta squared)	0.0367		
Fig. 2.4E	Two-way RM ANOVA					
	Matching:	Stacked				
	Assume sphericity?	Yes				
	Alpha	0.05				
	Source of Variation	% of total variation	P value	P value summary	Significant?	
	Chamber x Genotype	0.1415	0.7395	ns	No	
	Chamber	58.34	<0.0001	****	Yes	
	Genotype	0.8906	0.393	ns	No	
	Subject	19.71	0.5536	ns	No	
	ANOVA table	SS	DF	MS	F (DFn, DFd)	P value
	Chamber x Genotype	46.43	1	46.43	F (1, 17) = 0.1142	P=0.7395
	Chamber	19144	1	19144	F (1, 17) = 47.09	P<0.0001
	Genotype	292.3	1	292.3	F (1, 17) = 0.7681	P=0.3930
	Subject	6468	17	380.5	F (17, 17) = 0.9359	P=0.5536
	Residual	6911	17	406.5		
	Difference between row means		Difference between column means		Interaction CI	
	Mean of S1	93.74	Mean of <i>Eif4e2</i> ^{+/+}	68.48	Mean diff, A1 - B1	-3.34
	Mean of E	48.78	Mean of <i>Eif4e2</i> ^{-/-}	74.04	Mean diff, A2 - B2	-7.768
	Difference between means	44.95	Difference between means	-5.554	(A1 - B1) - (A2 - B2)	4.428
	SE of difference	6.551	SE of difference	6.337	95% CI of difference	-23.21 to 32.07
	95% CI of difference	31.13 to 58.77	95% CI of difference	-18.92 to 7.816	(B1 - A1) - (B2 - A2)	-4.428
					95% CI of difference	-32.07 to 23.21

Fig. 2.4F	Two-way RM ANOVA	Matching: Stacked				
	Assume sphericity?	Yes				
	Alpha	0.05				
	Source of Variation	% of total variation	P value	P value summary	Significant?	
	Chamber x Genotype	0.4588	0.6424	ns	No	
	Chamber	25.04	0.0028	**	Yes	
	Genotype	8.188	0.0514	ns	No	
	Subject	31.7	0.5774	ns	No	
	ANOVA table	SS	DF	MS	F (DFn, DFd)	P value
	Chamber x Genotype	92.84	1	92.84	F (1, 17) = 0.2235	P=0.6424
	Chamber	5068	1	5068	F (1, 17) = 12.20	P=0.0028
	Genotype	1657	1	1657	F (1, 17) = 4.391	P=0.0514
	Subject	6415	17	377.4	F (17, 17) = 0.9083	P=0.5774
	Residual	7062	17	415.4		
	Difference between row means		Difference between column means		Interaction CI	
	Mean of S1	51.12	Mean of <i>Eif4e2</i> ^{+/+}	56.07	Mean diff, A1 - B1	-16.36
	Mean of S2	74.25	Mean of <i>Eif4e2</i> ^{+/-}	69.3	Mean diff, A2 - B2	-10.1
	Difference between means	-23.13	Difference between means	-13.23	(A1 - B1) - (A2 - B2)	-6.261
	SE of difference	6.622	SE of difference	6.311	95% CI of difference	-34.20 to 21.68
95% CI of difference	-37.10 to -9.158	95% CI of difference	-26.54 to 0.09002	(B1 - A1) - (B2 - A2)	6.261	
				95% CI of difference	-21.68 to 34.20	
Fig. 2.4G	Two-way RM ANOVA	Matching: Stacked				
	Assume sphericity?	No				
	Alpha	0.05				
	Source of Variation	% of total variation	P value	P value summary	Significant?	Geisser-Greenhouse's epsilon
	Time x Genotype	6.017	0.0979	ns	No	
	Time	5.319	0.2162	ns	No	0.4436
	Genotype	0.1618	0.7547	ns	No	
	Subject	27.28	<0.0001	****	Yes	
	ANOVA table	SS	DF	MS	F (DFn, DFd)	P value
	Time x Genotype	95093	9	10566	F (9, 153) = 1.681	P=0.0979
	Time	84062	9	9340	F (3.993, 67.88) = 1.486	P=0.2162
	Genotype	2557	1	2557	F (1, 17) = 0.1008	P=0.7547
	Subject	431032	17	25355	F (17, 153) = 4.034	P<0.0001
	Residual	961635	153	6285		
	Difference between column means					
	Mean of <i>Eif4e2</i> ^{+/+}	307.2				
	Mean of <i>Eif4e2</i> ^{+/-}	299.8				
	Difference between means	7.347				
	SE of difference	23.14				
95% CI of difference	-41.47 to 56.16					
Fig. 2.4H	Unpaired t test	How big is the difference?			F test to compare variances	
	P value	0.6171	<i>Eif4e2</i> ^{+/+}	5.2	F, DFn, DFd	1.426, 9, 9
	P value summary	ns	<i>Eif4e2</i> ^{+/-}	5.8	P value	0.6053

	Significantly different (P < 0.05)?	No	Difference between means (B - A) ± SEM	0.6000 ± 1.179	P value summary	ns
	One- or two-tailed P value?	Two-tailed	95% confidence interval	-1.878 to 3.078	Significantly different (P < 0.05)?	No
	t, df	t=0.5087, df=18	R squared (eta squared)	0.01417		
Fig. 2.4I	Two-way RM ANOVA	Matching: Stacked				
	Assume sphericity?	Yes				
	Alpha	0.05				
	Source of Variation	% of total variation	P value	P value summary	Significant?	
	Chamber x Genotype	1.958	0.3508	ns	No	
	Chamber	58.75	0.0002	***	Yes	
	Genotype	4.654	0.0484	*	Yes	
	Subject	11.57	0.901	ns	No	
	ANOVA table	SS	DF	MS	F (DFn, DFd)	P value
	Chamber x Genotype	284.3	1	284.3	F (1, 12) = 0.9426	P=0.3508
	Chamber	8529	1	8529	F (1, 12) = 28.28	P=0.0002
	Genotype	675.7	1	675.7	F (1, 12) = 4.828	P=0.0484
	Subject	1679	12	139.9	F (12, 12) = 0.4640	P=0.9010
	Residual	3619	12	301.6		
	Difference between row means		Difference between column means		Interaction CI	
	Mean of S1	76.4	Mean of <i>Gigyf2^{+/+}:Eif4e2^{+/+}</i>	63.73	Mean diff, A1 - B1	16.37
	Mean of E	41.14	Mean of <i>Gigyf2^{-/-}:Eif4e2^{-/-}</i>	53.81	Mean diff, A2 - B2	3.488
	Difference between means	35.27	Difference between means	9.926	(A1 - B1) - (A2 - B2)	12.88
	SE of difference	6.632	SE of difference	4.517	95% CI of difference	-16.02 to 41.78
	95% CI of difference	20.82 to 49.72	95% CI of difference	0.08376 to 19.77	(B1 - A1) - (B2 - A2)	-12.88
					95% CI of difference	-41.78 to 16.02
Fig. 2.4J	Two-way RM ANOVA	Matching: Stacked				
	Assume sphericity?	Yes				
	Alpha	0.05				
	Source of Variation	% of total variation	P value	P value summary	Significant?	
	Chamber x Genotype	2.399	0.3208	ns	No	
	Chamber	40.78	0.0011	**	Yes	
	Genotype	0.4322	0.6922	ns	No	
	Subject	31.53	0.3925	ns	No	
	ANOVA table	SS	DF	MS	F (DFn, DFd)	P value
	Chamber x Genotype	396	1	396	F (1, 12) = 1.072	P=0.3208
	Chamber	6734	1	6734	F (1, 12) = 18.23	P=0.0011
	Genotype	71.36	1	71.36	F (1, 12) = 0.1645	P=0.6922
	Subject	5206	12	433.8	F (12, 12) = 1.175	P=0.3925
	Residual	4432	12	369.3		
	Difference between row means		Difference between column means		Interaction CI	
	Mean of S1	33.85	Mean of <i>Gigyf2^{+/+}:Eif4e2^{+/+}</i>	51.13	Mean diff, A1 - B1	-4.374

	Mean of S2	65.18	Mean of <i>Giyf2^{+/+}:Eif4e2^{+/-}</i>	47.9	Mean diff, A2 - B2	10.83
	Difference between means	-31.34	Difference between means	3.226	(A1 - B1) - (A2 - B2)	-15.2
	SE of difference	7.339	SE of difference	7.954	95% CI of difference	-47.18 to 16.78
	95% CI of difference	-47.33 to -15.35	95% CI of difference	-14.10 to 20.56	(B1 - A1) - (B2 - A2)	15.2
					95% CI of difference	-16.78 to 47.18
Fig. 2.4K	Two-way RM ANOVA	Matching: Stacked				
	Assume sphericity?	No				
	Alpha	0.05				
	Source of Variation	% of total variation	P value	P value summary	Significant?	Geisser-Greenhouse's epsilon
	Time x Genotype	1.208	0.9586	ns	No	
	Time	20.47	0.0044	**	Yes	0.2805
	Genotype	1.577	0.4676	ns	No	
	Subject	33.62	<0.0001	****	Yes	
	ANOVA table	SS	DF	MS	F (DFn, Dfd)	P value
	Time x Genotype	18802	9	2089	F (9, 108) = 0.3426	P=0.9586
	Time	318568	9	35396	F (2.525, 30.30) = 5.804	P=0.0044
	Genotype	24546	1	24546	F (1, 12) = 0.5629	P=0.4676
	Subject	523283	12	43607	F (12, 108) = 7.151	P<0.0001
	Residual	658606	108	6098		
	Difference between column means					
	Mean of <i>Eif4e2^{+/+}/Giyf2^{+/+}</i>	226.2				
	Mean of <i>Eif4e2^{+/-}/Giyf2^{+/-}</i>	199.4				
	Difference between means	26.76				
	SE of difference	35.66				
	95% CI of difference	-50.95 to 104.5				
Fig. 2.4L	Unpaired t test		How big is the difference?		F test to compare variances	
	P value	0.8683	<i>Eif4e2^{+/+}/Giyf2^{+/+}</i>	5.333	F, DFn, Dfd	1.421, 5, 7
	P value summary	ns	<i>Eif4e2^{+/-}/Giyf2^{+/-}</i>	5.125	P value	0.648
	Significantly different (P < 0.05)?	No	Difference between means (B - A) ± SEM	-0.2083 ± 1.230	P value summary	ns
	One- or two-tailed P value?	Two-tailed	95% confidence interval	-2.887 to 2.471	Significantly different (P < 0.05)?	No
	t, df	t=0.1694, df=12	R squared (eta squared)	0.002386		
Fig. S2.1B	Unpaired t test		How big is the difference?		F test to compare variances	
	P value	<0.0001	<i>Eif4e2^{+/+}:Emx1-Cre</i>	100	F, DFn, Dfd	2.955, 6, 5
	P value summary	****	<i>Eif4e2^{flx/flx}:Emx1-Cre</i>	61.63	P value	0.2547
	Significantly different (P < 0.05)?	Yes	Difference between means (B - A) ± SEM	-38.37 ± 6.214	P value summary	ns
	One- or two-tailed P value?	Two-tailed	95% confidence interval	-52.04 to -24.69	Significantly different (P < 0.05)?	No
	t, df	t=6.174, df=11	R squared (eta squared)	0.7761		
Fig. S2.1C	Unpaired t test		How big is the difference?		F test to compare variances	
	P value	0.0032	<i>Eif4e2^{+/+}:Emx1-Cre</i>	100	F, DFn, Dfd	5.288, 6, 5
	P value summary	**	<i>Eif4e2^{flx/flx}:Emx1-Cre</i>	50.46	P value	0.0879
	Significantly different (P < 0.05)?	Yes	Difference between means (B - A) ± SEM	-49.54 ± 13.21	P value summary	ns

	One- or two-tailed P value?	Two-tailed	95% confidence interval	-78.61 to -20.48	Significantly different (P < 0.05)?	No
	t, df	t=3.752, df=11	R squared (eta squared)	0.5613		
Fig. S2.1E	Unpaired t test		How big is the difference?		F test to compare variances	
	P value	<0.0001	<i>Eif4e2^{+/+}·Emx1-Cre</i>	100	F, DFn, Dfd	1.178, 7, 7
	P value summary	****	<i>Eif4e2^{flx/flx}·Emx1-Cre</i>	35.42	P value	0.8348
	Significantly different (P < 0.05)?	Yes	Difference between means (B - A) ± SEM	-64.58 ± 3.550	P value summary	ns
	One- or two-tailed P value?	Two-tailed	95% confidence interval	-72.19 to -56.97	Significantly different (P < 0.05)?	No
	t, df	t=18.19, df=14	R squared (eta squared)	0.9594		
Fig. S2.1F	Unpaired t test		How big is the difference?		F test to compare variances	
	P value	0.0059	<i>Eif4e2^{+/+}·Emx1-Cre</i>	100	F, DFn, Dfd	12.50, 7, 7
	P value summary	**	<i>Eif4e2^{flx/flx}·Emx1-Cre</i>	55.53	P value	0.0036
	Significantly different (P < 0.05)?	Yes	Difference between means (B - A) ± SEM	-44.47 ± 13.73	P value summary	**
	One- or two-tailed P value?	Two-tailed	95% confidence interval	-73.91 to -15.03	Significantly different (P < 0.05)?	Yes
	t, df	t=3.240, df=14	R squared (eta squared)	0.4285		
Fig. S2.2A	Unpaired t test		How big is the difference?		F test to compare variances	
	P value	0.4267	<i>Eif4e2^{+/+}·Emx1-Cre</i>	100	F, DFn, Dfd	2.471, 3, 3
	P value summary	ns	<i>Eif4e2^{flx/flx}·Emx1-Cre</i>	109.6	P value	0.477
	Significantly different (P < 0.05)?	No	Difference between means (B - A) ± SEM	9.617 ± 11.28	P value summary	ns
	One- or two-tailed P value?	Two-tailed	95% confidence interval	-17.99 to 37.22	Significantly different (P < 0.05)?	No
	t, df	t=0.8524, df=6	R squared (eta squared)	0.108		
Fig. S2.2B	Unpaired t test		How big is the difference?		F test to compare variances	
	P value	0.6067	4EHP +/+	100	F, DFn, Dfd	1.758, 3, 3
	P value summary	ns	4EHP +/-	90.95	P value	0.6544
	Significantly different (P < 0.05)?	No	Difference between means (B - A) ± SEM	-9.051 ± 16.67	P value summary	ns
	One- or two-tailed P value?	Two-tailed	95% confidence interval	-49.84 to 31.74	Significantly different (P < 0.05)?	No
	t, df	t=0.5429, df=6	R squared (eta squared)	0.04683		
Fig. S2.2C	Unpaired t test with Welch's correction		How big is the difference?		F test to compare variances	
	P value	0.4978	<i>Eif4e2^{+/+}·Emx1-Cre</i>	100	F, DFn, Dfd	20.81, 3, 3
	P value summary	ns	<i>Eif4e2^{flx/flx}·Emx1-Cre</i>	83.94	P value	0.0329
	Significantly different (P < 0.05)?	No	Difference between means (B - A) ± SEM	-16.06 ± 21.12	P value summary	*
	One- or two-tailed P value?	Two-tailed	95% confidence interval	-80.06 to 47.94	Significantly different (P < 0.05)?	Yes
	Welch-corrected t, df	t=0.7605, df=3.288	R squared (eta squared)	0.1496		
Fig. S2.3A	Two-way RM ANOVA					
	Assume sphericity?	Yes				
	Alpha	0.05				
	Source of Variation	% of total variation	P value	P value summary	Significant?	
	Time x Genotype	0.1297	0.7436	ns	No	
	Time	45.27	<0.0001	****	Yes	
	Genotype	0.09479	0.8211	ns	No	

	Subject	32.39	0.1876	ns	No	
	ANOVA table	SS	DF	MS	F (DFn, DFd)	P value
	Time x Genotype	11.62	1	11.62	F (1, 18) = 0.1103	P=0.7436
	Time	4054	1	4054	F (1, 18) = 38.50	P<0.0001
	Genotype	8.488	1	8.488	F (1, 18) = 0.05268	P=0.8211
	Subject	2900	18	161.1	F (18, 18) = 1.530	P=0.1876
	Residual	1895	18	105.3		
	Difference between row means		Difference between column means		Interaction CI	
	Mean of Naive	1.368	Mean of <i>Eif4e2^{+/+}:Emx1-Cre</i>	11.02	Mean diff, A1 - B1	-2.009
	Mean of 24 hrs	21.6	Mean of <i>Eif4e2^{flx/flx}:Emx1-Cre</i>	11.95	Mean diff, A2 - B2	0.1573
	Difference between means	-20.24	Difference between means	-0.9259	(A1 - B1) - (A2 - B2)	-2.166
	SE of difference	3.261	SE of difference	4.034	95% CI of difference	-15.87 to 11.54
	95% CI of difference	-27.09 to -13.38	95% CI of difference	-9.402 to 7.550	(B1 - A1) - (B2 - A2)	2.166
					95% CI of difference	-11.54 to 15.87
Fig. S2.3C	Unpaired t test		How big is the difference?		F test to compare variances	
	P value	0.0414	<i>Eif4e2^{+/+}:Emx1-Cre</i>	100	F, DFn, Dfd	1.087, 3, 3
	P value summary	*	<i>Eif4e2^{flx/flx}:Emx1-Cre</i>	59.49	P value	0.947
	Significantly different (P < 0.05)?	Yes	Difference between means (B - A) ± SEM	-40.51 ± 15.66	P value summary	ns
	One- or two-tailed P value?	Two-tailed	95% confidence interval	-78.83 to -2.191	Significantly different (P < 0.05)?	No
	t, df	t=2.587, df=6	R squared (eta squared)	0.5273		
Fig. S2.3D	Unpaired t test		How big is the difference?		F test to compare variances	
	P value	0.2115	<i>Eif4e2^{+/+}:Emx1-Cre</i>	100	F, DFn, Dfd	1.691, 3, 3
	P value summary	ns	<i>Eif4e2^{flx/flx}:Emx1-Cre</i>	75.18	P value	0.6767
	Significantly different (P < 0.05)?	No	Difference between means (B - A) ± SEM	-24.82 ± 17.75	P value summary	ns
	One- or two-tailed P value?	Two-tailed	95% confidence interval	-68.26 to 18.61	Significantly different (P < 0.05)?	No
	t, df	t=1.398, df=6	R squared (eta squared)	0.2458		
Fig. S2.3E	Unpaired t test		How big is the difference?		F test to compare variances	
	P value	0.6069	<i>Eif4e2^{+/+}:Emx1-Cre</i>	100	F, DFn, Dfd	2.006, 3, 3
	P value summary	ns	<i>Eif4e2^{flx/flx}:Emx1-Cre</i>	94.43	P value	0.582
	Significantly different (P < 0.05)?	No	Difference between means (B - A) ± SEM	-5.568 ± 10.26	P value summary	ns
	One- or two-tailed P value?	Two-tailed	95% confidence interval	-30.67 to 19.54	Significantly different (P < 0.05)?	No
	t, df	t=0.5427, df=6	R squared (eta squared)	0.04679		

Table S3.1: Details of statistical analyses for Chapter 3

Fig. 3.1E	Unpaired t test		How big is the difference?		F test to compare variances	
	P value	0.2067	<i>Eif4e2^{+/+}:Camk2a-Cre</i>	100	F, DFn, Dfd	2.680, 6, 7
	P value summary	ns	<i>Eif4e2^{flx/flx}:Camk2a-Cre</i>	89.05	P value	0.2232
	Significantly different (P < 0.05)?	No	Difference between means (B - A) ± SEM	-10.95 ± 8.237	P value summary	ns
	One- or two-tailed P value?	Two-tailed	95% confidence interval	-28.74 to 6.848	Significantly different (P < 0.05)?	No
t, df	t=1.329, df=13	R squared (eta squared)	0.1196			
Fig. 3.1F	Unpaired t test		How big is the difference?		F test to compare variances	
	P value	0.0067	<i>Eif4e2^{+/+}:Camk2a-Cre</i>	100	F, DFn, Dfd	2.162, 8, 7
	P value summary	**	<i>Eif4e2^{flx/flx}:Camk2a-Cre</i>	77.1	P value	0.3259
	Significantly different (P < 0.05)?	Yes	Difference between means (B - A) ± SEM	-22.90 ± 7.278	P value summary	ns
	One- or two-tailed P value?	Two-tailed	95% confidence interval	-38.41 to -7.387	Significantly different (P < 0.05)?	No
t, df	t=3.146, df=15	R squared (eta squared)	0.3976			
Fig. 3.2B	Two-way RM ANOVA					
	Assume sphericity?	Yes				
	Alpha	0.05				
	Source of Variation	% of total variation	P value	P value summary	Significant?	
	Time x Genotype	0.122	0.6279	ns	No	
	Time	77.24	<0.0001	****	Yes	
	Genotype	0.01866	0.8871	ns	No	
	Subject	14.35	0.1265	ns	No	
	ANOVA table	SS	DF	MS	F (DFn, DFd)	P value
	Time x Genotype	15.91	1	15.91	F (1, 16) = 0.2441	P=0.6279
	Time	10072	1	10072	F (1, 16) = 154.5	P<0.0001
	Genotype	2.433	1	2.433	F (1, 16) = 0.02081	P=0.8871
	Subject	1871	16	117	F (16, 16) = 1.794	P=0.1265
	Residual	1043	16	65.18		
	Difference between row means		Difference between column means		Interaction CI	
	Mean of Naive	2.209	Mean of <i>Eif4e2^{+/+}:Camk2a-Cre</i>	18.78	Mean diff, A1 - B1	-1.861
	Mean of 24 hrs	35.87	Mean of <i>Eif4e2^{flx/flx}:Camk2a-Cre</i>	19.3	Mean diff, A2 - B2	0.8148
	Difference between means	-33.66	Difference between means	-0.5232	(A1 - B1) - (A2 - B2)	-2.676
	SE of difference	2.708	SE of difference	3.627	95% CI of difference	-14.16 to 8.805
	95% CI of difference	-39.40 to -27.92	95% CI of difference	-8.213 to 7.166	(B1 - A1) - (B2 - A2)	2.676
					95% CI of difference	-8.805 to 14.16
Fig. 3.2C	Two-way RM ANOVA					
	Assume sphericity?	Yes				
	Alpha	0.05				
	Source of Variation	% of total variation	P value	P value summary	Significant?	
	Time x Genotype	0.288	0.4455	ns	No	
	Time	83.27	<0.0001	****	Yes	
	Genotype	0.2672	0.5243	ns	No	
	Subject	9.428	0.2891	ns	No	
	ANOVA table	SS	DF	MS	F (DFn, DFd)	P value
	Time x Genotype	84.79	1	84.79	F (1, 15) = 0.6138	P=0.4455
Time	24513	1	24513	F (1, 15) = 177.5	P<0.0001	
Genotype	78.66	1	78.66	F (1, 15) = 0.4251	P=0.5243	

	Subject	2776	15	185	F (15, 15) = 1.340	P=0.2891
	Residual	2072	15	138.1		
	Difference between row means			Difference between column means	Interaction CI	
	Mean of Naive	2.34		Mean of <i>Eif4e2^{+/+}:Camk2a-Cre</i>	27.71	Mean diff, A1 - B1
	Mean of 24 hrs	56.13		Mean of <i>Eif4e2^{flx/flx}:Camk2a-Cre</i>	30.76	Mean diff, A2 - B2
	Difference between means	-53.79		Difference between means	-3.047	(A1 - B1) - (A2 - B2)
	SE of difference	4.038		SE of difference	4.674	95% CI of difference
	95% CI of difference	-62.40 to -45.19		95% CI of difference	-13.01 to 6.915	(B1 - A1) - (B2 - A2)
						95% CI of difference
						-23.54 to 10.89
Fig. 3.2E	Two-way RM ANOVA	Matching: Stacked				
	Assume sphericity?	No				
	Alpha	0.05				
	Source of Variation	% of total variation	P value	P value summary	Significant?	Geisser-Greenhouse's epsilon
	Time x Genotype	2.92	0.4126	ns	No	
	Time	21.61	0.0002	***	Yes	0.8067
	Genotype	1.154	0.392	ns	No	
	Subject	25.43	0.0193	*	Yes	
	ANOVA table	SS	DF	MS	F (DFn, DFd)	P value
	Time x Genotype	1025	4	256.4	F (4, 68) = 1.002	P=0.4126
	Time	7588	4	1897	F (3.227, 54.85) = 7.417	P=0.0002
	Genotype	405.4	1	405.4	F (1, 17) = 0.7716	P=0.3920
	Subject	8931	17	525.4	F (17, 68) = 2.054	P=0.0193
	Residual	17392	68	255.8		
Fig. 3.2F	Two-way RM ANOVA	Matching: Stacked				
	Assume sphericity?	No				
	Alpha	0.05				
	Source of Variation	% of total variation	P value	P value summary	Significant?	Geisser-Greenhouse's epsilon
	Quadrant x Genotype	11.58	0.0796	ns	No	
	Quadrant	5.882	0.3134	ns	No	0.8681
	Genotype	0.00004083	0.397	ns	No	
	Subject	0.0009193	>0.9999	ns	No	
	ANOVA table	SS	DF	MS	F (DFn, DFd)	P value
	Quadrant x Genotype	1164	3	388.2	F (3, 51) = 2.389	P=0.0796
	Quadrant	591.6	3	197.2	F (2.604, 44.27) = 1.214	P=0.3134
	Genotype	0.004107	1	0.004107	F (1, 17) = 0.7550	P=0.3970
	Subject	0.09247	17	0.00544	F (17, 51) = 3.348e-005	P>0.9999
	Residual	8286	51	162.5		
Fig. 3.2G	Two-way RM ANOVA	Matching: Stacked				
	Assume sphericity?	No				
	Alpha	0.05				
	Source of Variation	% of total variation	P value	P value summary	Significant?	Geisser-Greenhouse's epsilon
	Time x Genotype	3.31	0.0206	*	Yes	
	Time	60.71	<0.0001	****	Yes	0.5912
	Genotype	0.1562	0.5169	ns	No	
	Subject	8.666	0.1659	ns	No	
	ANOVA table	SS	DF	MS	F (DFn, DFd)	P value
	Time x Genotype	1959	4	489.7	F (4, 96) = 3.050	P=0.0206

	Time	35930	4	8983	F (2.365, 56.76) = 55.94	P<0.0001
	Genotype	92.47	1	92.47	F (1, 24) = 0.4327	P=0.5169
	Subject	5129	24	213.7	F (24, 96) = 1.331	P=0.1659
	Residual	15416	96	160.6		
	Bonferroni's multiple comparisons test	Mean Diff.	95.00% CI of diff.	Below threshold ?	Summary	Adjusted P Value
	<i>Eif4e2^{+/+}:Camk2a-Cre - Eif4e2^{flx/flx}:Camk2a-Cre</i>					
	1	7.266	-12.78 to 27.32	No	ns	>0.9999
	2	-16.19	-29.47 to -2.915	Yes	*	0.0118
	3	-2.81	-19.16 to 13.54	No	ns	>0.9999
	4	-0.1481	-11.10 to 10.81	No	ns	>0.9999
	5	3.219	-5.336 to 11.77	No	ns	>0.9999
Fig. 3.2H	Two-way RM ANOVA	Matching: Stacked				
	Assume sphericity?	No				
	Alpha	0.05				
	Source of Variation	% of total variation	P value	P value summary	Significant?	Geisser-Greenhouse's epsilon
	Quadrant x Genotype	2.095	0.5565	ns	No	
	Quadrant	21.92	0.0013	**	Yes	0.7153
	Genotype	1.744E-08	0.9563	ns	No	
	Subject	0.0001367	>0.9999	ns	No	
	ANOVA table	SS	DF	MS	F (DFn, DFd)	P value
	Quadrant x Genotype	288.7	3	96.24	F (3, 72) = 0.6976	P=0.5565
	Quadrant	3022	3	1007	F (2.146, 51.50) = 7.301	P=0.0013
	Genotype	0.000002404	1	0.000002404	F (1, 24) = 0.003062	P=0.9563
	Subject	0.01884	24	0.0007852	F (24, 72) = 5.691e-006	P>0.9999
	Residual	9933	72	138		
Fig. 3.3B	Two-way RM ANOVA	Matching: Stacked				
	Assume sphericity?	Yes				
	Alpha	0.05				
	Source of Variation	% of total variation	P value	P value summary	Significant?	
	Time x Genotype	0.1254	0.6731	ns	No	
	Time	75.97	<0.0001	****	Yes	
	Genotype	0.01295	0.893	ns	No	
	Subject	11.8	0.4836	ns	No	
	ANOVA table	SS	DF	MS	F (DFn, DFd)	P value
	Time x Genotype	21.81	1	21.81	F (1, 17) = 0.1843	P=0.6731
	Time	13220	1	13220	F (1, 17) = 111.7	P<0.0001
	Genotype	2.253	1	2.253	F (1, 17) = 0.01866	P=0.8930
	Subject	2053	17	120.8	F (17, 17) = 1.020	P=0.4836
	Residual	2012	17	118.4		
	Difference between row means		Difference between column means		Interaction CI	
	Mean of Naive	1.783	Mean of <i>Eif4e2^{+/+}:Camk2a-Cre</i>	20.7	Mean diff, A1 - B1	-1.03
	Mean of 1 hr	39.14	Mean of <i>Eif4e2^{flx/flx}:Camk2a-Cre</i>	20.22	Mean diff, A2 - B2	2.005
	Difference between means	-37.36	Difference between means	0.4877	(A1 - B1) - (A2 - B2)	-3.035
	SE of difference	3.534	SE of difference	3.571	95% CI of difference	-17.95 to 11.88
	95% CI of difference	-44.81 to -29.90	95% CI of difference	-7.045 to 8.021	(B1 - A1) - (B2 - A2)	3.035
					95% CI of difference	-11.88 to 17.95

Fig. 3.3D	Two-way RM ANOVA	Matching: Stacked				
	Assume sphericity?	Yes				
	Alpha	0.05				
	Source of Variation	% of total variation	P value	P value summary	Significant?	
	Arm x Genotype	10.05	0.007	**	Yes	
	Arm	4.844	0.0506	ns	No	
	Genotype	0.7381	0.6203	ns	No	
	Subject	61.29	0.0171	*	Yes	
	ANOVA table	SS	DF	MS	F (DFn, Dfd)	P value
	Arm x Genotype	9958	1	9958	F (1, 21) = 8.926	P=0.0070
	Arm	4798	1	4798	F (1, 21) = 4.301	P=0.0506
	Genotype	731	1	731	F (1, 21) = 0.2529	P=0.6203
	Subject	60703	21	2891	F (21, 21) = 2.591	P=0.0171
	Residual	23428	21	1116		
	Difference between row means		Difference between column means		Interaction CI	
	Mean of Familiar	133.6	Mean of <i>Eif4e2^{+/+}:Camk2a-Cre</i>	139.8	Mean diff, A1 - B1	-37.44
	Mean of Novel	154.1	Mean of <i>Eif4e2^{flx/flx}:Camk2a-Cre</i>	147.8	Mean diff, A2 - B2	21.47
	Difference between means	-20.45	Difference between means	-7.98	(A1 - B1) - (A2 - B2)	-58.91
	SE of difference	9.859	SE of difference	15.87	95% CI of difference	-99.91 to -17.90
	95% CI of difference	-40.95 to 0.05671	95% CI of difference	-40.98 to 25.02	(B1 - A1) - (B2 - A2)	58.91
					95% CI of difference	17.90 to 99.91
	Bonferroni's multiple comparisons test	Predicted (LS) mean diff.	95.00% CI of diff.	Below threshold ?	Summary	Adjusted P Value
	Familiar - Novel					
	<i>Eif4e2^{+/+}:Camk2a-Cre</i>	-49.9	-84.28 to -15.52	Yes	**	0.0042
	<i>Eif4e2^{flx/flx}:Camk2a-Cre</i>	9.009	-23.91 to 41.92	No	ns	>0.9999
Fig. 3.3E		<i>Eif4e2^{+/+}:Camk2a-Cre</i>	<i>Eif4e2^{flx/flx}:Camk2a-Cre</i>		Unpaired t test	
	Theoretical mean	0	0		P value	0.0015
	Actual mean	18.58	-2.546		P value summary	**
	Number of values	11	12		Significantly different (P < 0.05)?	Yes
					One- or two-tailed P value?	Two-tailed
					t, df	t=3.641, df=21
	One sample t test				How big is the difference?	
	t, df	t=4.790, df=10	t=0.5965, df=11		<i>Eif4e2^{+/+}:Camk2a-Cre</i>	18.58
	P value (two tailed)	0.0007	0.5629		<i>Eif4e2^{flx/flx}:Camk2a-Cre</i>	-2.546
	P value summary	***	ns		Difference between means (B - A) ± SEM	-21.13 ± 5.804
	Significant (alpha=0.05)?	Yes	No		95% confidence interval	-33.20 to -9.061
					R squared (eta squared)	0.387
	How big is the discrepancy?				F test to compare variances	
	Discrepancy	18.58	-2.546		F, DFn, Dfd	1.320, 11, 10
	SD of discrepancy	12.87	14.78		P value	0.6694
	SEM of discrepancy	3.88	4.267		P value summary	ns
	95% confidence interval	9.941 to 27.23	-11.94 to 6.847		Significantly different (P < 0.05)?	No
	R squared (partial eta squared)	0.6965	0.03133			
Fig. 3.3F	Unpaired t test		How big is the difference?		F test to compare variances	
	P value	0.6203	<i>Eif4e2^{+/+}:Camk2a-Cre</i>	279.7	F, DFn, Dfd	1.678, 11, 10

	P value summary	ns	<i>Eif4e2^{flx/flx}:Camk2a-Cre</i>	295.6	P value	0.4235
	Significantly different (P < 0.05)?	No	Difference between means (B - A) ± SEM	15.96 ± 31.74	P value summary	ns
	One- or two-tailed P value?	Two-tailed	95% confidence interval	-50.04 to 81.97	Significantly different (P < 0.05)?	No
	t, df	t=0.5029, df=21	R squared (eta squared)	0.0119		
Fig. 3.4B	Two-way RM ANOVA	Matching: Stacked				
	Assume sphericity?	Yes				
	Alpha	0.05				
	Source of Variation	% of total variation	P value	P value summary	Significant?	
	Arm x Genotype	27.17	0.0007	***	Yes	
	Arm	12.66	0.0142	*	Yes	
	Genotype	1.005	0.2842	ns	No	
	Subject	19.23	0.9637	ns	No	
	ANOVA table	SS	DF	MS	F (DFn, DFd)	P value
	Arm x Genotype	39603	1	39603	F (1, 23) = 15.11	P=0.0007
	Arm	18453	1	18453	F (1, 23) = 7.040	P=0.0142
	Genotype	1465	1	1465	F (1, 23) = 1.202	P=0.2842
	Subject	28028	23	1219	F (23, 23) = 0.4649	P=0.9637
	Residual	60287	23	2621		
	Difference between row means		Difference between column means		Interaction CI	
	Mean of Familiar	169.7	Mean of <i>Eif4e2^{+/+}:Gad2-Cre</i>	194.3	Mean diff, A1 - B1	-45.5
	Mean of Novel	208.1	Mean of <i>Eif4e2^{flx/flx}:Gad2-Cre</i>	183.5	Mean diff, A2 - B2	67.17
	Difference between means	-38.45	Difference between means	10.84	(A1 - B1) - (A2 - B2)	-112.7
	SE of difference	14.49	SE of difference	9.882	95% CI of difference	-172.6 to -52.70
	95% CI of difference	-68.43 to -8.473	95% CI of difference	-9.606 to 31.28	(B1 - A1) - (B2 - A2)	112.7
					95% CI of difference	52.70 to 172.6
	Bonferroni's multiple comparisons test	Predicted (LS) mean diff.	95.00% CI of diff.	Below threshold ?	Summary	Adjusted P Value
	Familiar - Novel					
	<i>Eif4e2^{+/+}:Gad2-Cre</i>	-94.79	-144.9 to -44.67	Yes	***	0.0003
	<i>Eif4e2^{flx/flx}:Gad2-Cre</i>	17.88	-30.27 to 66.03	No	ns	0.765
Fig. 3.4C		<i>Eif4e2^{+/+}:Gad2-Cre</i>	<i>Eif4e2^{flx/flx}:Gad2-Cre</i>		Unpaired t test with Welch's correction	
	Theoretical mean	0			P value	0.001
	Actual mean	24.1	-4.914		P value summary	***
	Number of values	12	13		Significantly different (P < 0.05)?	Yes
					One- or two-tailed P value?	Two-tailed
					Welch-corrected t, df	t=3.910, df=18.53
	One sample t test				How big is the difference?	
	t, df	t=6.731, df=11	t=0.7560, df=12		<i>Eif4e2^{+/+}:Gad2-Cre</i>	24.1
	P value (two tailed)	<0.0001	0.4642		<i>Eif4e2^{flx/flx}:Gad2-Cre</i>	-4.914
	P value summary	****	ns		Difference between means (B - A) ± SEM	-29.02 ± 7.421
	Significant (alpha=0.05)?	Yes	No		95% confidence interval	-44.58 to -13.46
					R squared (eta squared)	0.4521
	How big is the discrepancy?				F test to compare variances	
	Discrepancy	24.1	-4.914		F, DFn, Dfd	3.570, 12, 11
	SD of discrepancy	12.4	23.44		P value	0.0434
	SEM of discrepancy	3.581	6.5		P value summary	*

	95% confidence interval	16.22 to 31.98	-19.08 to 9.249		Significantly different (P < 0.05)?	Yes
	R squared (partial eta squared)	0.8047	0.04547			
Fig. 3.4D	Unpaired t test		How big is the difference?		F test to compare variances	
	P value	0.2842	<i>Elf4e2^{+/+}:Gad2-Cre</i>	388.6	F, DFn, DFd	1.208, 11, 12
	P value summary	ns	<i>Elf4e2^{flx/flx}:Gad2-Cre</i>	367	P value	0.7475
	Significantly different (P < 0.05)?	No	Difference between means (B - A) ± SEM	-21.67 ± 19.76	P value summary	ns
	One- or two-tailed P value?	Two-tailed	95% confidence interval	-62.55 to 19.21	Significantly different (P < 0.05)?	No
	t, df	t=1.097, df=23	R squared (eta squared)	0.04968		
Fig. 3.4E	Two-way RM ANOVA	Matching: Stacked				
	Assume sphericity?	Yes				
	Alpha	0.05				
	Source of Variation	% of total variation	P value	P value summary	Significant?	
	Time x Genotype	0.03617	0.8862	ns	No	
	Time	45.73	<0.0001	****	Yes	
	Genotype	0.01144	0.9352	ns	No	
	Subject	26.86	0.5143	ns	No	
	ANOVA table	SS	DF	MS	F (DFn, DFd)	P value
	Time x Genotype	4.136	1	4.136	F (1, 16) = 0.02115	P=0.8862
	Time	5230	1	5230	F (1, 16) = 26.75	P<0.0001
	Genotype	1.308	1	1.308	F (1, 16) = 0.006813	P=0.9352
	Subject	3072	16	192	F (16, 16) = 0.9819	P=0.5143
	Residual	3129	16	195.5		
	Difference between row means		Difference between column means		Interaction CI	
	Mean of Naive	0.5933	Mean of <i>Elf4e2^{+/+}:Gad2-Cre</i>	12.84	Mean diff, A1 - B1	-0.2967
	Mean of 24 hrs	24.7	Mean of <i>Elf4e2^{flx/flx}:Gad2-Cre</i>	12.46	Mean diff, A2 - B2	1.059
	Difference between means	-24.11	Difference between means	0.3813	(A1 - B1) - (A2 - B2)	-1.356
	SE of difference	4.661	SE of difference	4.619	95% CI of difference	-21.12 to 18.41
	95% CI of difference	-33.99 to -14.22	95% CI of difference	-9.410 to 10.17	(B1 - A1) - (B2 - A2)	1.356
					95% CI of difference	-18.41 to 21.12
Fig. 3.5B	Two-way RM ANOVA	Matching: Stacked				
	Assume sphericity?	Yes				
	Alpha	0.05				
	Source of Variation	% of total variation	P value	P value summary	Significant?	
	Time x Treatment	0.5452	0.5203	ns	No	
	Time	25.97	0.0005	***	Yes	
	Treatment	10.84	0.0887	ns	No	
	Subject	45.34	0.0433	*	Yes	
	ANOVA table	SS	DF	MS	F (DFn, DFd)	P value
	Time x Treatment	555.9	1	555.9	F (1, 14) = 0.4349	P=0.5203
	Time	26485	1	26485	F (1, 14) = 20.72	P=0.0005
	Treatment	11049	1	11049	F (1, 14) = 3.346	P=0.0887
	Subject	46229	14	3302	F (14, 14) = 2.583	P=0.0433
	Residual	17894	14	1278		
	Difference between row means		Difference between column means		Interaction CI	
	Mean of Familiar	119.7	Mean of WT + VEH	168.6	Mean diff, A1 - B1	29.77
	Mean of Novel	179.1	Mean of WT + ANISO	130.2	Mean diff, A2 - B2	46.99
	Difference between means	-59.43	Difference between means	38.38	(A1 - B1) - (A2 - B2)	-17.22
	SE of difference	13.05	SE of difference	20.98	95% CI of difference	-73.22 to 38.78

	95% CI of difference	-87.42 to -31.43	95% CI of difference	-6.621 to 83.39	(B1 - A1) - (B2 - A2)	17.22
					95% CI of difference	-38.78 to 73.22
Fig. 3.5C		WT + VEH	WT + ANISO		Unpaired t test	
	Theoretical mean	0	0		P value	0.9658
	Actual mean	20.48	20.12		P value summary	ns
	Number of values	6	10		Significantly different (P < 0.05)?	No
					One- or two-tailed P value?	Two-tailed
					t, df	t=0.04368, df=14
	One sample t test			How big is the difference?		
	t, df	t=5.550, df=5	t=3.336, df=9		WT + VEH	20.48
	P value (two tailed)	0.0026	0.0087		WT + ANISO	20.12
	P value summary	**	**		Difference between means (B - A) ± SEM	-0.3657 ± 8.373
	Significant (alpha=0.05)?	Yes	Yes		95% confidence interval	-18.32 to 17.59
					R squared (eta squared)	0.0001363
	How big is the discrepancy?			F test to compare variances		
	Discrepancy	20.48	20.12		F, DFn, Dfd	4.448, 9, 5
	SD of discrepancy	9.041	19.07		P value	0.1149
	SEM of discrepancy	3.691	6.03		P value summary	ns
	95% confidence interval	11.00 to 29.97	6.477 to 33.76		Significantly different (P < 0.05)?	No
	R squared (partial eta squared)	0.8603	0.5529			
Fig. 3.5D	Unpaired t test		How big is the difference?		F test to compare variances	
	P value	0.0887	WT + VEH	337.1	F, DFn, Dfd	3.026, 9, 5
	P value summary	ns	WT + ANISO	260.4	P value	0.2355
	Significantly different (P < 0.05)?	No	Difference between means (B - A) ± SEM	-76.76 ± 41.97	P value summary	ns
	One- or two-tailed P value?	Two-tailed	95% confidence interval	-166.8 to 13.24	Significantly different (P < 0.05)?	No
	t, df	t=1.829, df=14	R squared (eta squared)	0.1929		
Fig. 3.5F	Unpaired t test		How big is the difference?		F test to compare variances	
	P value	0.001	<i>Eif4e2^{+/+}:Camk2a-Cre</i>	100	F, DFn, Dfd	1.966, 5, 5
	P value summary	**	<i>Eif4e2^{flx/flx}:Camk2a-Cre</i>	63.6	P value	0.476
	Significantly different (P < 0.05)?	Yes	Difference between means (B - A) ± SEM	-36.40 ± 7.962	P value summary	ns
	One- or two-tailed P value?	Two-tailed	95% confidence interval	-54.14 to -18.66	Significantly different (P < 0.05)?	No
	t, df	t=4.572, df=10	R squared (eta squared)	0.6764		
Fig. 3.5H	Unpaired t test		How big is the difference?		Unpaired t test	
	Theoretical mean	0	0		P value	0.26
	Actual mean	23.2	12.53		P value summary	ns
	Number of values	14	10		Significantly different (P < 0.05)?	No
					One- or two-tailed P value?	Two-tailed
					t, df	t=1.156, df=22
	One sample t test			How big is the difference?		
	t, df	t=5.145, df=13	t=1.398, df=9		<i>Rptor^{+/+}:Camk2a-Cre</i>	23.2
	P value (two tailed)	0.0002	0.1955		<i>Rptor^{flx/flx}:Camk2a-Cre</i>	12.53
	P value summary	***	ns		Difference between means (B - A) ± SEM	-10.67 ± 9.228

	Significant (alpha=0.05)?	Yes	No		95% confidence interval	-29.81 to 8.468
					R squared (eta squared)	0.05728
	How big is the discrepancy?			F test to compare variances		
	Discrepancy	23.2	12.53		F, DFn, Dfd	2.821, 9, 13
	SD of discrepancy	16.87	28.34		P value	0.0879
	SEM of discrepancy	4.509	8.962		P value summary	ns
	95% confidence interval	13.46 to 32.94	-7.742 to 32.80		Significantly different (P < 0.05)?	No
	R squared (partial eta squared)	0.6707	0.1785			
Fig. 3.5I	Unpaired t test		How big is the difference?		F test to compare variances	
	P value	0.6938	<i>Rptor^{flx/flx};Camk2a-Cre</i>	407.6	P value	0.2145
	P value summary	ns	<i>Rptor^{flx/flx};Camk2a-Cre</i>	417.6	P value summary	ns
	Significantly different (P < 0.05)?	No	Difference between means (B - A) ± SEM	10.04 ± 25.17	Significantly different (P < 0.05)?	No
	One- or two-tailed P value?	Two-tailed	95% confidence interval	-42.16 to 62.24	F, DFn, Dfd	2.300, 13, 9
	t, df	t=0.3989, df=22	R squared (eta squared)	0.007183		
Fig. S3.2A	Unpaired t test		How big is the difference?		F test to compare variances	
	P value	0.6689	<i>Eif4e2^{+/+};Gad2-Cre</i>	37.93	P value	0.0852
	P value summary	ns	<i>Eif4e2^{flx/flx};Gad2-Cre</i>	44.44	P value summary	ns
	Significantly different (P < 0.05)?	No	Difference between means (B - A) ± SEM	6.507 ± 14.92	Significantly different (P < 0.05)?	No
	One- or two-tailed P value?	Two-tailed	95% confidence interval	-25.29 to 38.31	F, DFn, Dfd	3.978, 8, 7
	t, df	t=0.4362, df=15	R squared (eta squared)	0.01253		
Fig. S3.2B	Unpaired t test		How big is the difference?		F test to compare variances	
	P value	0.4258	<i>Eif4e2^{+/+};Gad2-Cre</i>	2.556	P value	0.663
	P value summary	ns	<i>Eif4e2^{flx/flx};Gad2-Cre</i>	3.25	P value summary	ns
	Significantly different (P < 0.05)?	No	Difference between means (B - A) ± SEM	0.6944 ± 0.8484	Significantly different (P < 0.05)?	No
	One- or two-tailed P value?	Two-tailed	95% confidence interval	-1.114 to 2.503	F, DFn, Dfd	1.411, 8, 7
	t, df	t=0.8186, df=15	R squared (eta squared)	0.04276		
Fig. S3.2C	Two-way RM ANOVA					
	Assume sphericity?	Yes				
	Alpha	0.05				
	Source of Variation	% of total variation	P value	P value summary	Significant?	
	Time x Genotype	0.2729	0.6756	ns	No	
	Time	54.79	<0.0001	****	Yes	
	Genotype	0.2853	0.6444	ns	No	
	Subject	20.62	0.6181	ns	No	
	ANOVA table	SS	DF	MS	F (DFn, DFd)	P value
	Time x Genotype	480.9	1	480.9	F (1, 16) = 0.1817	P=0.6756
	Time	96554	1	96554	F (1, 16) = 36.49	P<0.0001
	Genotype	502.7	1	502.7	F (1, 16) = 0.2213	P=0.6444
	Subject	36343	16	2271	F (16, 16) = 0.8584	P=0.6181
	Residual	42336	16	2646		
	Difference between row means		Difference between column means		Interaction CI	
	Mean of E	56.3	<i>Eif4e2^{+/+};Gad2-Cre</i>	111.8	Mean diff, A1 - B1	14.78
	Mean of S1	159.9	<i>Eif4e2^{flx/flx};Gad2-Cre</i>	104.4	Mean diff, A2 - B2	0.1644
	Difference between means	-103.6	Difference between means	7.474	(A1 - B1) - (A2 - B2)	14.62
	SE of difference	17.15	SE of difference	15.89	95% CI of difference	-58.08 to 87.32

	95% CI of difference	-139.9 to -67.23	95% CI of difference	-26.20 to 41.15	(B1 - A1) - (B2 - A2)	-14.62
					95% CI of difference	-87.32 to 58.08
Fig. S3.2D	Two-way RM ANOVA	Matching: Stacked				
	Assume sphericity?	Yes				
	Alpha	0.05				
	Source of Variation	% of total variation	P value	P value summary	Significant?	
	Time x Genotype	0.7079	0.4407	ns	No	
	Time	38.35	<0.0001	****	Yes	
	Genotype	0.07304	0.8708	ns	No	
	Subject	42.75	0.0479	*	Yes	
	ANOVA table	SS	DF	MS	F (DFn, DFd)	P value
	Time x Genotype	521	1	521	F (1, 16) = 0.6251	P=0.4407
	Time	28220	1	28220	F (1, 16) = 33.86	P<0.0001
	Genotype	53.75	1	53.75	F (1, 16) = 0.02733	P=0.8708
	Subject	31463	16	1966	F (16, 16) = 2.360	P=0.0479
	Residual	13335	16	833.4		
	Difference between row means		Difference between column means		Interaction CI	
	Mean of S1	63.16	<i>Eif4e2^{+/+};Gad2-Cre</i>	89.93	Mean diff, A1 - B1	-10.05
	Mean of S2	119.2	<i>Eif4e2^{flx/flx};Gad2-Cre</i>	92.38	Mean diff, A2 - B2	5.164
	Difference between means	-56	Difference between means	-2.444	(A1 - B1) - (A2 - B2)	-15.22
	SE of difference	9.623	SE of difference	14.78	95% CI of difference	-56.02 to 25.58
	95% CI of difference	-76.40 to -35.60	95% CI of difference	-33.78 to 28.89	(B1 - A1) - (B2 - A2)	15.22
					95% CI of difference	-25.58 to 56.02

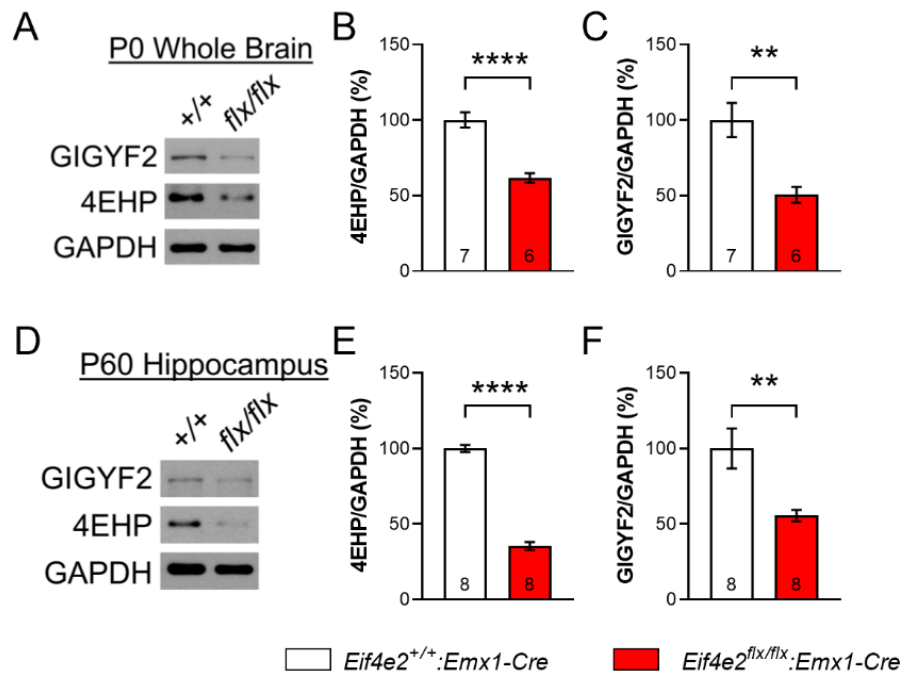


Figure S2.1. Codeletion of 4EHP and GIGYF2 occurs as early as P0 in the brain of 4EHP-eKO mice.

A Western blot analysis of GIGYF2 and 4EHP levels in P0 whole brain from 4EHP-WT (+/+) versus 4EHP-eKO (flx/flx) mice. GAPDH was used as loading control. **B** and **C** Quantification of band intensity from A, presented as percent control. **D** Western blot analysis of GIGYF2 and 4EHP levels in P60 hippocampus from 4EHP-WT (+/+) versus 4EHP-eKO (flx/flx) mice. GAPDH was used as loading control. **E** and **F** Quantification of band intensity from D, presented as percent control. Data are presented as mean \pm s.e.m.; **p<0.01, ****p<0.0001; calculated by unpaired t-test. Sample size is located within bar graphs.

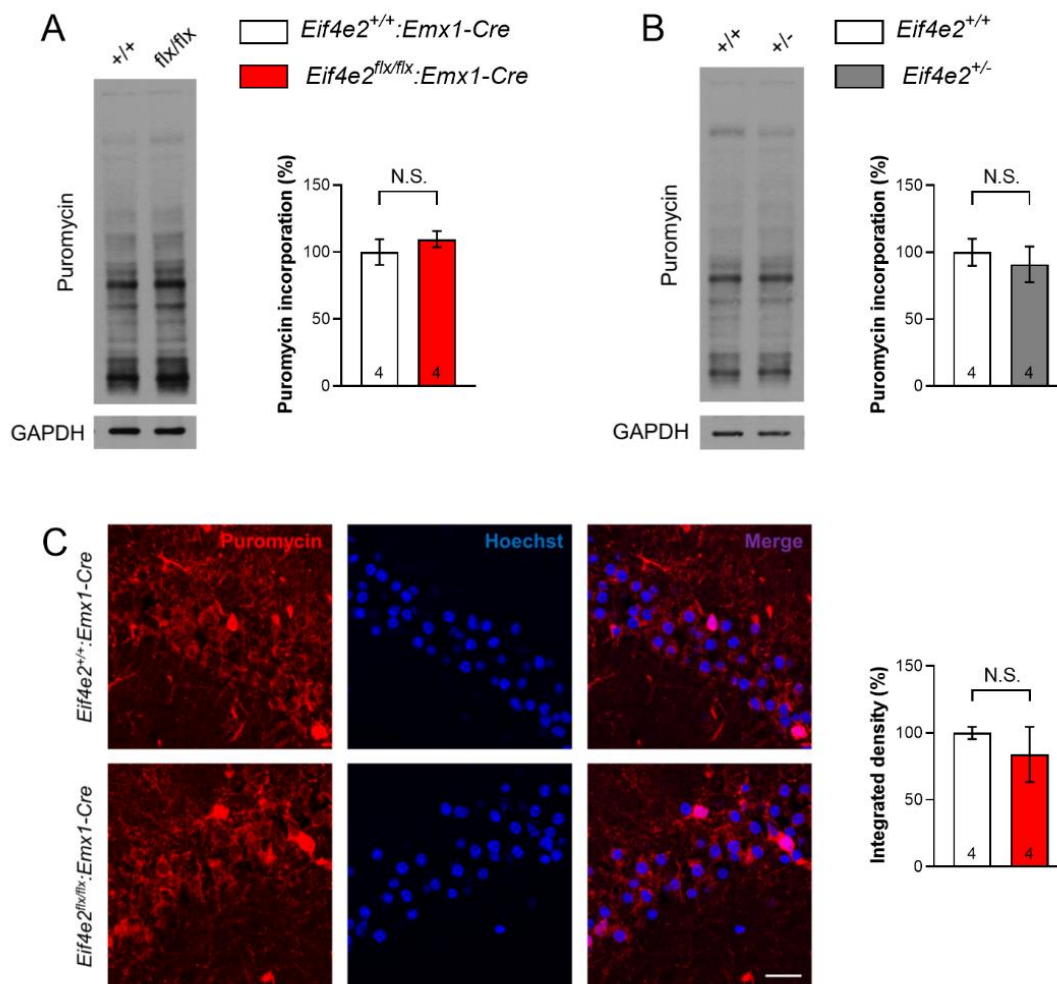


Figure S2.2. Analysis of global protein synthesis.

A Puromycin incorporation into hippocampal slices from 4EHP-WT and 4EHP-eKO mice measured by western blot (left panel) and quantification (right panel) normalized to GAPDH. **B** Puromycin incorporation into hippocampal slices from 4EHP^{+/+} and 4EHP^{+/-} mice measured by western blot (left panel) and quantification (right panel) normalized to GAPDH. **C** Puromycin incorporation into hippocampal slices from 4EHP-WT and 4EHP-eKO mice measured by immunofluorescence (left panel) and quantification (right panel). Puromycin staining is colored in red and Hoechst-stained nucleus in blue. Quantification of puromycin integrated density was performed on whole image using image J. Scale bar represents 20 μ m. Data are presented as mean \pm s.e.m.; N.S., not significant; calculated by unpaired t-test. Sample size is located within bar graphs.

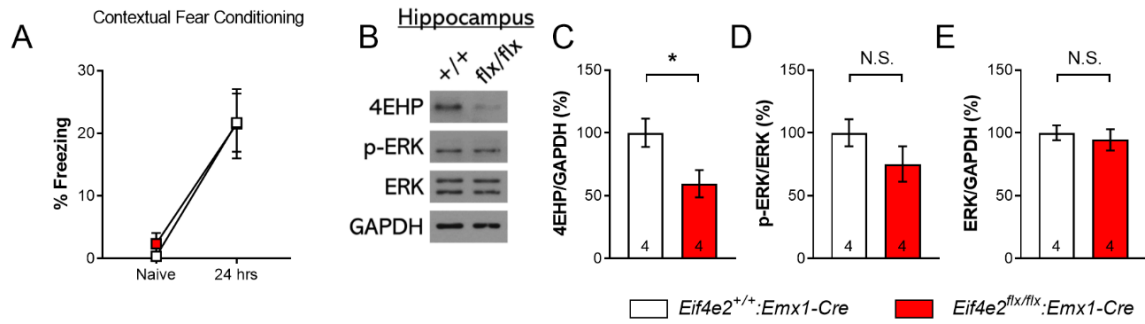


Figure S2.3. Analysis of long-term contextual fear memory and p-ERK.

A Mice were placed into a soundproof box (context) with an electric grid floor. Freezing time was recorded for 2 min (Naïve) before receiving a mild foot shock (0.7 mA, 1 sec). Mice were placed back in the box after 24 hr and freezing behavior recorded, n=11 (4EHP-WT), n=9 (4EHP-eKO). **B** Western blot analysis of ERK activation (p-ERK) in the hippocampus of 4EHP-eKO versus 4EHP-WT mice. **C** Quantification of 4EHP normalized to GAPDH. **D** Quantification of p-ERK normalized to total ERK. **E** Quantification of total ERK normalized to GAPDH. Data are presented as mean \pm s.e.m.; *p<0.05, N.S., not significant; calculated by unpaired t-test. Sample size is located within bar graphs.

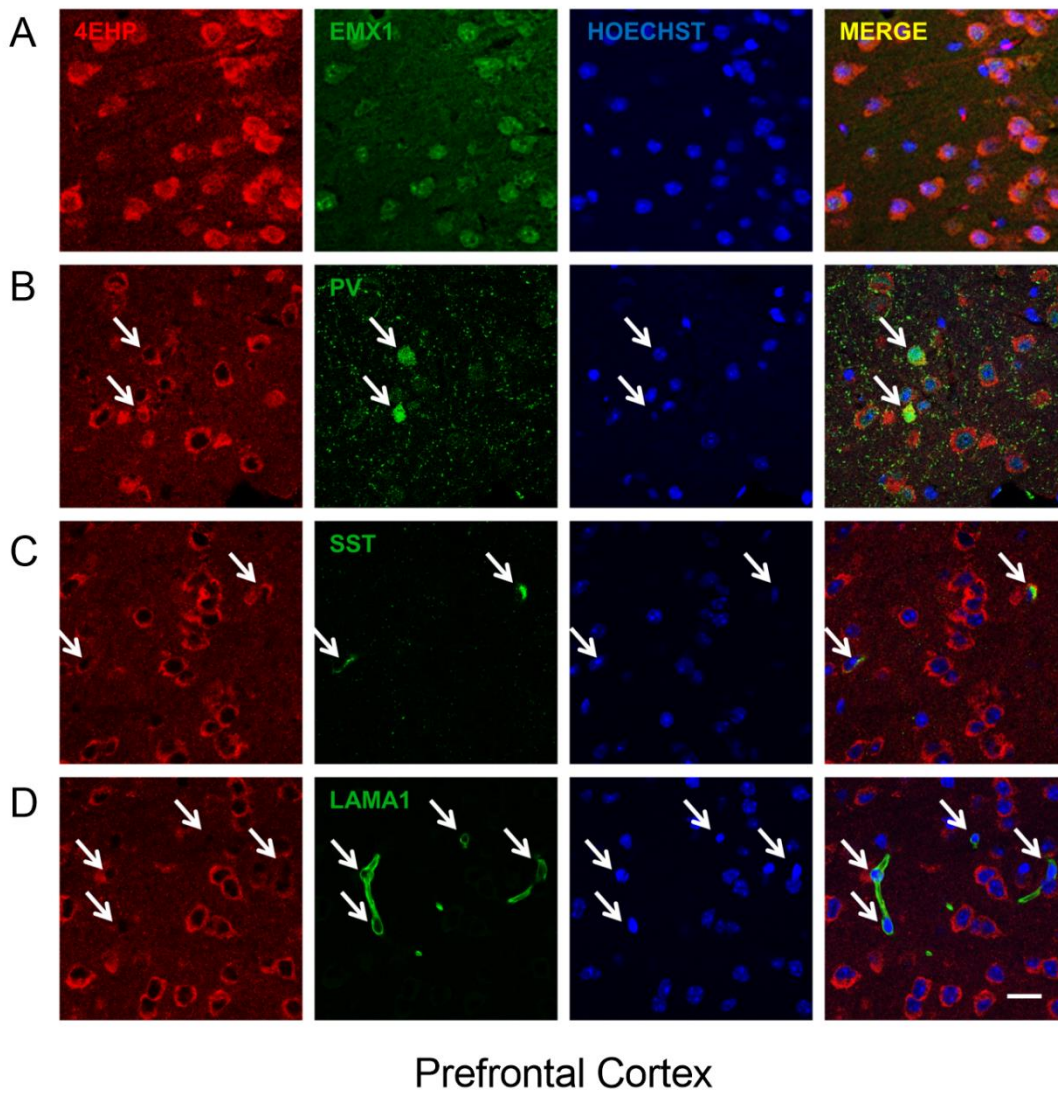


Figure S3.1. 4EHP expression pattern in the prefrontal cortex.

Analysis of cell-type-specific expression of 4EHP by colocalization with **A** Empty Spiracles Homeobox 1 (EMX1, defining excitatory neurons), **B** parvalbumin (PV, defining a subset of inhibitory neurons), **C** somatostatin (SST, defining another subset of inhibitory neurons), and **D** laminin (LAMA1, defining endothelial cells) in the prefrontal cortex of wildtype mice. 4EHP expression is colored in red, the cell type marker in green, and Hoechst-stained nucleus in blue. Arrows indicate a positive signal for the cell type maker. Scale bar represents 20 μm .

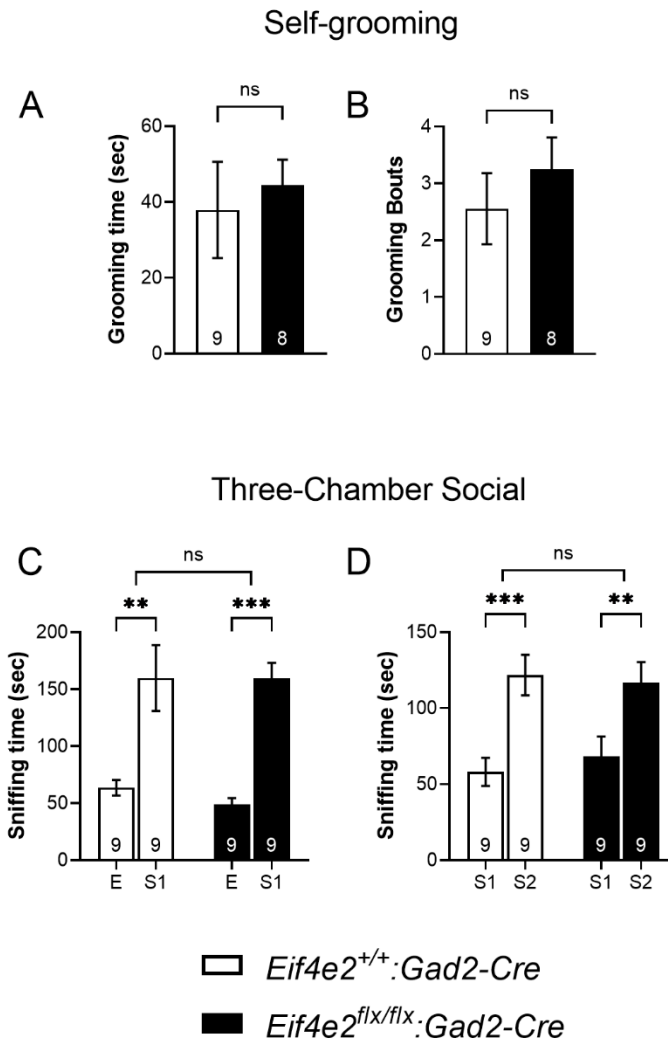


Figure S3.2. Inhibitory interneuron-specific deletion of 4EHP does not affect ASD-like behaviors.

Assessment of ASD-like behaviors in mice lacking 4EHP expression specifically in inhibitory neurons defined by *Gad2*. **A** Total time spent grooming. **B** Number of grooming bouts. **C** Sniffing time between either an empty cage (E) or a cage containing a stranger mouse (S1). **D** Sniffing time between either the previously encountered stranger mouse (S1) or a novel stranger mouse (S2). Data are presented as mean \pm s.e.m.; ** $p < 0.01$, *** $p < 0.001$, ns., not significant; calculated by unpaired t-test or 2-way ANOVA with Bonferroni multiple comparisons test. Sample size is located within bar graphs.